COMPARISON OF SEDIMENT ACCUMULATION AND ACCRETION IN IMPOUNDED AND UNIMPOUNDED MARSHES OF THE DELAWARE ESTUARY

by

Brandon Michael Boyd

A thesis submitted to the Faculty of the University of Delaware in partial fulfillment of the requirements for the degree of Master of Science in Marine Studies

Summer 2012

COMPARISON OF SEDIMENT ACCUMULATION AND ACCRETION IN IMPOUNDED AND UNIMPOUNDED MARSHES OF THE DELAWARE ESTUARY

by

Brandon Michael Boyd

Approved: ____
Christopher K. Sommerfield, Ph.D.
Professor in charge of thesis on behalf of the Advisory Committee

Approved: ____
Nancy M. Targett, Ph.D.
Dean of the College of Earth, Ocean, and Environment

Approved: ____
Charles G. Riordan, Ph.D.
Vice Provost for Graduate and Professional Education

ACKNOWLEDGMENTS

I would like to thank my loving family especially my grandmother, Leontine, my mother, Stephanie, and my father, Michael, for their continued support of my academic pursuits. They showed me I could achieve whatever I want in life. I am also thankful for my girlfriend, Kaytee, whose patience and cooking during the completion of this thesis was much appreciated. I thank God for blessing me with my many friends and brothers in Louisiana and Delaware, whose support during this work was warmly received, and with a love for our coastal world that has made the pursuit of this work possible.

I would like to thank my committee for their helpful criticism, Dr. William Ullman, Dr. David Velinsky, and especially, my advisor, Dr. Christopher Sommerfield. Chris has taught me how to be a better student and researcher and I look forward to my learning more from him during pursuit of my Ph.D.

Sediment cores for this project were collected by the Delaware Department of Natural Resources and Environmental Control's (DNREC) Delaware Coastal Programs (DCP) Office staff and analysis of these cores was started by my lab members, Dack Stuart and Jared Halonen. I thank them all for starting this project as it would not be possible for me to have done any of it alone. Dr. David Carter of DNREC DCP and James Joachimowski of DE Division of Fish and Wildlife provided site information.

This research was partial funded by a fellowship from the National Oceanic and Atmospheric Administration's National Estuarine Research Reserve System

(NERR). I thank Dr. Bob Scarborough and the Delaware NERR for seeing the potential in me to make a contribution to our understanding of Delaware's coastal resources. This thesis is an expansion of the DNREC DCP's Coastal Impoundment Accretion Rate Study, which involved contributions from the following individuals: Bartholomew Wilson, Drexel Siok, Christina Pinkerton, Kenneth Smith III, Tiffany Johnson, Kat Hoenke, Brian Kelly, Jocelyn Robinson, Gabrielle Lyons, and Mike Rhodes.

TABLE OF CONTENTS

LIST OF TABLES

LIST OF FIGURES

ABSTRACT

Coastal marshes represent a small land area relative to the ecosystem services they provide. Humans have altered the coastal environment in a number of ways, one being the tidal restriction of marshes. One type of tidal restriction involves marsh impoundments, which are managed by humans to provide ecological benefits including mosquito control and waterfowl habitat. In the state of Delaware, impounded marshes are faced with rising sea level just like their unrestricted counterpart. Currently, coastal managers are concerned about the fate of these systems and are considering what actions (if any) can be taken to preserve them. Accretion, or vertical growth of the marsh platform by accumulation of mineral and organic material, is an important part of understanding marsh elevation change through time. This study compares impounded and unimpounded tidal marshes of coastal Delaware to examine 1) the relative accretionary status of selected managed and natural marshlands, 2) the relative influences of mineral and organic solids accumulation on rates of accretion. Accretion rates were measured using ^{137}Cs and ^{210}Pb radiometric methods, which are commonly used in tidal marsh studies but not always together. This study explores the value of using both radiometric methods and compares the results.

Gravimetric, loss-on-ignition, and radionuclide analyses were conducted on over 500 subsamples of 44 marsh cores collected at eleven sites along the western coast of the Delaware Estuary. Radionuclide analysis was performed via gamma spectroscopy, which allows simultaneous measurement of ^{137}Cs and ^{210}Pb activity.

Accretion and accumulation rates were calculated using activity-depth profiles of ^{137}Cs and excess ^{210}Pb, using the 1964 reference horizon and the Constant Initial Concentration model, respectively.

The two radionuclide methods were found to provide similar results, suggesting that ^{137}Cs and ^{210}Pb are effective sediment chronometers in the study area. For unimpounded marshes, mineral and organic mass accumulation averaged 0.22 g cm^{-2} y^{-1} and 0.06 g cm^{-2} y^{-1}, respectively. For impounded marshes, mineral and organic mass accumulation averaged 0.08 g cm^{-2} y^{-1} and 0.03 g cm^{-2} y^{-1}, respectively. Accretion rates for unimpounded marshes averaged 0.57 cm y^{-1} and, for unimpounded marshes, 0.28 cm y^{-1}. Overall, rates of accumulation and accretion determined for this study were comparable to rates reported in the literature for U.S. East Coast marshes.

Impounded marshes investigated exhibited lower accretion rates and lower mineral sediment inventories than the unimpounded marshes. Impounded and unimpounded marshes were found to show a similar direct relationship between accretion rates and accumulated mass; accretion increased with increasing organic and mineral mass accumulation. However, accretion was more sensitive to organic accumulation than mineral sediment accumulation. In the case of impounded marshes, accretion rates appear to be limited by mineral sediment accumulation. The implication is that these marshes are deficient in suspended mineral sediment supplied by tidal flooding and deposition, perhaps due to the impoundment works.

Accretion rates determined for the impounded marshes (0.11–0.72 cm y^{-1} range, 0.25±0.16 cm y^{-1} mean) fell at or below the rate of relative sea-level rise for middle Delaware Estuary (0.36±0.06 cm y^{-1} at Reedy Point). Where the rate of marsh accretion is deficient, coastal flooding and inundation related to future sea-level rise will be most pronounced. Coastal managers should consider sediment management among the various adaptation strategies implemented by the state of Delaware to mitigate effects of rising sea level on the impounded marshlands.

Chapter 1

INTRODUCTION

1.1 Marsh Sediment Accumulation and Accretion

Marsh accretion is the vertical growth of the landscape by a combination of detrital mineral sediment and organic matter accumulation along with burial of vegetative biomass. Sediment is transported to the marsh in suspension via tidal, flood, or stream flow. This material can be autochthonous or allochthonous in origin and either organic or mineral in composition. In tidal marshes, mineral material can be composed of marine sediments, eroded marsh material, or eroded watershed material. Organic material can also be imported from outside the marsh in the form of plant litter and detritus, but the marsh sediment column is composed of mostly of root material and buried litter (Reed 1995). Together, organic and mineral material make up the volume of solids in the sediment column, whereas the total volume is composed of solids and pore space filled with water or air (Bricker-Urso et al. 1989).

Accretion is only one component of surface elevation change in a marsh; decomposition of organics, fluctuation in root volume, autocompaction, and isostatic subsidence are other factors (Nyman et al. 1993). The feedback system of sea-level rise, accretion, and soil processes that lead to elevation change are illustrated in Figure 1. The concentration of suspended sediment in tide water along with hydroperiod (the frequency and duration of tidal inundation) are fundamental factors affecting sediment delivery to tidal marshes (Friedrichs and Perry 2001). On a tidal time scale, sediment deposition rate and trapping efficiency tend to decrease with increasing distance away from source waters as a function of initial concentration and settling velocity (Moskalski and Sommerfield 2012). The ability of a marsh to permanently trap sediment depends on the hydrologic, biologic, and topographic properties of the marsh itself (Temmerman et al. 2005; van Proosdij et al. 2006). For example, tidal amplitude, storm magnitude and frequency, distance from sediment sources, stem density, vegetative cover, nutrient supply, plant grazing, peat accumulation, groundwater content, and ice rafting influence patterns and rates of sediment accumulation and accretion (Gleason et al. 1979; Reed et al. 2008; Mudd et al. 2010).

The rate of accretion of a marsh is sometimes misunderstood to be synonymous with elevation change in an absolute sense. As described above, accretion is the rate of vertical growth of the marsh; knowledge of local sediment and crustal movements is needed to relate accretion and vertical elevation change. Subsidence is downward movement of the earth's surface due to a combination of subsurface processes. The measured accretion rate (net accretion) corrected for subsidence is the "absolute rate" of accretion, which is closely related to actual changes in topographic elevation (Figure 2). In coastal Delaware, subsidence is primarily an adjustment of earth's crust following the retreat of the Laurentide ice sheet after the last glacial maximum (Davis 1987; Nikitina et al. 2000).

Plant stem density is a biological influence on sediment deposition and marsh accretion on the longer term. On the marsh platform plant stems and leaves create frictional drag and reduce the speed of overmarsh flows, enhancing particle settling (Leonard and Luther 1995; Nepf 1999). Additionally, particles become trapped on stems and leaves themselves (Yang 1999). Lab experiments have shown increasing stem density can increase accretion rates (Gleason et al. 1979). In the highly depositional Yangtze Delta, Yang (1999) found trapping by two species of *Scirpus* was an important factor in accretion processes, and that the plants protected the sediment surface against wave erosion. Rooth and Stevenson (2000) compared accretion in marshes dominated by the invasive *Phragmites australis* to those dominated by native plants. They found an increase in trapping by *Phragmites* and also that other attributes of the plant (litter production, belowground biomass) were responsible for increased accretion rate.

Coastal storms create a transient, high-energy environment in and around marshes. The wind-forced setup and surge of storms influences sediment delivery to the marsh surface. On the Gulf Coast of the United States, a number of accretion and marsh elevation studies have focused on hurricanes as a mode of sediment transport to marshes (Cahoon et al. 1995; Turner et al. 2007). Some of these studies found hurricanes to be a necessary mode of sediment transport and especially important for mineral deposition. Winter storms are also an important source of mineral material (Reed 1989; Roman et al. 1997). In Delaware, Stumpf (1983) found that subtropical northeaster storms caused significant accretion events, hypothesizing that they may be the only mode of mineral sedimentation on the back marsh and in areas not flooded during most tides. Moskalski (2010), working in Delaware’s St. Jones National Estuarine Research Reserve (NERR), showed that among different types of storms strong northeasters were the events most effective at causing synchronously high water and high turbidity in the St. Jones Estuary, thereby creating a regime conducive for high rates of deposition.

Regression analysis of accumulation and accretion is often used to determine the relative contributions of organic and mineral mass accumulation to accretion—the coefficient of determination explains the contribution of accumulation to the variability in accretion. Nyman et al. (1993) showed a correlation coefficient of 0.95 for organic accumulated mass and accretion and 0.70 for mineral accumulated mass and accretion in marshes in Terrebonne Parish, Louisiana. Turner et al. (2000) applied regression analysis to data from marshes on the U.S. Gulf and East coasts and found that organic accumulation accounted for 59% of the variation in accretion rates. Chmura and Hung (2001) found that accumulated organic matter accounted for 87% of the variation in accretion rates in eastern Canada marshes. Neubauer (2008), reviewing U.S. Gulf and East coast tidal freshwater and salt marshes, found a correlation coefficient of 0.53. The common findings of these studies are twofold: 1) accretion in established salt and brackish marshes is mostly influenced by organic accumulation; and 2) the importance of mineral accumulation in accretion varies geographically (Neubauer 2008).

While natural biological and physical factors influence marsh accretion, human-altered hydrology adds further complexity to the marsh system (Crain et al. 2009). Impounded marshes (marshes in which tidal exchange is altered from its natural state) make up a small but important portion of marshland on the U.S. East Coast, often being managed for increased ecological and socioeconomical benefit (Montague et al. 1987; Kennish 2001). Because the flow of tide water is manipulated, suspended sediment delivery to impounded marshlands is partly a function of local management practices, which can alternatively inhibit or enhance tidal sediment deposition, and by extension marsh accretion on the longer term. For this reason, understanding marsh accretion and sustainability in the face of sea-level rise is particularly relevant to impounded wetlands, and is a major concern among coastal managers in the state of Delaware and beyond (Delaware Coastal Programs 2011).

1.2 Impounded Marshes

Impounded marshes are marshes in which humans have modified or altogether removed the tidal flow. There are different management systems for impounded marshes, but most consist of a diked perimeter, such as spoil banks, levees, or dunes, and a water control structure, such as weirs, tide gates, or pumps. Impoundment is often done to achieve a certain management goal, such as to create agricultural land, provide mosquito control, or increase waterfowl habitat. Marshes can also be unintentionally impounded by bridges, roads, railways and other human structures whose construction can impose tidal restrictions. Impounding a marsh can result in lower water tables, reduced surface elevation, and decreased soil salinity (Sturdevant 2003). Impounded marshes represent a small but significant percentage of coastal wetlands on the U.S. East Coast. For example, 3.7 – 4.8 % (12,000 – 15,000 acres) of the coastal wetland in Delaware are in some manner impounded (Wetlands Research Associates Inc. 1995), 3% (5200 acres) in North Carolina, 14% (70,500 acres) in South Carolina, 2% (8200 acres) in Georgia, and 16% (30,900 acres) in Florida (Montague et al. 1987).

Interest in the ecological consequences of impoundments has focused on effects on soil chemistry, biomass, nutrient fluxes and plant and microbial community changes (Montague et al. 1987; Boumans and Day 1994; Portnoy and Giblin 1997; Sturdevant 2003; Stocks and Grassle 2003). Only within the past two decades have the hydrologic and accretionary attributes of impoundments been investigated and compared natural marshes. Cahoon and Groat (1990) conducted a literature review of impoundment studies and found a lack of studies focusing on accretion and soil processes. The majority of impoundment accretion studies have been conducted on the Gulf coast of Louisiana (Cahoon and Turner 1989; Knaus and van Gent 1989; Cahoon and Groat 1990; Cahoon 1994; Reed et al. 1997). This is likely due to the fact that 280,000 acres or 19.5% of Louisiana's coastal wetlands are impounded (Day and Holz 1990).

Interest in restoration of impounded marshes has given rise to the question of whether they can survive the increased tidal flow and water levels accompanying removal of water control structures (Anisfeld et al. 1999). Impounded marshes with accretion rates lower than the rate of local sea-level rise are another restoration concern. Impounded marshes with accretionary deficits will be more susceptible to submergence and thus convert to open water if management structures fall into disrepair (Reed et al. 1997; Anisfeld et al. 1999). While there have been some studies of surface elevation and sedimentation in impoundments (Cahoon and Turner 1989; Reed 1992; Cahoon 1994; Reed et al. 1997, 1999), few studies on long-term sediment accretion have been reported in the literature (Bryant and Chabreck 1998; Anisfeld et al. 1999). The available information is summarized below.

The study of impounded marsh accretion originated on the Louisiana Chenier Plain in marshes that were hydraulically restricted by spoil banks from exploratory dredging (DeLaune et al. 1989). Researchers found that sedimentation rates were lower behind spoil banks than in nearby natural marshes (Taylor 1988; Cahoon and Turner 1989). Reed (1992) studied the effect of flow restriction on sediment deposition in Southern Terrebonne Parish, Louisiana, and found lower rates inside weirs than on the unrestricted adjacent marsh. While these studies studied sediment accretion in disturbed marshes, few have focused specifically on impounded marsh accretion.

Bouman and Day (1994) found lower rates of short-term sedimentation in impounded marshes compared to unimpounded marshes in Louisiana NWRs. Using sediment traps, Reed et al. (1997) showed that impoundments in the Mississippi Delta were deficient in mineral sediment when compared to natural reference marshes. Bryant and Chabreck (1998) measured long-term accretion using ^{137}Cs in National Wildlife Refuge (NWR) impoundments in southwestern Louisiana. They found lower surface elevations in impoundments versus natural marshes, and lower accretion rates in all impoundments versus natural marshes, except for one impoundment that remained permanently flooded. In Long Island Sound, Anisfeld et al. (1999) related the change in accretion and soil properties (bulk density, organic accumulation, and mineral accumulation) in impoundments versus previously impounded, tidally restored marshes. They found that, while mineral accumulation was similar in impounded and unimpounded marshes, organic accumulation was lower in impounded marshes. These studies have shown that accretion rates in impounded marshes are often lower than unimpounded reference marshes.

A comparison of accretion rates reported in the literature shows that rates are often lower in marsh impoundments than in nearby unimpounded marshes (See Tables 2 and 3). Accretion rates are highest on the Gulf Coast at, 0.30 – 1.1 cm y^{-1}, and are in the range of 0.35 – 0.60 cm y^{-1} on the Mid-Atlantic Coast. Impounded marsh accretion studies using the radiometric methods have determined rates of 0.29 – 0.90 cm y^{-1} in Louisiana and 0.19 – 0.39 cm y^{-1} in impounded marshes of Long Island Sound, NY.

Impoundment of Delaware Estuary marshes, primarily in the tidal fresh region, was first largely motivated by the agricultural interest of European settlers, farming *Spartina patens* (salt hay) for fodder and other crops (Daiber 1986). Today, marsh impoundments under federal, state, and private ownership are primarily managed for waterfowl habitat and mosquito control (Wetlands Research Associates Inc. 1995). The present study focuses on selected Delaware impounded marshes. The findings add to our general understanding of sediment accumulation and accretion in impounded marshes and how they differ from unimpounded marshes.

1.3 Measuring Rates of Marsh Sediment Accumulation and Accretion

Rates of marsh sediment accumulation (mass/area/time) and accretion (length/time) average over time spans ranging from storm events to millennia (Richard 1978; Plater et al. 2000), but the time spans tend to be operationally limited by a given methodology. For example, short-term deposition (tidal to months) measured using sediment traps or marker beds captures tidal, seasonal, and storm-driven conditions (Stumpf 1983; Reed 1989; Moskalski and Sommerfield 2012). Intermediate sediment accumulation (years to decades) quantified by radionuclide chronometers (e.g., ^{137}Cs and ^{210}Pb) average over short-term variations in deposition and erosion, and reflect conditions related to sea-level change, climate, and land-use practices. Long-term (centuries to millennia) rates of accumulation and accretion determined by radiocarbon dating are used to investigate marsh stratigraphy and to construct geologic records of sea-level rise, coastal change, and organic carbon sequestration (Kearney et al. 1994; Roman et al. 1997; Nikitina et al. 2000; Drexler 2011). Accretion rates averaged over long time spans are often lower than those measured over short spans for the same site, a difference which can be attributed to decomposition and compaction (DeLaune et al. 1989), but also to episodic deposition (Neubauer 2008).

This study employs excess ^{210}Pb ($t_{1/2}$=22.3 y) and ^{137}Cs ($t_{1/2}$=30.2 y) methods to measure rates of sediment accumulation and accretion averaged over the past 50–100 years. The ^{210}Pb method utilizes the specific activity (or inventory) of ^{210}Pb in the sediment column to calculate sedimentation rates (Krishnaswamy et al. 1971). The total amount of ^{210}Pb in the sediment column includes "supported" activity produced by in-situ decay of mineral-bound ^{226}Ra (a daughter of ^{238}U), and "unsupported" activity produced by ^{210}Pb fallout from the atmosphere. Atmospheric ^{210}Pb is a consequence of ^{222}Rn emanation from continental rocks ($^{226}Ra \rightarrow ^{222}Rn \rightarrow ^{210}Pb$), and upon wash-out by precipitation results in U-series disequilibrium in terrestrial soils and aquatic waters. Being particle reactive, dissolved ^{210}Pb is scavenged by suspended particles and buried via sediment accumulation (Appleby 2008). Unsupported ^{210}Pb activity present in excess of supported ^{210}Pb is known as "excess" ^{210}Pb ($^{210}Pb_{xs}$ hereafter). In soils and sediments the activity-depth profile of $^{210}Pb_{xs}$ is used for sediment chronometry. The range of this method is ~100 years (~5 half-lives) from the time of deposition, after which $^{210}Pb_{xs}$ is no longer measurable.

The ^{137}Cs geochronology method takes advantage of the fallout and burial of ^{137}Cs associated with northern hemisphere nuclear bomb testing starting around 1954 and peaking in 1963 – 1964 (hereafter, 1964); (DeLaune et al. 1978; Ritchie and McHenry 1990). Whereas ^{210}Pb gives a relative chronology referenced to the top of the sediment column, under ideal circumstances ^{137}Cs provides two absolute age markers. Sediment accumulation and accretion rates based on ^{210}Pb and ^{137}Cs methods are well-suited for direct comparison to tide-gauge records of relative sea level because they average over similar time scales of measurement (Kearney et al. 1994; Roman et al. 1997). As described earlier, the vertical movement of the crust underlying the marsh platform must be taken into consideration when comparing accretion rates to rates of relative sea-level rise.

1.4 Hypothesis

The guiding hypothesis for this research is that marsh accretion rates in the study area vary between impounded and unimpounded marshlands in ways that reflect rates of mineral and organic mass accumulation, ultimately as a consequence of sediment delivery and vegetative growth, decomposition and burial. Specifically, because of tidal restriction, accretion in marsh impoundments is limited by the supply of allochthonous mineral sediment and thus exhibit accretionary deficits with respect to the local rate of relative sea-level rise. Conversely, unimpounded marshes are not limited by mineral or organic matter and thus accrete at or above rates of relative sea-level rise.

Chapter 2

SITE DESCRIPTION

2.1 The Delaware Estuary

The marsh sites sampled for this study fringe the tidal Delaware River and its drowned river valley, the Delaware Estuary. The marshes in the river and estuary grade from tidal freshwater near the head of tides to salt at the confluence of the bay and Atlantic Ocean (Figure 3). The Holocene evolution of Delaware Estuary and its tidal marshes from the ancestral bay is marked by a northwestern migration of sediment deposition and flooding of lowlands and tributary channels (Fletcher et al. 1990). The fringing marshes formed from flooding of the Wisconsinan drainage system and sediment deposition (Kraft 1979; Knebel et al. 1988). Sea-level rise since the peak of the Wisconsin glaciation 18,000 years ago was a major influence on formation of Delaware marshes. The average rate of sea-level rise for the past 2000 years is 1.2 mm y^{-1}, determined using ^{14}C age date of basal peat deposits (Nikitina et al. 2000). The local rate of subsidence, measured in Dover, DE is ~ 4 mm y^{-1} (Davis 1987). Based on the 1956 – 2011 tide-gauge record for Reedy Point (See Figure 3 for gauge location), the rate of relative sea-level rise is higher at 3.63 ± 0.58 mm y^{-1} (*http://tidesandcurrents.noaa.gov*). Sea-level trends from tide gauges include local subsidence and thus provide trends of sea level *relative* to the eustatic sea level.

Coastal tidal wetlands make up 13% of Delaware's land area (Kraft 1979). Common vegetation in these marshes are: *Spartina alterniflora* and *S. patens* in salt marshes; *Phragmites australis*, *Distichlis spicata*, *Tyhpa anusgtifolia*, *S. cynosuroides*, and *Hibiscus moscheutos*, as well as the common salt marsh species in brackish marshes; and a larger variety of species in tidal fresh marshes (Tiner 2001). Delaware Estuary marshes are subject to semidiurnal, symmetrical tides (mean range of 1.25 m at the mouth of Delaware Bay increasing to 2.4 m at the head of tide) with strong meteorological events adding significantly to the astronomical tide (Tiner 1985). Starting with the fishing practices of the native population and continuing with European settlement to the present, wetlands of Delaware Estuary have seen a range of human impacts including development, dredging and channeling, impounding, and waste disposal (Daiber and Roman 1988; Wetlands Research Associates Inc. 1995; Tiner 2001; Philipp 2005).

2.2 Marsh Study Sites

In support of the "Coastal Impoundment Accretion Rate Study" of the Delaware Department of Natural Resources and Environmental Control (DNREC), conducted as part of the agency's sea-level rise initiative (Delaware Coastal Programs 2011), state and federally managed marsh impoundments were targeted for study by the DNREC Coastal Programs group in 2008. In coordination with DNREC, the research described in this thesis was conducted to determine the accretionary status of the marsh impoundments, and the results will be used by DNREC to devise a coastal marsh management strategy (if needed). The present research expands on the goals of the Coastal Impoundment Accretion Rate Study in that it addresses the specific influences of organic and mineral mass accumulation on measured rates of accretion. The locations of the studied marshes are shown in Figure 3. A total of three sediment cores were collected at each marsh location unless otherwise noted.

2.2.1 Brackish Marshes Sites

2.2.1.1 Lukens Marsh

Lukens Marsh is a brackish marsh located in New Castle County south of Wilmington, Delaware (Figure 4).

2.2.1.2 Rivers Edge Marsh

Rivers Edge Marsh is a brackish marsh located in New Castle County south of Wilmington, Delaware (Figure 5).

2.2.1.3 Blackbird Creek Marsh

The Blackbird Creek Reserve, an inland reserve located about ~9 km from Delaware Estuary, was formed in 1993 as the 22^{nd} reserve by the National Oceanic and Atmospheric Administration (NOAA) (Delaware National Estuarine Research Reserve 1999). The Reserve's 4.8 km^2 area is situated on 9.2 km of Blackbird Creek, a tidal creek of the Delaware Estuary that varies from low-salinity brackish to freshwater. The Blackbird Creek NERR watershed is mostly agricultural (39%) or forested (22%) with residential development on the rise. Wetlands and forestlands account for 25% and 22% of watershed land cover, respectively. *Spartina alterniflora* is the dominant vegetation cover (29%). Because of the low salinity waters in the wetlands of the reserve, vegetation is diverse (Delaware National Estuarine Research Reserve 1999). Two cores were collected from the western end of the NERR (Figure 6).

2.2.1.4 Buttonwood Marsh

Just downriver from Lukens Marsh, Buttonwood is an impounded marsh by a 460 m long dike and is separated from Broad Dyke by an industrial park (Figure 7).

This impoundment was equipped with tidal flap gates since 1950. In 2011, after core collection, the flap gates were replaced with a self-regulating tidegates that allow for tidal flushing.

2.2.1.5 Broad Dyke Marsh

Broad Dyke is impounded by a 340 m dike (Figure 8). Perhaps one of the oldest impounded marshes in the United States, this marsh was diked in 1655 by Dutch settlers. Previously managed as a freshwater impoundment with water only flowing out, automated tide gate was installed in 1995 to assist in *Phragmites* control.

2.2.1.6 Gambacorta Marsh

Located between the natural marsh sites of Lukens Marsh and Rivers Edge, Gambacorta Marsh is impounded by an 800 m long dike (Figure 9). This 41 acre marsh is adjacent to the Delaware River and bordered by urban development and commercial parks on the remaining sides. Previously used for waste disposal, the site has been a focus of the DNREC Division of Fish and Wildlife's restoration efforts (Delaware Division of Fish & Wildlife 2001).

2.2.2 Salt Marsh Sites

2.2.2.1 Pickering Beach Marsh

This unimpounded marsh is located south of Little Creek and north of Ted Harvey Conservation Area (Figure 10).

2.2.2.2 Little Creek Marsh

Little Creek site is the south impoundment unit (Little Creek Impoundment) of the Little Creek State Wildlife Area (Figure 11). It provides habitat for waterfowl, land birds, and shorebirds. Up until the late 1980s, brackish estuary water, not freshwater, was used to manipulate water levels in this impoundment. This management, contrary to other impoundments managed with freshwater, maintained salt and brackish marsh vegetation. Now, water level management is achieved by freshwater input with some tidal flushing is used.

2.2.2.3 Port Mahon Marsh

Port Mahon is the northern impoundment unit in Little Creek State Wildlife Area and provides waterfowl, land bird, and small game habitat (Figure 12). It is located east of the Dover Air Force Base, directly adjacent to fuel tank farms. In a similar fashion to Little Creek impounded marsh, this impounded marsh was managed with estuary water and now primarily with freshwater.

2.2.2.4 Ted Harvey Conservation Area

Ted Harvey Conservation Area is composed of two adjacent impounded units (Figure 13). A total of six cores were collected, three in each unit. This site is just shoreward of the St. Jones NERR, the southern counterpart of the Blackbird Creek NERR, and is renowned among bird-watching enthusiasts. Ted Harvey impoundment has been managed the same way as the Little Creek impounded marsh.

2.2.2.5 Prime Hook National Wildlife Refuge

Prime Hook National Wildlife Refuge was established in 1963 and is composed of four units on ~40 km^2 managed by the U.S. Wildlife and Fisheries Service (Figure 14). The freshwater impoundment Units II and III were constructed in 1988 to create habitat for migratory waterfowl while Units I and IV remained tidal salt marshes (U.S. Fish and Wildlife Service 2010). Prime Hook has seen human influence in the form of mosquito ditching and invasions of *Phragmites*. Its recent ecological history and current management issues make it an instructive case study for understanding how wetland management practices affect marsh sediment transport and accretion. Tidal Unit I and impounded Unit II make up the north of the Refuge (Figure 15), whereas impounded Unit III and tidal Unit IV make up the south of the Refuge (Figure 16).

In 2010, the U.S. Fish and Wildlife Service released an environmental assessment concerning the restoration of a dune that was breached during back-to-back Nor'easters in late 2009. Two breaches of the barrier beach between Delaware Bay and Unit II restored tidal flow, killing ~80 % of the freshwater vegetation (Prime Hook National Wildlife Refuge 2010). Most recently, a draft comprehensive conservation planning document released by the refuge outlines various management plans (Prime Hook National Wildlife Refuge 2012). Regardless of the plan chosen, understanding of the accretionary status of the impounded and unimpounded units will help managers plan the habitat type and land use of the marsh units.

Chapter 3

METHODS

3.1 Site Selection

Marsh coring sites were selected by DNREC Coastal Programs. According to DNREC, “Sites were chosen within impounded and reference (natural marsh) sites throughout the State based upon a wetland area change analysis (using a time-series of available imagery), and basins that have been identified as needing detailed study to aid in their management to optimize the future available habitat (Delaware Coastal Programs 2011).” Dr. Sommerfield’s lab at the University of Delaware, School of Marine Science and Policy, was contracted to perform radionuclide measurements for cores collected by Coastal Programs staff. The radionuclide data form the basis of the research described in this thesis.

3.2 Marsh Core Collection

Cores were collected between November 2008 and August 2011. Core barrels were prepared using 4” PVC pipe cut to ~1.5 m lengths, and collected by pressing or driving the barrel by mallet into the marsh surface. The liner and intact core was retrieved using a tripod-mounted winch. Cores were then plugged and capped to preserve the integrity of the core and prevent porewater loss. Three cores were collected at eight of the eleven impoundment sites: twelve cores at the Prime Hook NWR (three cores per unit), six cores at the Ted Harvey Conservation Area (three in each impoundment), and two cores at the Blackbird Creek NERR.

After collection, cores were extruded vertically and subsampled in 2-cm thick intervals. Samples were either immediately dried or refrigerated until further analysis in the lab. ^{210}Pb and ^{137}Cs activities, water content, and loss-on-ignition (LOI) were determined on every other sample interval (i.e., 0–2 cm, 4–6 cm, 8–10 cm), which provided sufficient resolution for radionuclide geochronology. For calculating radionuclide inventories, activities and bulk density were interpolated over skipped intervals using a cubic spline function.

3.3 Physical Properties

Physical properties of the sediment aid in interpretation of the radionuclide profiles and can be used to infer changes in sediment accumulation and marsh accretion. A total of 647 samples were processed for water content and LOI analysis. Water content was determined gravimetrically by drying samples ~24 h at 100°C (Bennett and Lambert 1971). In order to determine the amount of organic matter in the samples, LOI was measured by combusting ~4 g of sediment powder in a muffle furnace at 550°C for 4 hours (Heiri et al. 2001). The mass of the residual ash was taken as the amount of non-combustible mineral sediment in the sample.

Water content and LOI can be used to determine porosity and bulk density of the core subsamples. Fractional porosity (ϕ) was calculated as follows:

$$\phi = \frac{WC * \rho_s}{WC * \rho_s + (1 - WC)\rho_w} \qquad 1$$

where WC is water content, ρ_s is the density of solids, and ρ_w is the density of the porewater.

The dry bulk density (ρ_d) of the sediment was calculated as:

$$\rho_d = (1 - \phi) * [(LOI * \rho_{org}) + ((1 - LOI) * \rho_{min})] \qquad 2$$

where *LOI* is the fractional mass lost on ignition, ρ_{org} is the assigned density of organic solids (1.15 g cm^{-3}), and ρ_{min} is the assigned density of mineral solids (2.65 g cm^{-3}).

To determine the volumetric composition of the sediment column, the specific volume of water (V_w), mineral solids (V_{min}) and organic solids (V_{org}) was calculated as follows:

$$V_t = V_w + V_{min} + V_{org} \quad (3)$$

where V_t is the total volume, V_w is equivalent to ϕ, and V_{min} and V_{org} are calculated as the mass of solids divided by density. Physical property data for skipped core intervals were interpolated by cubic spline.

Mineral sediment and organic matter inventories (g cm^{-2}) above the 1964 ^{137}Cs age horizon were calculated for the cores to compare the relative proportions of mineral and organic solids buried among sampling sites. The 1964 horizon was not identified in all cores, so when not present the 1964 age-depth value was interpolated using accretion rates based on $^{210}Pb_{xs}$ chronology.

3.4 Radionuclide Measurements

A total of 580 subsamples from 44 cores were analyzed for radionuclide activity. These samples were prepared by packing dry sediment powder into 60-ml volume plastic jar using a plastic tamp and rubber mallet. Jars were filled to a height of 1 cm above the bottom when enough material was available, or half the jar height in the case of smaller samples. The counting geometry of all samples was identical to that of the standard reference material used for calibration of the gamma detectors. For this study the National Institute of Standards and Technology (NIST) Standard Reference Material 4357: Ocean Sediment Environmental Radioactivity Standard was used for detector calibration (Inn et al. 2001). This natural matrix reference material has physical properties similar to the marsh sediments investigated in this study.

Samples were counted for 24 h on one of two Canberra Model 2020 low-energy Germanium detectors connected to a Canberra Model 1720 Desktop Inspector. Activities of the following radionuclides were determined: ^{210}Pb (46.5 keV), ^{226}Ra (186.1 keV), ^{214}Pb (351.9 keV), ^{214}Bi (610.0 keV) and ^{137}Cs (661.7 keV). An example gamma spectrum with the peaks of interest is shown in Figure 19. The NIST radionuclide standard SRM 4357 was used to create a calibration curve for various sample weights and geometries. This natural-matrix standard was presented to the detectors in the same geometry as the core samples, eliminating the need for a separate correction for ^{210}Pb self-absorption.

The minimum detectable activity (MDA), the smallest significant count that could be detected, is a statistic based on the methods used and is unique to any gamma spectroscopy scheme (Gilmore 2008). For this study the average MDAs for ^{210}Pb and ^{137}Cs were 3.0 ± 0.1 mBq g^{-1} and 2.7 ± 0.001 mBq g^{-1}, respectively. Uncertainties in activity concentration are reported in this thesis as the 1 σ error (Gilmore 2008).

In order to calculate ^{210}Pb$_{xs}$ from the total activity, the ^{226}Ra parent activity was calculated by deconvolution of the ^{226}Ra-^{235}U doublet photopeak (^{226}Ra at 186.1 keV and ^{235}U at 185.7 keV appear as one peak on gamma spectra) following a method outlined by Gilmore (2008). In this method a correction factor of 0.571 is applied to the doublet to account for interference by ^{235}U, assuming a natural ^{235}U/^{238}U ratio and secular equilibrium of ^{226}Ra with ^{238}U. In all cases, ^{226} Ra activity determined in this manner converged with the activity of supported ^{210}Pb at depth in the cores (below the upper zone of excess activity), confirming that these assumptions were met. As this method does not involve ^{222}Rn progeny, loss of ^{222}Rn from the sample is not an issue (Zhang et al. 2009). The uncertainty reported for ^{226}Ra activity concentration is based on the background error of the entire ^{226}Ra-^{235}U doublet.

3.5 Radionuclide Profiles and Inventories

Accretion rates derived from ^{137}Cs measurements were based on age-depth relationship of the 1964 fallout peak in the sediment column.. The 1954 reference age-depth is less desirable due to the low level of 1954 fallout, loss of ^{137}Cs by decay, possible “tailing” due to plant bioturbation (Delaune et al. 1978). It was not used in this study. The ^{137}Cs accretion rate is calculated as follows:

$$S = \frac{T_C - T_H}{z} \qquad 6$$

where S is the linear sedimentation rate (accretion rate in this study), T_C is the year of sample collection, T_H is 1964, the reference year of interest, and z is the depth of the reference horizon.

The Constant Initial Concentration (CIC) model was used determine accretion rates from activity-depth profiles of $^{210}Pb_{xs}$ (Robbins 1978). The CIC model specifies that the initial concentration of $^{210}Pb_{xs}$ is constant and does not vary with changes in sediment accumulation (open system). The model is described as:

$$C_z = C_0 e^{-\lambda t} \qquad 7$$

where C_z is the specific activity of $^{210}Pb_{xs}$ (mBq g^{-1}) at depth z, C_0 is the initial specific activity of $^{210}Pb_{xs}$, λ is the decay constant (0.0311 y^{-1} for ^{210}Pb), and t is time in years. From the CIC model an average accretion rate can be calculated from the slope of a regression of specific activity versus depth, substituting z/S for t in Eq. 7:

$$S = \frac{-\lambda z}{\ln(C_z/C_0)} \qquad 8$$

where S is the accretion rate and z is the length (cm) of sediment column between C_0 and C_z. The $^{210}Pb_{xs}$ value at the bottom of the surface mixed layer (if present) was used as the initial concentration. As with the ^{137}Cs rates, accretion rates calculated using the CIC model were multiplied by accumulated mineral and organic mass (g cm^{-2}) to compute mass accumulation rates (g cm^{-2} y^{-1}).

In this study radionuclide inventories were used to examine the completeness of the sedimentary record, and the relative proportions of direct atmospheric and tidal sources of ^{137}Cs and ^{210}Pb delivery to the marsh platform. Inventories of ^{137}Cs and $^{210}Pb_{xs}$ where calculated by integrating the specific activity over the depth profile:

$$I = \sum_{i=1}^{z} \rho_{si} x_i C_i \tag{9}$$

where, I is the radionuclide inventory (mBq cm^{-2}), ρ_s is the dry bulk density (g cm^{-3}), x is the thickness of the core interval in cm (2 cm for all cores), C is the specific activity (mBq g^{-1}) and i indicates the ith interval down core. Statistical Methods

Statistical analysis was applied to accretion rates to determine (1) if the ^{137}Cs and $^{210}Pb_{xs}$ methods estimated the same accretion rates and (2) if the accretion rates calculated in impounded marshes are lower than those from unimpounded marshes. The former objective was evaluated comparing the ^{137}Cs and $^{210}Pb_{xs}$ accretion rates from each core using a two-tailed, paired *t*-test at the 95% confidence interval. The latter objective was evaluated by means of unbalanced, mixed nested analyses of variance (ANOVA) (Logan 2010). Marsh sites were separated into two types: impounded and unimpounded and the accretion rates were nested inside of their respective site (*Type* (fixed) -> *Site* (random) ->*Accretion* (response)). This same ANOVA model was used to determine if mineral and organic inventories were different in impounded and unimpounded marshes.

3.6 Computer Software

The R statistical package and following add on packages were was utilized for mapping, plotting and statistical analysis: maps, maptools, PBSmapping, Rgooglemaps, rgdal, sp gdata, gplots, plotrix, PBSmapping, and nlme package (*http://www.r-project.org/*).

Chapter 4

RESULTS AND INTERPRETATION

4.1 Physical Properties Profiles and Correlations

Physical properties data for all cores are presented in Appendix A. Sediment water content in the unimpounded marshes sampled ranged from 13 to 92 % (by weight) and, for impoundments, ranged from 8 to 94 %. These values are consistent with observations from other studies show that the marsh sediment column is primarily composed of water (Bricker-Urso et al. 1989). Fractional porosity ranged from 0.49 to 0.95 for unimpounded marshes and 0.19 to 0.94 impounded marshes.

LOI values ranged from 6 to 79 % in core samples from unimpounded marshes and from 2 to 84 % in impounded marshes. LOI correlated directly with water content (Figure 18) and inversely with dry bulk density (Figure 19). Unimpounded brackish marsh samples had the lowest range of LOI values and dry bulk densities (Figure 19, Panel B). The lowest LOI and bulk density values were associated with samples from impounded salt marshes (Figure 19, Panel C). The range of LOIs is similar to that reported by others for estuarine and coastal marshes (Bricker-Urso et al. 1989; Kim et al. 1997; Stuart 2010). The strong correlation between LOI and water content suggests that a substantial fraction of water in the sediment column is associated with organic matter and is not merely held within interconnected pore space between solids. This relationship has been observed previously in organic-rich marshes where the sediment is composed mostly of organic matter (Bricker-Urso et al. 1989).

Selected profiles of volume composition and LOI are discussed here to emphasize the broad range of variability among the coring sites. Core NCRE-2 from River's Edge showed a sediment profile with organic volume remaining fairly uniform and mineral volume increasing downcore with decreasing water content (Figure 20). The sediment column is mostly composed of water, ranging from ~ 80 % near the surface and 65 % in the bottom part of the core. The LOI profile indicates an organic content of over 20 % (by mass) above 22 cm, decreasing to 10 % down to 89 cm. In the uppermost sediment column the organic fraction (composed of mostly living biomass) resists compaction and creates a matrix for both mineral sediment and water. This is one reason why the organic matter volume remains largely invariant while the organic mass (LOI values) decreases. In the case of mineral sediment, it is compacted and dewatered under the weight of the overlying column thereby increasing the mineral volume relative to water volume. This core is representative of the other cores collected from unimpounded brackish marsh sites.

The two impounded and unimpounded marsh units at Prime Hook NWR exhibited a wide range in volume composition and LOI values. Core PM-4 (from impounded Unit II) had high organic content at the surface, but below 10 cm depth it changed abruptly with increasing mineral volume and decreasing water content (Figure 21), a change most likely related to changing sedimentation conditions after impoundment of the unit in 1988. The large variability in mineral volume in this profile is representative of the other cores collected from impounded salt marshes.

In contrast, the composition of core PM-10 (from unimpounded Unit IV) was characteristic for a salt marsh with low mineral volume compared to organic volume and high water volume down-core (Figure 22). In general, salt water marshes have a large below ground biomass with *Spartina patens* rhizomes extending as far as ~ 30 cm below the surface, and as far as ~50 cm in the case of *Phragmites australis*, which favors tidal fresh to brackish waters (Windham 2001). As described in NCRE-2, living roots resist compaction as the sediment layers are buried.

Down-core mineral sediment and organic matter inventories were integrated from the surface to the depth coinciding with the year 1964 based on ^{137}Cs activity peak. When no peak was present, the depth of the 1964 reference year was computed using the accretion rate given by $^{210}Pb_{xs}$ chronologies (see Table 1). Organic matter inventories for cores from unimpounded marshes ranged from 0.86 to 4.65 g cm^{-2} and averaged 2.68 ± 1.25 g cm^{-2}. For cores from impounded marsh sites, organic matter inventories ranged from 0.47 to 3.00 g cm^{-2} and averaged 1.43 ± 0.71 g cm^{-2}. Mineral sediment inventories from cores collected in unimpounded marshes ranged from 0.45 to 3.00 g cm^{-2} and averaged 10.40 ± 8.42 g cm^{-2}. For cores from impounded marshes, mineral sediment inventories ranged from 0.61 to 7.80 g cm^{-2} and averaged 3.97 ± 2.44 g cm^{-2}. Overall, the three cores from each marsh location exhibited similar mineral and organic inventories.

4.2 ^{137}Cs and $^{210}Pb_{xs}$ Activities and Inventories

All cores obtained for this study contained ^{137}Cs activity above the detection limit and $^{210}Pb_{xs}$ with depth. The 1964 ^{137}Cs fallout peak was identified in all 17 cores from unimpounded marshes and in 20 of the 27 cores from impounded marshes. In 16 cores from unimpounded marshes and 21 cores from impounded marshes, $^{210}Pb_{xs}$ exhibited a monotonic decrease in activity with depth. For these cores the profiles were linearly regressed for accretion rate determination following Equation 8.

Radionuclide profiles for all cores are presented in Appendix C and the original data in Appendix B. Profiles of interest are discussed below.

Core NCRE-2 from the River's Edge unimpounded marsh displayed a complete ^{137}Cs burial record and a steady-state distribution of $^{210}Pb_{xs}$ (Figure 20). The ^{137}Cs profile had a distinct peak (1964) at ~37 cm. The ^{137}Cs profile exhibited tailing at the base of the profile, and near the surface the activity dropped to below MDA. The tailing is interpreted to be a consequence of downward mixing by plants roots (DeLaune et al., 1978) and perhaps benthic infauna (Olsen et al. 1981).

Core LC-1 from the Little Creek impounded marsh demonstrates the usefulness of using both ^{137}Cs and ^{210}Pb in accretion studies (Figure 23). There was no distinct peak in the ^{137}Cs profile to use in calculation of accretion and accumulation rates, and the up-core trend in activity is suggestive of resedimentation of ^{137}Cs reworked from other sites. In this case, the $^{210}Pb_{xs}$ profile was used to calculate accretion for the core, which was 0.48 cm y^{-1}.

Inventories of $^{210}Pb_{xs}$ and ^{137}Cs were calculated for forty-three and forty-two cores, respectively (see Table 1). The range of inventories for both nuclides were similar for both unimpounded and impounded marsh cores (Figure 24). The ^{137}Cs inventories ranged from 27.8 to 425.9 mBq cm^{-2} and averaged 203.7 ± 86.4 mBq cm^{-2}. The $^{210}Pb_{xs}$ inventories ranged from 139.2 to 1499.0 mBq cm^{-2} and averaged 710.9 ± 323.20 mBq cm^{-2}. Thirty-three of the cores had $^{210}Pb_{xs}$ inventories that were higher than the theoretical inventory supported for by atmospheric deposition (327 – 523 mBq cm^{-2}) based on flux measurements reported by Graustein and Turekian (1986). Similarly, many of the ^{137}Cs inventories met or exceeded atmospherically sourced reference inventories decay corrected to the years of the present study (82 – 250 mBq cm^{-2}); (Graustein and Turekian 1986). This suggests that there exist non-atmospheric sources of ^{137}Cs and ^{210}Pb to the study locations, presumably tidal or watershed influx of radionuclides associated with mobile sedimentary particles and redistributed soils, in the case of ^{137}Cs.

4.3 Mass Accumulation Rates

Accumulation rates determined for all cores are tabulated in Table 1. There was good agreement between mineral and organic accumulation rates determined by the ^{137}Cs and $^{210}Pb_{xs}$ methods (Figure 25). Comparison of the ^{137}Cs and $^{210}Pb_{xs}$ methods showed no difference in mineral mass accumulation (paired *t*-test: $t(28) = 0.35$, two-tailed, $p = 0.73$) but slightly higher rates of organic mass accumulation for the ^{137}Cs method, 0.01 g cm^{-2} y^{-1} on average (paired *t*-test: $t(28) = 2.44$, one-tailed, $p = 0.01$). Although the minimum values of mineral accumulation for unimpounded and impounded marsh were similar, the unimpounded marshes had higher rates overall. Organic accumulation was also higher in the unimpounded marshes than in impounded marshes.

Based on the ^{137}Cs chronology, mineral accumulation in unimpounded marshes ranged from 0.01 to 0.54 g cm^{-2} y^{-1} and averaged 0.22 ± 0.18 g cm^{-2} y^{-1}. Mineral accumulation in impounded marshes ranged from 0.01 to 0.18 g cm^{-2} y^{-1} and averaged 0.08 ± 0.05 g cm^{-2} y^{-1}. Organic accumulation in unimpounded marshes ranged from 0.02 to 0.10 g cm^{-2} y^{-1} and averaged 0.06 ± 0.03 g cm^{-2} y^{-1}, and in impounded marshes ranged from 0.01 to 0.07 g cm^{-2} y^{-1} and averaged 0.03 ± 0.02 g cm^{-2} y^{-1}.

For unimpounded marshes, organic accumulation rates reported in the literature for Gulf Coast and East Coast marshes ranged from 0.01 to 0.19 g cm^{-2} y^{-1}, which captures the range presented in this study, but the upper limit of organic accumulation rates presented here fall above the maximum found in U.S. Northeast marshes and near the median of U.S. Southeast marshes (Neubauer 2008). Mineral accumulation rates reported in the literature for Gulf Coast and East Coast marshes ranges from 0.01 to 0.79 g cm^{-2} y^{-1} (Neubauer 2008). The mineral accumulation rates from this study fall within the literature range similarly to the organic accumulation rates described above.

Anisfeld et al. (1999), working in Long Island Sound, measured rates of organic accumulation of 0.023 ± .004 g cm^{-2} y^{-1} and mineral accumulation of 0.10 ± 0.02 g cm^{-2} y^{-1} in impounded marshes. The organic accumulation rates of Anisfeld et al. (1999) are comparable to those of this study, but the mineral accumulation rates are above the average. The authors attributed high rates of mineral accumulation in impounded marshes to a combination of water level management and low surface elevation. Bryant and Chabreck (1998) using similar radionuclide methods found organic mass accumulation was higher in unimpounded marshes than impounded marshes. The rates of accumulation presented here for Delaware impounded marshes are ~10 times lower than those measured in the impounded units of NWRs in southwestern Louisiana (Bryant and Chabreck 1998).

4.4 Accretion Rates

Accretion rates for all of the cores examined for this study are listed in Table 1. Comparison of accretion rates calculated using ^{137}Cs and $^{210}Pb_{xs}$ methods shows close agreement between the two approaches (Figure 26). The agreement of the accretion methods was further analyzed using paired *t*-test. For the cores with accretion rates calculated from both ^{137}Cs and $^{210}Pb_{xs}$ methods, no statistical difference between the rates from the two methods was found (paired *t* test: $t(30) = 1.38$, two-tailed, $p = 0.176$).

Accretion rates for unimpounded marshes ranged from 0.20 to 1.07 cm y^{-1} (0.57 ± 0.28 cm y^{-1} mean) using the ^{137}Cs method, and from 0.26 to 0.97 cm y^{-1} (0.50 ± 0.19 cm y^{-1}) using $^{210}Pb_{xs}$. For impounded marshes, accretion rates ranged from 0.11 to 0.72 cm y^{-1} (0.25 ± 0.16 cm y^{-1}) and from 0.10 to 0.87 cm y^{-1} (0.30 ± 0.17 cm y^{-1}) based on ^{137}Cs and $^{210}Pb_{xs}$, respectively. Overall, accretion rates were highest for impounded and unimpounded marshes in the brackish marsh region of the Delaware Estuary.

Accretion rates for unimpounded marshes were generally higher than for the impounded marshes (Figure 27). Statistical analysis shows that accretion rates for unimpounded sites were significantly higher than rates from impounded sites based on unbalanced, mixed nested ANOVA (^{137}Cs accretion: $F_{1,12} = 7.83$, $p = 0.016$ and $^{210}Pb_{xs}$: $F_{1,12} = 9.01$, $p = 0.011$). Impounded marshes having accretion rates lower than unimpounded reference marshes is consistent with impounded marsh accretion studies (Bryant and Chabreck 1998; Anisfeld al. 1999). In order shed light on why accretion rates are lower in impounded marshes, the contributions of organic and mineral mass are examined.

Chapter 5

DISCUSSION

5.1 Organic versus Mineral Contributions to Accretion

The process of marsh accretion involves organic and mineral mass accumulation, which are well-known to be interrelated at some level. Researchers have sought to determine the specific contributions of organic and mineral mass accumulation to accretion by regression analysis of radiometrically determined accumulation and accretion rates (Bricker-Urso et al. 1989; Nyman et al. 1993; Turner et al. 2000; Chmura and Hung 2004). A similar regression analysis approach was employed in this study. The main questions to address are: 1) how does accumulation differ in unimpounded and impounded marshes; and 2) how are mass accumulation and accretion related in these systems? Recalling that rates of mineral and organic accumulation and accretion were higher in unimpounded marshes, it stands to reason that accretion in impounded marshes might be limited by mineral and (or) organic mass accumulation.

Organic accumulation is a consequence of both deposition of detrital organic matter and stem and leaf litter and burial of living and dead belowground biomass (i.e., root material). Together, these pools comprise the organic inventory of the sediment column. This organic inventory, or accumulated organic mass, showed a strong relationship with accretion rates for both the unimpounded and impounded marshes examined in this study. Unimpounded and impounded marshes exhibited nearly identical regression trendline slopes (Figure 28), suggesting that accretion in both types of marshes responds similarly to organic mass accumulation. Regression analysis indicated that accretion is also related to mineral sediment accumulation (Figure 28), but that the rate of accretion is more sensitive to organic accumulation than to mineral accumulation.

Mineral accumulation, a result of suspended mineral sediment deposition from tidal water, creates the mineral inventory of the sediment column. This mineral inventory, or accumulated mineral mass, is highly correlated with accretion rates in unimpounded marshes ($R^2 = 0.82$, Figure 28). The correlation for impounded marshes is much weaker, $R^2 = 0.23$, and suggests that accumulation of mineral mass alone does contribute to accretion observed in these systems, at least to the same extent as in impounded marshes. The reduced or nonexistent allochthonous sediment supply in impounded marshes (due to tidal restriction) may explain the difference.

Results of regression analysis for unimpounded marsh accumulation and accretion for this study are similar to previous findings discussed previously for U.S. Gulf and East Coast marshes. Regression relationships between mass accumulation and accretion have been found to vary geographically and usually do not hold for tidal freshwater marshes (e.g. Neubauer, 2008). Nonetheless, regression relationships reported in the literature are broadly similar to those presented herein for Delaware Estuary brackish and salt marshes. The main similarities between the present results and those shown through research elsewhere are as follows: 1) accretion is more sensitive to organic mass accumulation than mineral mass accumulation; 2) organic mass accumulation explains more of the variability in accretion rates than mineral mass accumulation; and 3) mineral and organic mass accumulation are positively correlated.

As noted above regression analysis suggests that mineral and organic mass accumulation rates are at some level interrelated in unimpounded marshes but to a lesser extent in impounded marshes (Figure 29). Indeed, there appears to be no statistically significant relationship of accumulated organic and mineral mass in impounded marshes (R^2 = 0.13), perhaps due to a lack in feedback between mineral and organic accumulation. For example, plants trap mineral material and contribute to sedimentation (Leonard et al. 2002), and minerals provide nutrients to marsh plants and provide a substrate on which plants grow.

The regression analysis further suggests that impounded marshes have the potential to accrete in the same manner as their unrestricted counterparts. Moreover, the strong relationship between accumulated organic and mineral mass (see Figure 29) suggests the two are coupled in unimpounded marshes, perhaps by a feedback loop involving plant growth, sediment trapping and deposition, and mass accumulation.

To summarize, three conclusions regarding relations between mass accumulation and accretion are as follows: 1) organic accumulation is requisite for brackish and salt marsh accretion in the Delaware Estuary because it sets the lower limit of the accretion rate; 2) mineral sediment accumulation contributes to accretion and determines the upper limit of the accretion rate; and 3) mineral sediment deficiency in marsh impoundments, perhaps due to tidal restriction and sediment delivery (among other factors such as plant destruction by migratory waterfowl and dewatering and decomposition associated with impoundment), reduces the accretion rate compared to unimpounded marshlands.

5.2 Accretion Rates and Relative Sea-level Rise

Rates of brackish and salt marsh accretion for the unimpounded sites considered in this study are comparable to similarly measured rates reported for other U.S. East Coast marshes (Table 2). Accretion rates rate based on ^{137}Cs and ^{210}Pb chronology are generally on the order 0.35 – 0.50 cm y^{-1}, with some of the variability related to methodological differences and spatial variability within and among sampling locations.

Interestingly, rates of impounded marsh accretion are consistently lower than that of unimpounded marsh across different geographic regions (Table 3), although, there are some regional differences. For example, East Coast marsh impoundments exhibit lower accretion rates more so than for impoundments in Louisiana. This is most likely due to differences in management practices, mineral sediment supply during storms, and length of the plant growth season.

A concern among coastal managers in Delaware is the rate of impounded marsh accretion, specifically, whether accretion occurs at pace with relative sea-level rise. In Figure 30 rates of accretion measured at all of the study sites are plotted along with the estuary-wide mean rate of relative sea-level rise. As shown in the figure, most of the impounded marshes display an apparent accretionary deficit with respect to local sea level rise. The Blackbird Creek NERR and Prime Hook NWR Units I and IV are the only unimpounded sites that exhibit an accretionary deficit. The accretion rates determined for the Blackbird Creek NERR are lower than most of the impounded marshes examined in this study, perhaps because this site is most distal from the main source of fine-grained sediment, the Delaware Estuary. The Prime Hook NWR unimpounded units have been previously managed for mosquito control, and accretion there is most likely affected by the neighboring impounded marsh. In exclusion of the

Blackbird Creek NERR and Prime Hook locations, the other unimpounded marshes examined in this study appear to be “keeping up” with relative sea-level rise.

Chapter 6

CONCLUSIONS

In this study radiometrically determined rates of sediment accumulation and accretion in brackish and salt marshes of the Delaware Estuary were measured in order to examine the accretionary status of historically impounded marshlands. Specific objectives were to quantify rates of mineral and organic mass accumulation averaged over the past several decades, and assess whether deficiencies in mass accumulation have limited marsh accretion overall. The major conclusions of this study are listed below:

1. The 1964 peak of ^{137}Cs and the $^{210}Pb_{xs}$ CIC modeled rates of accretion and accumulation were largely in agreement
2. The rates of accumulation and accretion measured in this study were similar to other U.S. East Coast marshes
3. Both mineral and organic mass accumulation rates were higher in unimpounded marshes than impounded marshes
4. Impounded marshes exhibited the a similar direct relationship between accretion and accumulated organic mass as unimpounded marshes with accretion limited by mineral accumulation
5. The unimpounded marshes appear to be “keeping up” with relative sea-level rise while the impounded marshes are currently in a state of accretionary deficit.

Future studies on tidal freshwater marshes of the Delaware Estuary could provide further information on the controls on accretion in impounded marshes because, like the impoundments, the tidal fresh marsh are typically highly minerogenic as opposed to the organogenic brackish and salt marshes of the lower estuary. In order to further understand Delaware Estuary marsh morphology in response to human intervention and sea-level rise, elevation surveys and studies of short-term deposition could give insight into the effects of topography, sediment delivery, tidal processes, and variations in accretion on various timescales.

Based on the conclusions of this study, impounded marshes in Delaware should have a sediment management plan incorporated into their management goals. Over the next 50 – 100 years, the marshes investigated may be lower than mean sea level unless the accretionary deficit is mitigated by increased mineral sediment accumulation. As experienced recently in Prime Hook NWR, over topping or destruction of impoundment structures have potential to inundate other impounded marshes in Delaware. The intrusion of salt and increased tidal flooding will likely overwhelm the vegetation and impounded marshes will revert to open water. Impounded marshes with seasonal operation of tidal gates have been shown to have similar mineral accumulation rates to reference marshes (Anisfeld et al. 1999). Additionally, thin-layer application sediment emplacement in the marshes could be a viable method to promote growth (e.g. Ray 2007). Use of material removed through maintenance dredging of the Delaware Estuary shipping channel might be one option. Managers should consider ways of diverting sediment-rich tidal water into impounded marshes, either on a schedule or permanently, and evaluate the response of these systems before shoreline erosion and increase storm frequency destroy these valuable resources.

TABLES & FIGURES

Table 1: **Accumulation rates, accretion rates, and radionuclide inventories.**

Core	Site[a]	Year[b]	Accretion (cm y^{-1})		Mineral Accumulation (g cm^{-2} y^{-1})		Organic Accumulation (g cm^{-2} y^{-1})		Radionuclide Inventory (mBq cm^{-2})		Accumulated Mass Since 1964 (g cm^{-2})	
			^{137}Cs	$^{210}Pb_{xs}$	^{137}Cs	$^{210}Pb_{xs}$	^{137}Cs	$^{210}Pb_{xs}$	^{137}Cs	$^{210}Pb_{xs}$	Organic	Mineral
BBRC1	U	2009	0.29	0.6	0.09	0.21	0.03	0.06	199.4	1112.3	1.34	4.19
BBRC2	U	2009	0.20	0.72	0.09	0.22	0.02	0.08	213.1	571.4	0.86	4.05
LC1	I	2011	---	0.48	---	---	---	---	101.2	927.7	2.08	7.44
LC2	I	2011	0.28	0.32	0.10	0.10	0.02	0.02	183.4	530.1	0.89	4.86
LC3	I	2011	---	0.29	---	0.09	---	0.03	127.3	847.3	1.66	6.18
MH1	I	2011	---	0.32	---	0.09	---	0.03	27.8	471.2	1.46	5.69
MH2	I	2011	---	0.19	---	0.16	---	0.02	192.7	1162.9	1.31	7.81
MH3	I	2011	0.11	0.18	0.02	0.03	0.01	0.01	73.7	232.7	0.47	1.15
NCBD1	I	2011	0.28	0.22	0.04	0.13	0.04	0.02	171.2	672.3	1.79	1.71
NCBD2	I	2010	0.54	0.23	0.17	0.1	0.05	0.02	229.5	708.6	2.30	7.77
NCBD3	I	2010	0.37	0.24	0.05	0.11	0.05	0.03	171.3	903.5	2.40	2.07
NCBW1	I	2010	0.28	0.26	0.13	0.21	0.05	0.03	275.4	1359.8	2.24	6.19
NCBW2	I	2010	---	---	---	---	---	---	172.6	139.2	---	---

Table 1 continued

Core	Site[a]	Year[b]	Accretion (cm y^{-1})		Mineral Accumulation (g cm^{-2} y^{-1})		Organic Accumulation (g cm^{-2} y^{-1})		Radionuclide Inventory (mBq cm^{-2})		Accumulated Mass Since 1964 (g cm^{-2})	
			^{137}Cs	$^{210}Pb_{xs}$	^{137}Cs	$^{210}Pb_{xs}$	^{137}Cs	$^{210}Pb_{xs}$	^{137}Cs	$^{210}Pb_{xs}$	Organic	Mineral
NCBW3	I	2010	0.28	---	0.18	---	0.03	---	266.7	660.1	---	---
NCGB1	I	2010	0.72	0.87	0.14	---	0.07	---	258.7	796.4	3.00	6.33
NCGB2	I	2010	0.2	---	0.02	---	0.02	---	155.3	316.5	1.12	1.01
NCGB3	I	2010	---	0.44	---	---	---	---	334.2	1444.0	2.34	3.09
NCLM1	U	2010	0.72	0.36	0.39	0.19	0.08	0.04	300.1	634.3	3.66	17.83
NCLM2	U	2010	0.8	0.53	0.54	0.35	0.08	0.06	349.1	785.4	3.84	25.02
NCLM3	U	2010	0.72	0.49	0.32	0.23	0.08	0.06	287.0	1264.8	3.78	14.77
NCRE1	U	2010	1.07	0.73	0.51	0.39	0.1	0.07	425.9	750.4	4.64	23.56
NCRE2	U	2010	0.8	0.42	0.31	0.22	0.08	0.04	235.7	808.3	3.57	14.47
NCRE3	U	2010	0.72	0.28	0.32	0.13	0.08	0.03	252.1	608.3	3.68	14.78
PK1	U	2011	0.45	0.35	0.15	0.11	0.05	0.04	252.0	929.4	2.57	6.90
PK2	U	2011	1.04	0.97	0.49	0.42	0.1	0.09	---	1499.4	4.65	23.09
PK3	U	2011	0.74	0.48	0.23	0.15	0.06	0.04	230.6	960.9	2.98	10.79
PM1	U	2009	0.47	0.45	0.19	0.24	0.04	0.04	261.2	502.3	1.93	8.42
PM2	U	2009	0.29	0.26	0.1	0.18	0.04	0.03	194.9	1007.2	2.02	4.56
PM7	U	2010	0.54	0.44	0.05	0.06	0.04	0.03	137.2	433.1	1.84	2.34
PM3	I	2009	0.11	---	0.05	---	0.01	---	222.6	393.3	0.61	2.38
PM4	I	2009	0.11	---	0.01	---	0.02	---	170.7	409.2	1.02	0.61
PM8	I	2010	0.11	0.10	0.04	0.11	0.02	0.01	220.2	566.9	0.84	1.64
PM5	I	2009	0.20	0.12	0.02	0.06	0.02	0.01	222.0	680.3	1.05	0.78
PM6	I	2011	---	0.42	---	0.10	---	0.04	112.1	367.5	1.99	1.90

Table 1 continued

Core	Site[a]	Year[b]	Accretion ($cm\ y^{-1}$)		Mineral Accumulation ($g\ cm^{-2}\ y^{-1}$)		Organic Accumulation ($g\ cm^{-2}\ y^{-1}$)		Radionuclide Inventory ($mBq\ cm^{-2}$)		Accumulated Mass Since 1964 ($g\ cm^{-2}$)	
			^{137}Cs	$^{210}Pb_{xs}$	^{137}Cs	$^{210}Pb_{xs}$	^{137}Cs	$^{210}Pb_{xs}$	^{137}Cs	$^{210}Pb_{xs}$	Organic	Mineral
PM9	I	2011	0.19	0.31	---	---	---	---	---	---	---	---
PM10	U	2011	0.36	0.52	0.01	0.04	0.04	0.05	93.3	260.5	1.77	0.68
PM11	U	2011	0.28	0.33	0.01	0.02	0.03	0.03	88.0	393.4	1.41	0.45
PM12	U	2011	0.23	---	0.02	---	0.02	---	43.2	303.5	1.05	0.96
TH1	I	2011	0.19	---	0.07	---	0.01	---	36.4	624.4	0.69	3.45
TH2	I	2011	0.15	0.27	0.11	0.18	0.02	0.02	279.0	643.6	0.71	5.17
TH3	I	2011	0.28	0.21	0.10	0.05	0.03	0.02	249.9	654.6	1.34	4.80
TH4	I	2011	0.19	0.20	0.10	0.21	0.02	0.01	208.3	877.3	0.84	4.66
TH5	I	2011	0.36	0.39	0.15	0.14	0.03	0.03	262.7	708.0	1.60	7.00
TH6	I	2011	0.11	0.20	0.04	0.10	0.01	0.02	267.4	645.5	0.50	1.70

[a] "U" refers to unimpounded marsh sites and "I" refers to impounded marsh sites. [b] "Year" refers to the year the core was collected.

Table 2: Unimpounded marsh accretion rates reported in the literature.

Location	Rate ($cm\ y^{-1}$)	Method	Study
Long Island, NY	0.64	^{210}Pb	Armento & Woodwell (1975)[a]
Aransas NWR, TX	0.44 ± 0.16[c]	^{137}Cs (1964)	Callaway et al. (1997)
San Bernard NWR, TX	0.62 ± 0.15[c]	^{137}Cs (1964)	"
Biloxi Bay, MI	0.56 ± 0.09[c]	^{137}Cs (1964)	"
Barataria Bay, LA	0.59 - 1.40[b]	^{137}Cs (1964)	Hatton et al. (1993)
Lafourche Parish, LA	0.61 - 0.70	^{137}Cs (1954)	DeLaune et al. (1989)
"	0.33 - 0.59	^{137}Cs (1964)	"
"	0.42 - 0.43	^{210}Pb	"
Terrebonne Parish, LA	0.80 - 1.08	^{137}Cs (1954)	DeLaune et al. (1989)
"	0.72 - 0.98	^{137}Cs (1964)	"
"	0.58 - 0.89	^{210}Pb	"
Cameron Parish, LA	0.59 - 0.83	^{137}Cs (1954)	DeLaune et al. (1989)
"	0.45 - 0.70	^{137}Cs (1964)	"
"	0.55	^{210}Pb	"
Southwestern Louisiana	0.48 - 0.70	^{137}Cs (1964)	Bryant and Chabreck (1998)
Rhode Island	0.15 - 0.58	^{210}Pb	Bricker-Urso et al. (1989)
Nauset Marsh, MA	0.38 - 0.45	^{137}Cs	Roman et al. (1997)
"	0.26 - 0.40	^{210}Pb	"
"	0.10 - 0.34	^{14}C	"
Long Island Sound, NY	0.25 - 0.44	^{137}Cs (1964)	Anisfeld et al. (1999)
"	0.11 - 0.59	^{210}Pb	"
Delaware	0.39	^{137}Cs	Kraft et al. (1992)
"	0.42	^{210}Pb	"

Table 2 continued

Location	Rate (cm y^{-1})	Method	Study
Delaware	0.35 ± 0.07	^{137}Cs	Kim et al. (1997)
"	0.37 ± 0.02	^{207}Bi	"
"	0.57 ± 0.28	^{137}Cs (1964)	This Study
"	0.50 ± 0.19	^{210}Pb	"

[a] Rate taken from Stumpf (1983), [b] rates from range of brackish and salt marsh

Table 3: Impounded marsh accretion rates reported in the literature.

Location	Rate (cm y^{-1})	Method	Study
Southwestern Louisiana	0.29 - 0.90	^{137}Cs (1964)	Bryant and Chabreck (1998)
Long Island Sound, NY	0.19 - 0.39	^{137}Cs (1964)	Anisfeld et al. (1999)
"	0.14 - 0.23	^{210}Pb	"
Delaware	0.25 ± 0.16	^{137}Cs (1964)	This study
"	0.30 ± 0.17	^{210}Pb	"

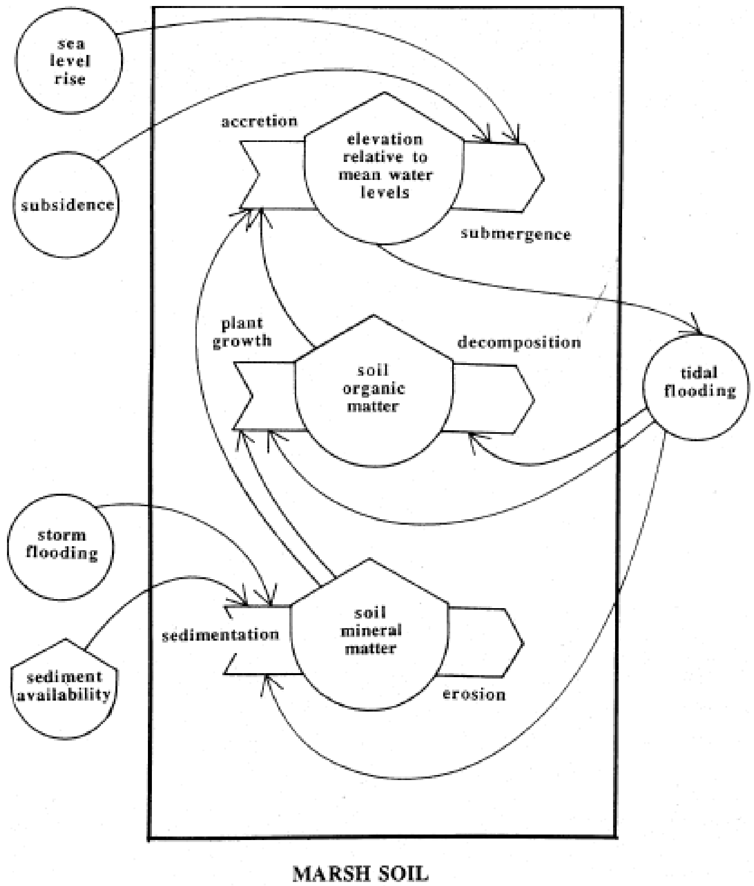

Figure 1: **Conceptual model of soil formation in tidal marshes. Figure from Nyman et al. (1993).**

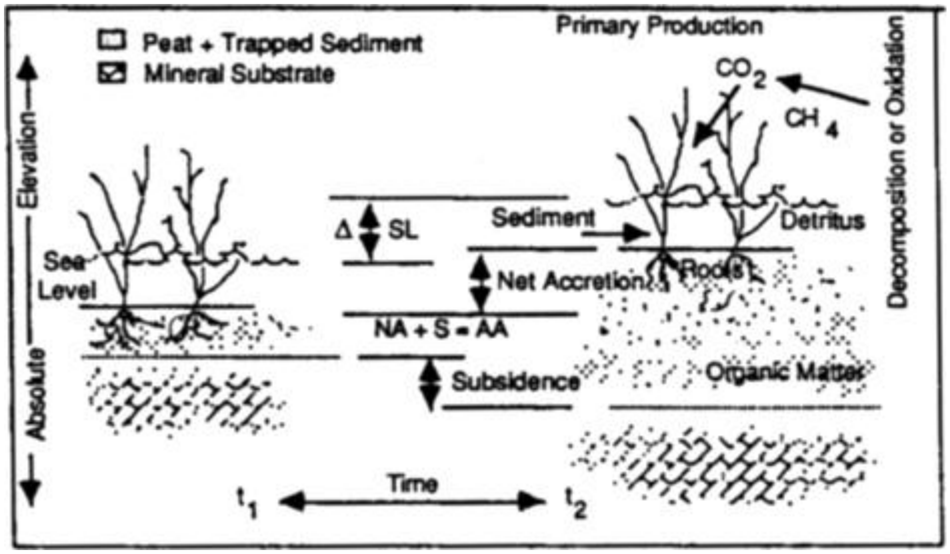

Figure 2: **Model of accretion and sea-level rise showing the relationship among net accretion, subsidence and absolute accretion. (S L = Eustatic Sea-Level Change, NA = Net Accretion, S = Subsidence, AA = Absolute Accretion). Figure from DeLaune et al. (1989).**

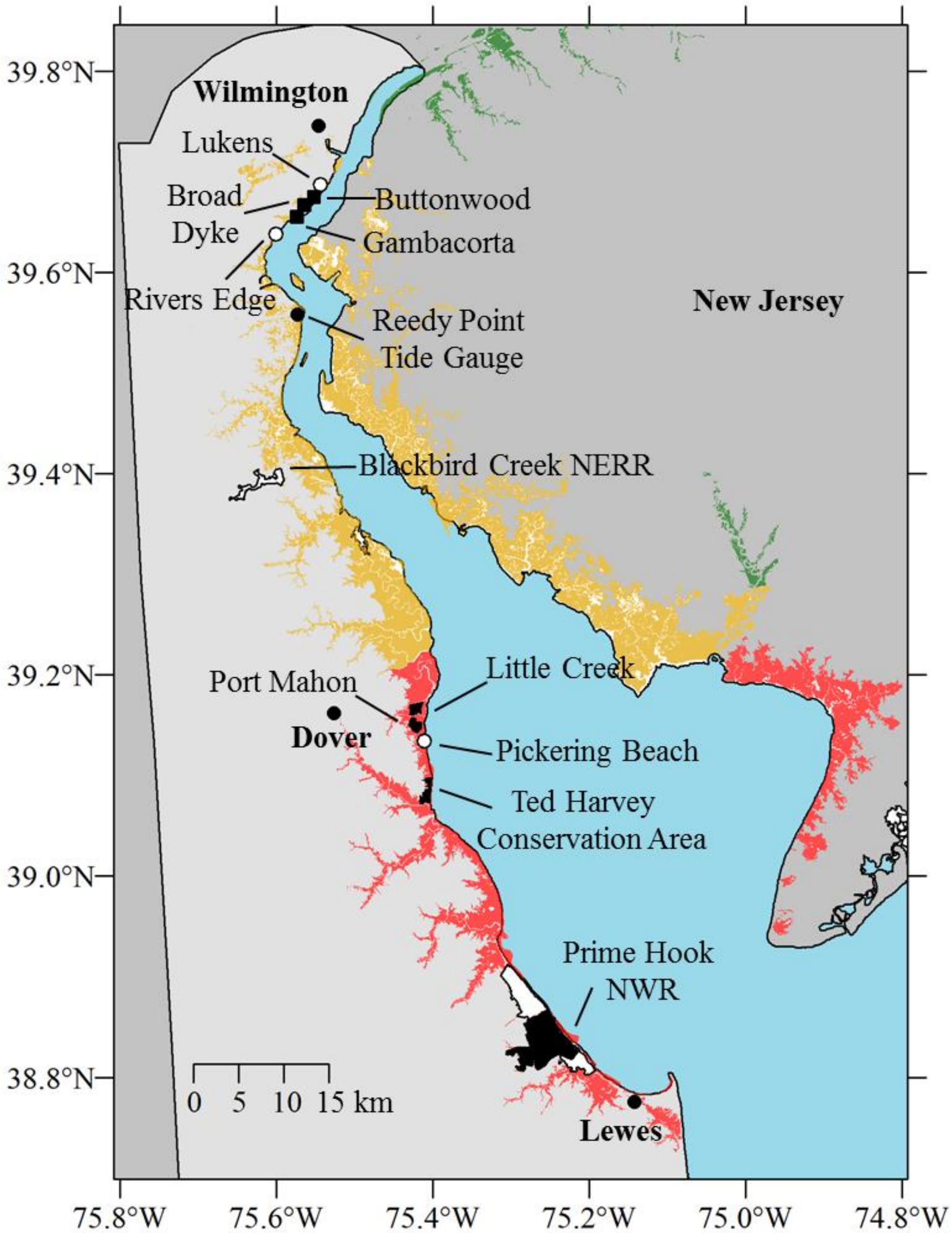

Figure 3: **Map of the state of Delaware (light grey) showing the US Fish and Wildlife Service habitat classifications for the Delaware Estuary. Salt marsh is in red, brackish marsh in orange and tidal fresh in green. Unimpounded study sites are shown in white and impounded sites in black.**

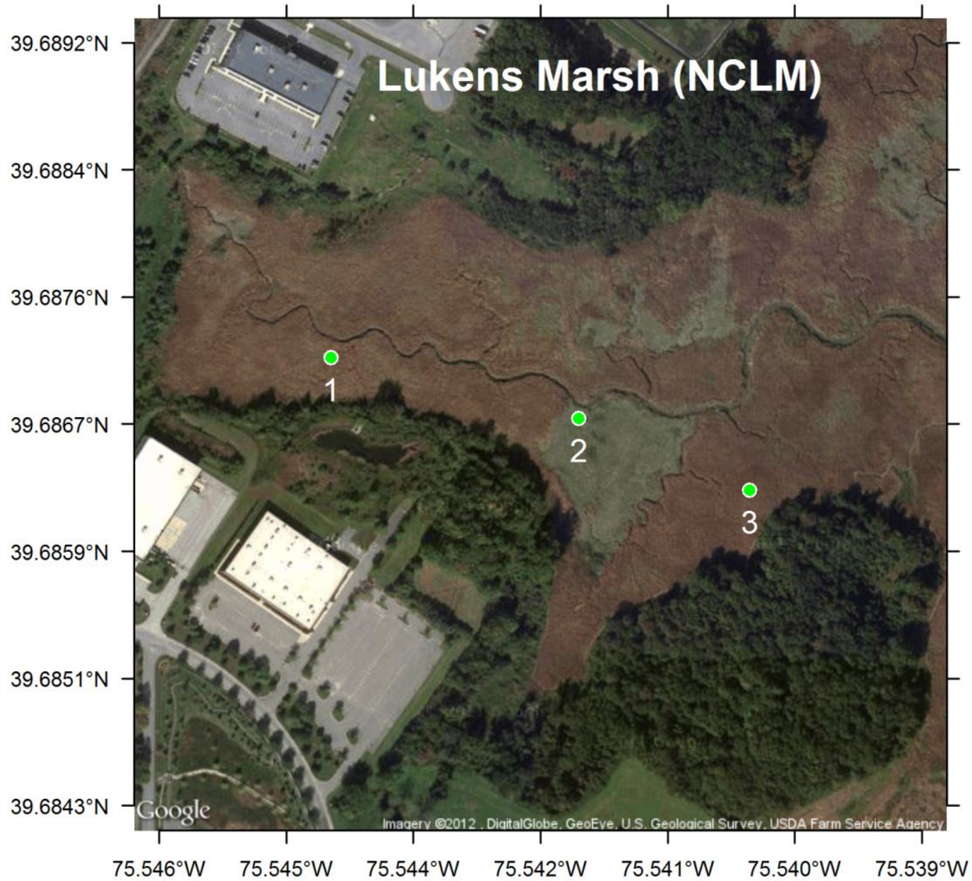

Figure 4: **Map of Lukens Marsh, an unimpounded marsh site, showing the locations of cores NCLM-1, NCLM-2, and NCLM-3.**

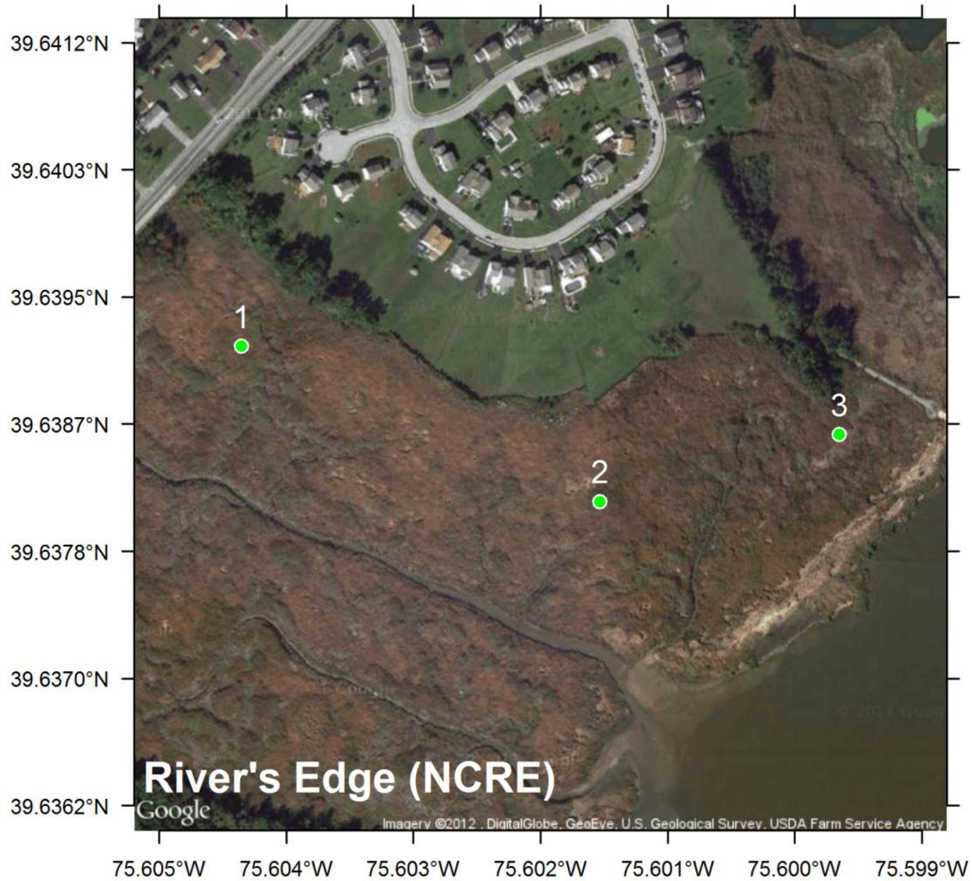

Figure 5: Map of Rivers Edge, an unimpounded marsh site, showing the locations of cores NCRE-1, NCRE-2, and NCRE-3.

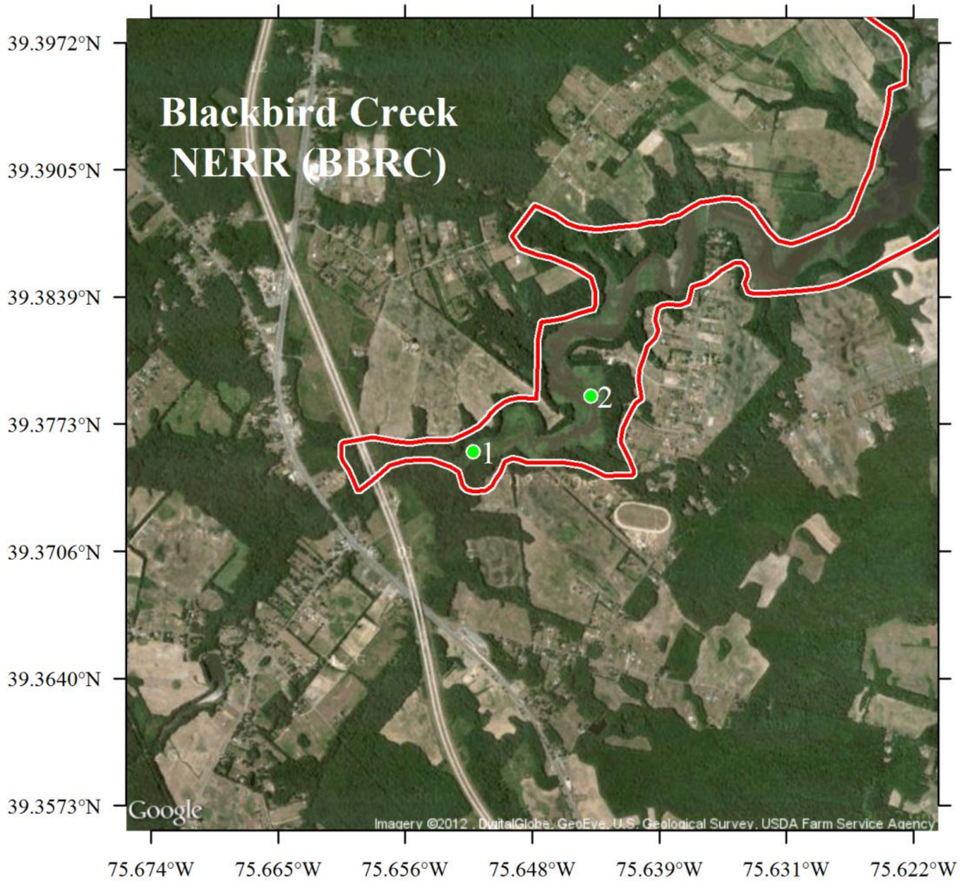

Figure 6: **Map of Blackbird Creek, an unimpounded marsh coring site, showing the locations of BBRC-1 and BBRC-2. The boundaries of the Blackbird Creek NERR are shown in red.**

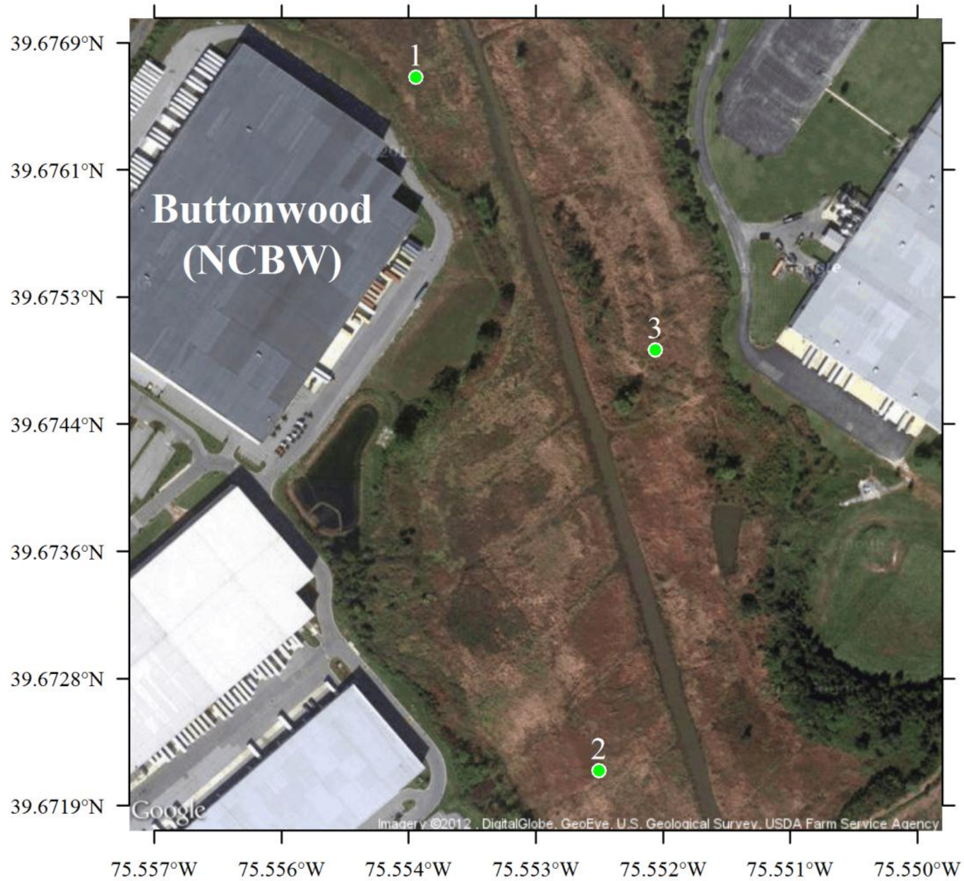

Figure 7: Map of Buttonwood marsh, an impounded marsh site, showing the locations of cores NCBW-1, NCBW-2, and NCBW-3.

Figure 8: **Map of Broad Dyke impounded marsh showing the locations of cores NCBD-1, NCBD-2, and NCBD3.**

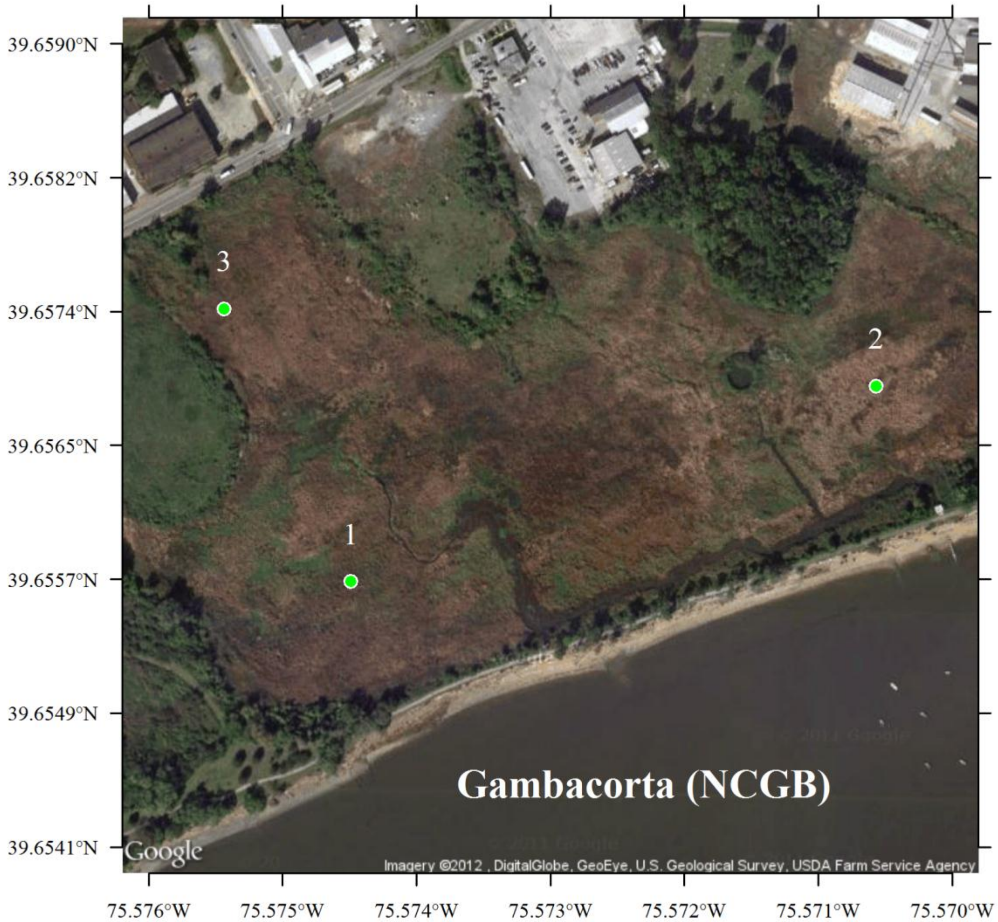

Figure 9: Map of Gambacorta marsh, an unimpounded marsh site, Delaware showing the locations of cores NCGB-1, NCGB-2, and NCGB-3.

Figure 10: Map of Pickering Beach marsh, an unimpounded marsh site near Dover, Delaware, just south of Little Creek, showing the locations of cores PK-1, PK-2, and PK-3.

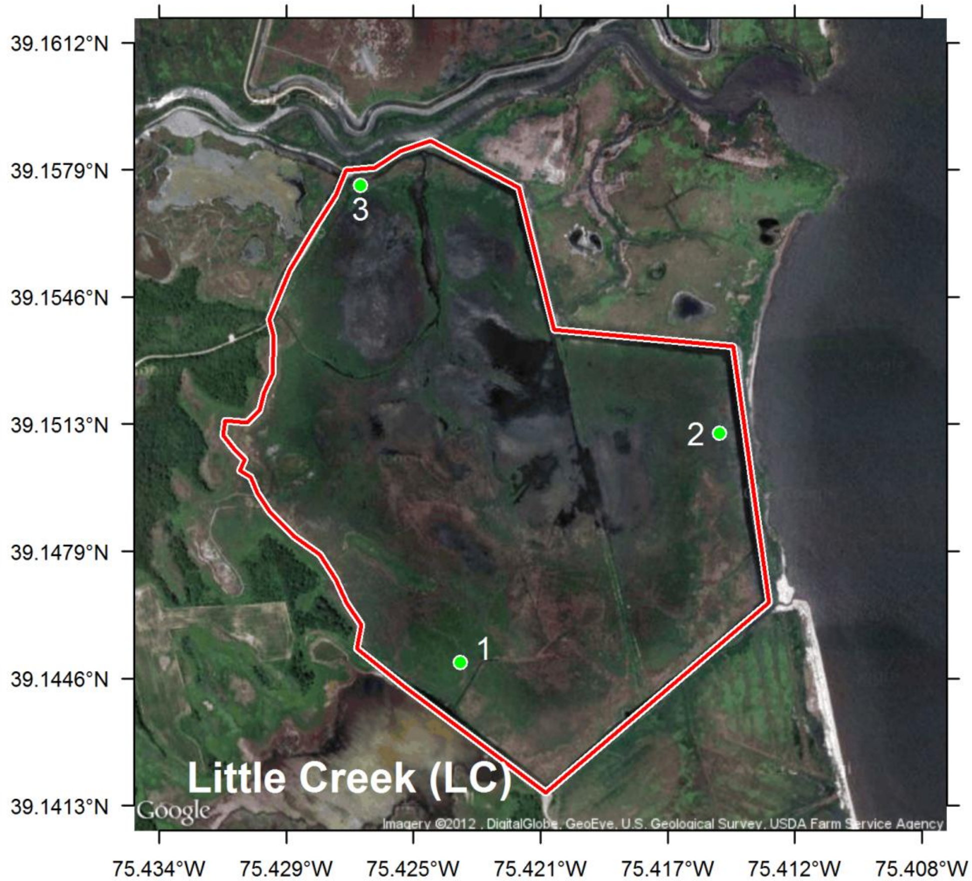

Figure 11: Map of Little Creek marsh, an impounded marsh site, located near Dover, Delaware, just south of the Little Creek, showing the locations of cores LC-1, LC-2, and LC-3.

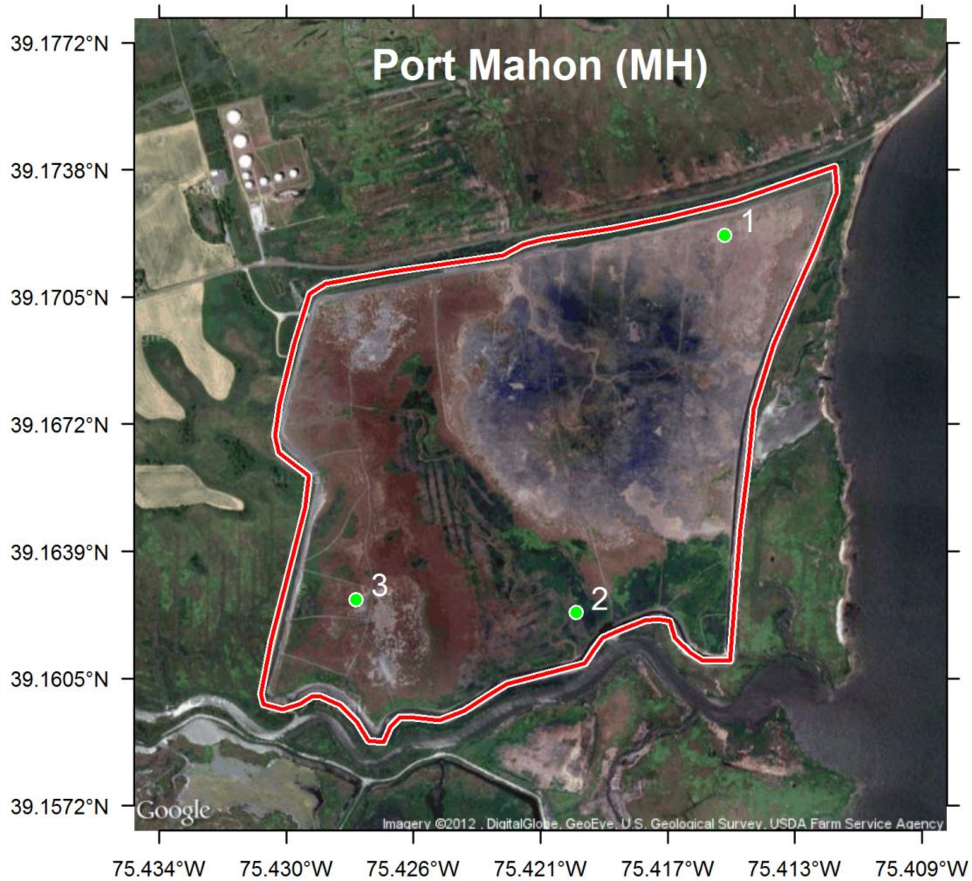

Figure 12: Map of Port Mahon marsh, an impounded marsh site, near Dover, Delaware, just north of the Little Creek, showing the locations of cores MH-1, MH-2, and MH-3.

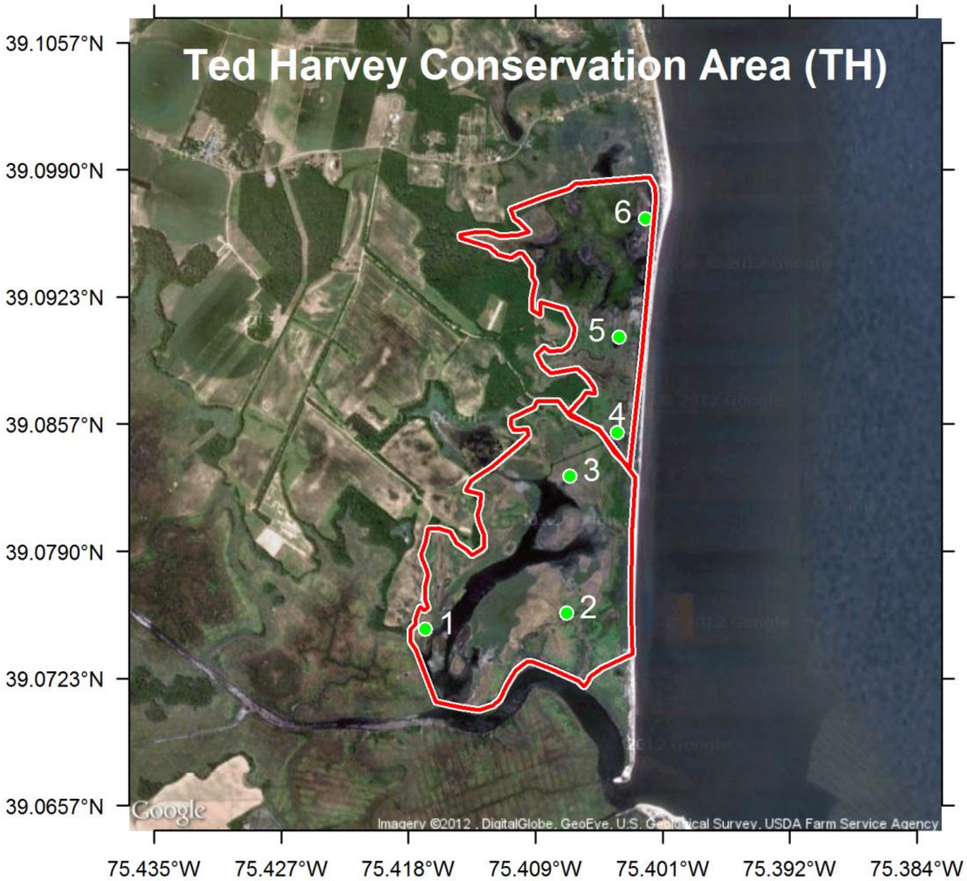

Figure 13: Map of Ted Harvey State Conservation Area, an impounded marsh site just north of the Lower St. Jones Estuary, showing the locations of cores TH-1, TH-2, TH-3, TH-4, TH-5, and TH-6.

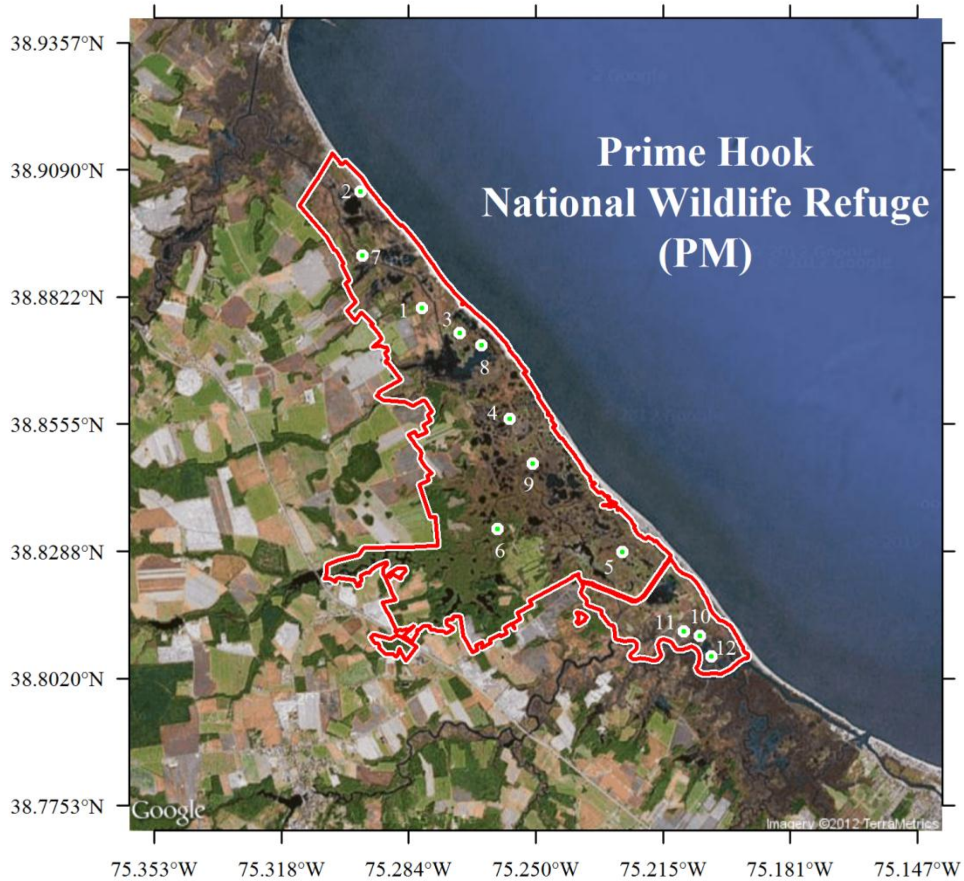

Figure 14: Map of Prime Hook National Wildlife Refuge near Lewes, Delaware showing locations of PM cores 1-12. The outline of the refuge is marked by the red and white line.

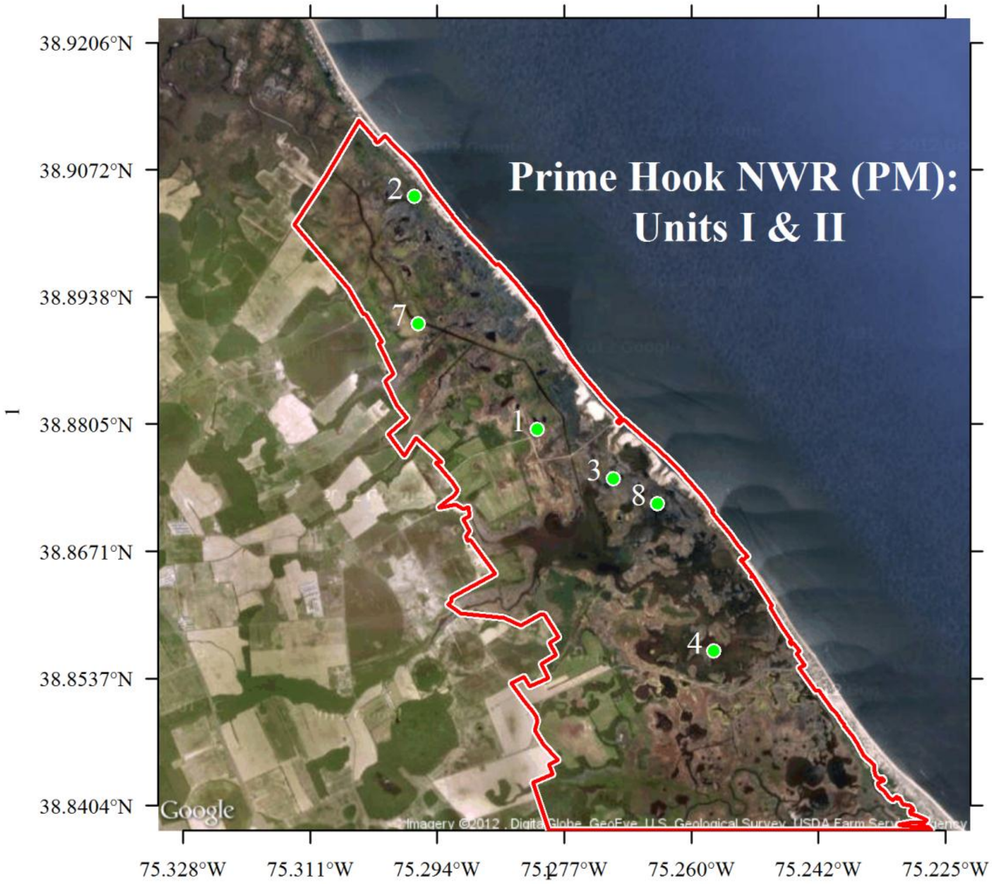

Figure 15: Map of Prime Hook National Wildlife Refuge showing unimpounded Unit I (cores PM-1, PM-2, and PM-7) and impounded Unit II (cores PM-3, PM-8, and PM-4). The outline of the refuge is marked by the red and white line.

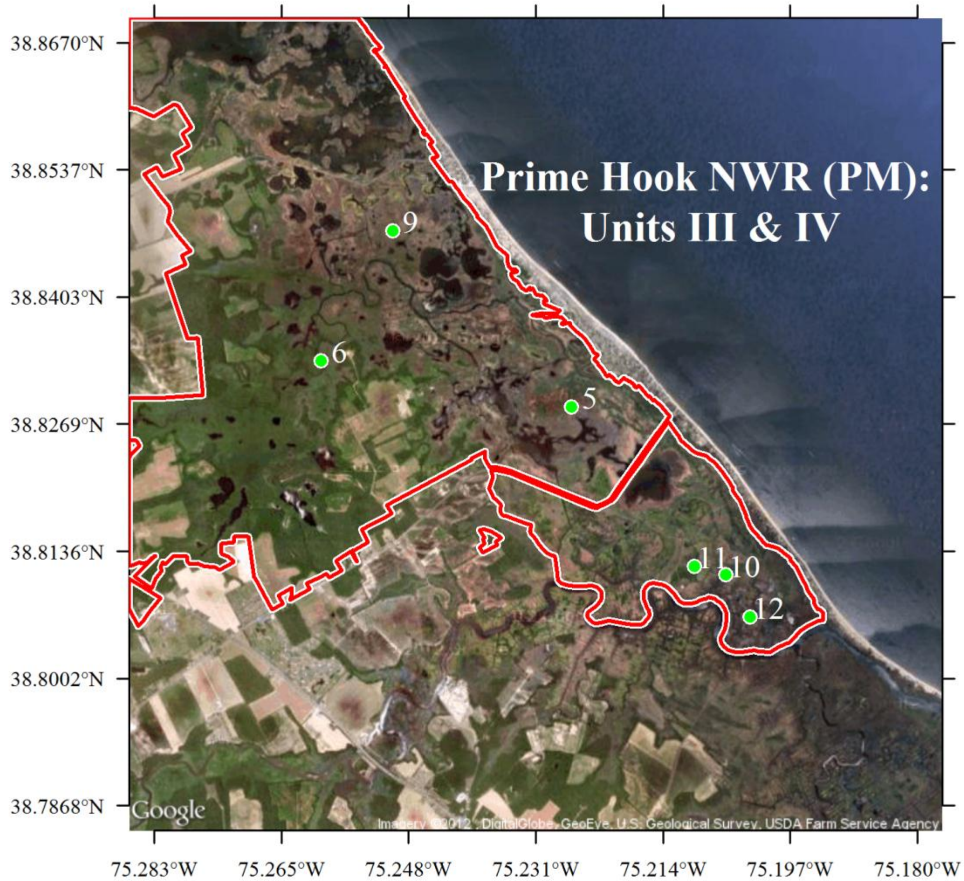

Figure 16: **Map of Prime Hook National Wildlife Refuge showing impounded Unit III (cores PM-5, PM-6, and PM-9) and unimpounded Unit IV (cores PM-10, PM-11, and PM-12). The outline of the refuge is marked by the red and white line.**

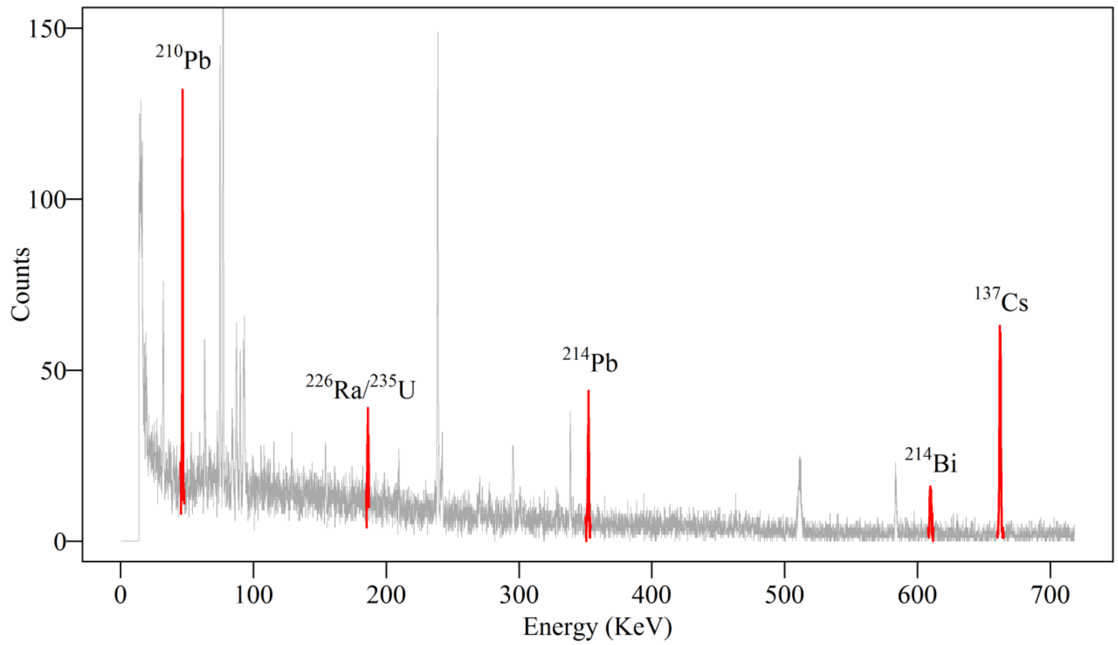

Figure 17: Examples gamma-ray energy spectra (sample NCGB-1 32-34 cm) showing the photopeaks of nuclides used in this study.

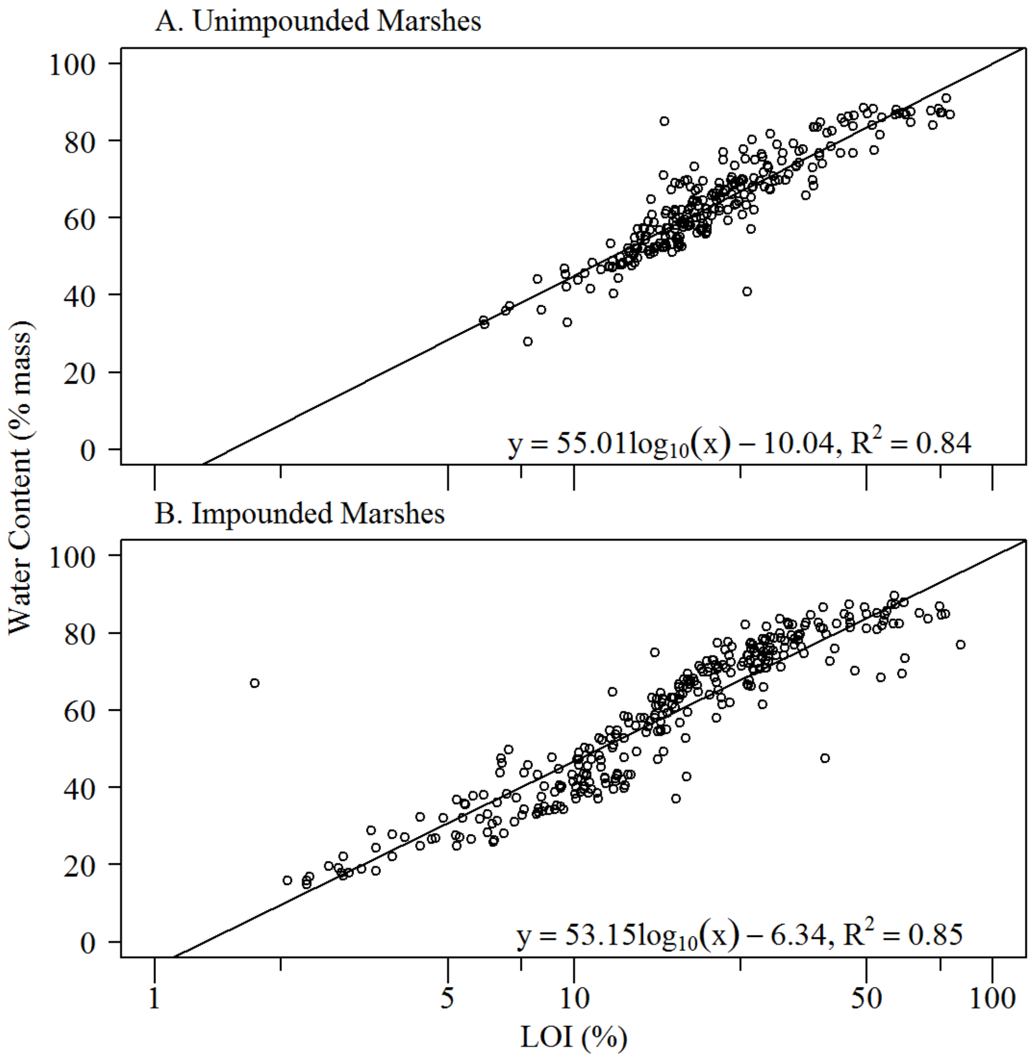

Figure 18: **Loss-on-ignition (LOI) versus water content. Data for unimpounded marshes are shown in panel A and impounded marshes in panel B.**

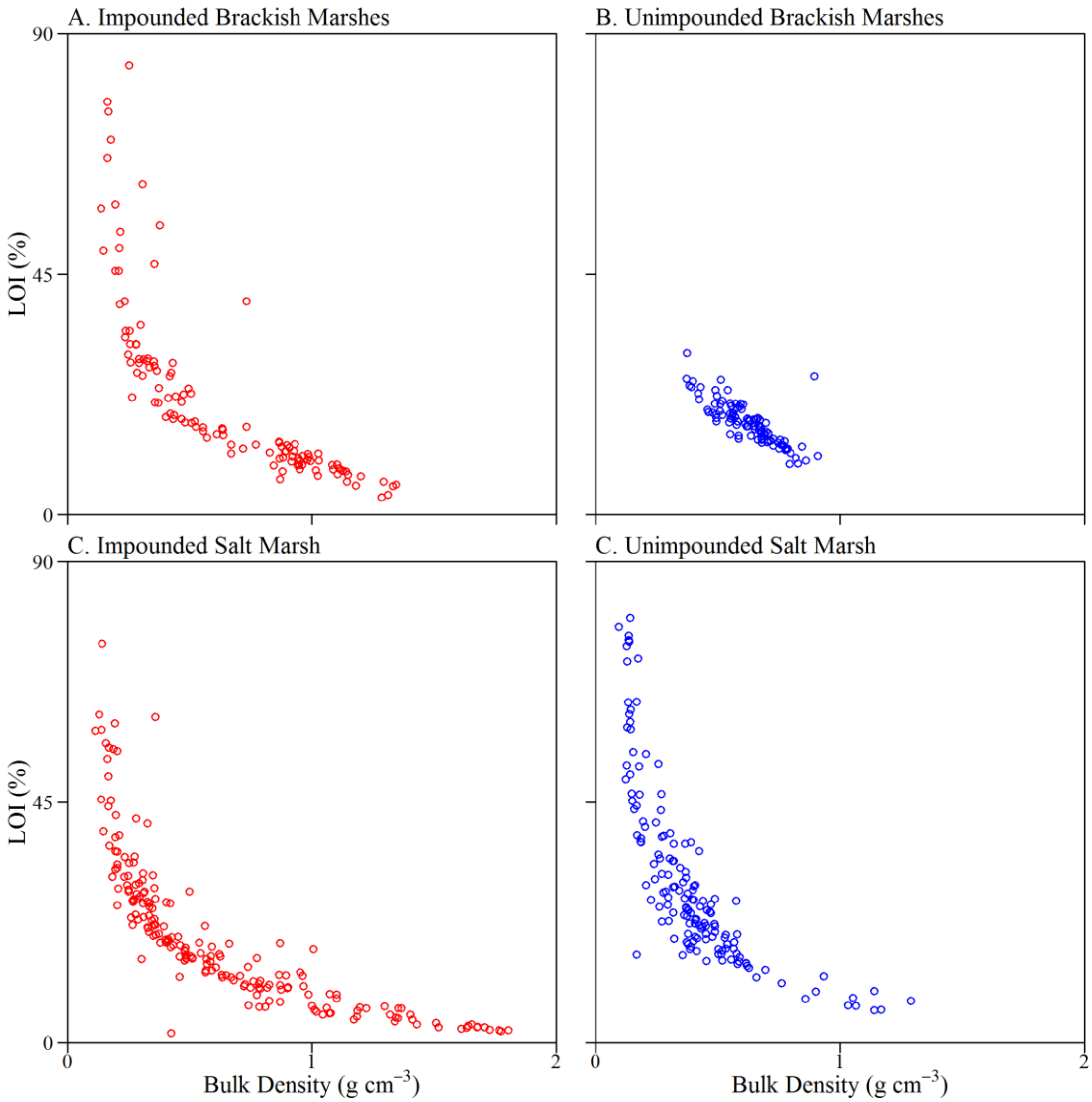

Figure 19: Dry bulk density versus LOI for all core samples.

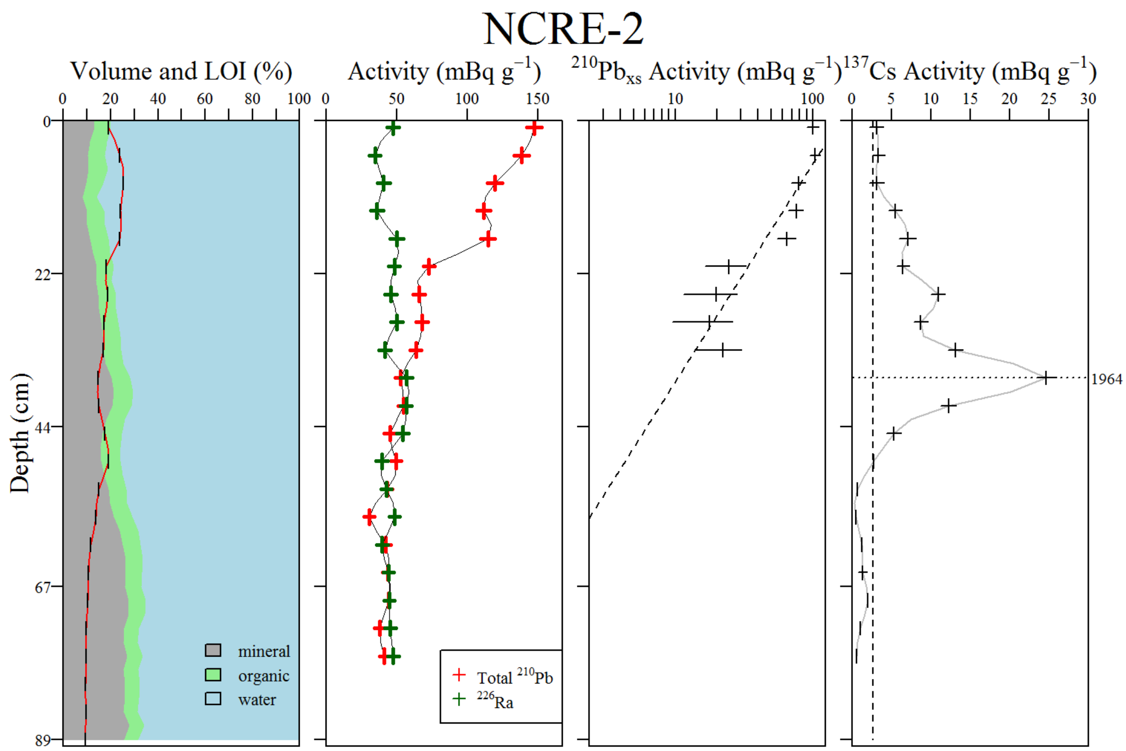

Figure 20: Profiles of volume composition, LOI, and, $^{210}Pb_{xs}$ and ^{137}Cs activity for core NCRE-2 from the River's Edge unimpounded marsh site.

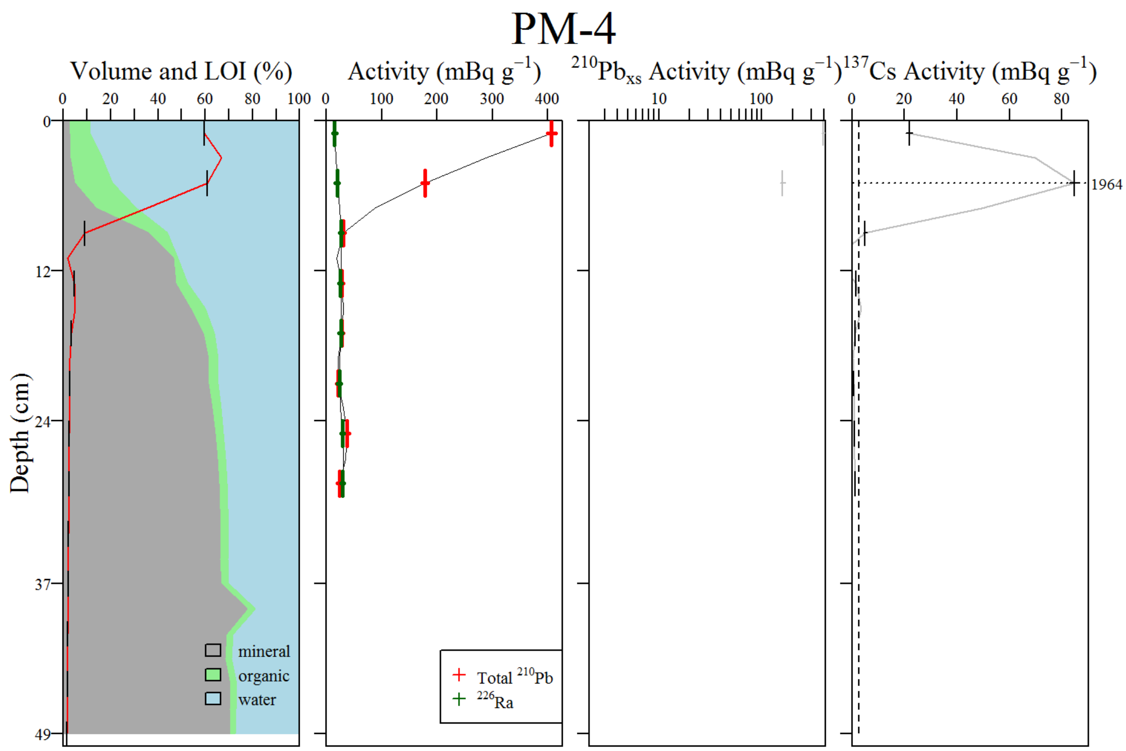

Figure 21: Profiles of volume composition, LOI, and, $^{210}Pb_{xs}$ and ^{137}Cs activity for core PM-4 from the Prime Hook NWR impounded Unit II.

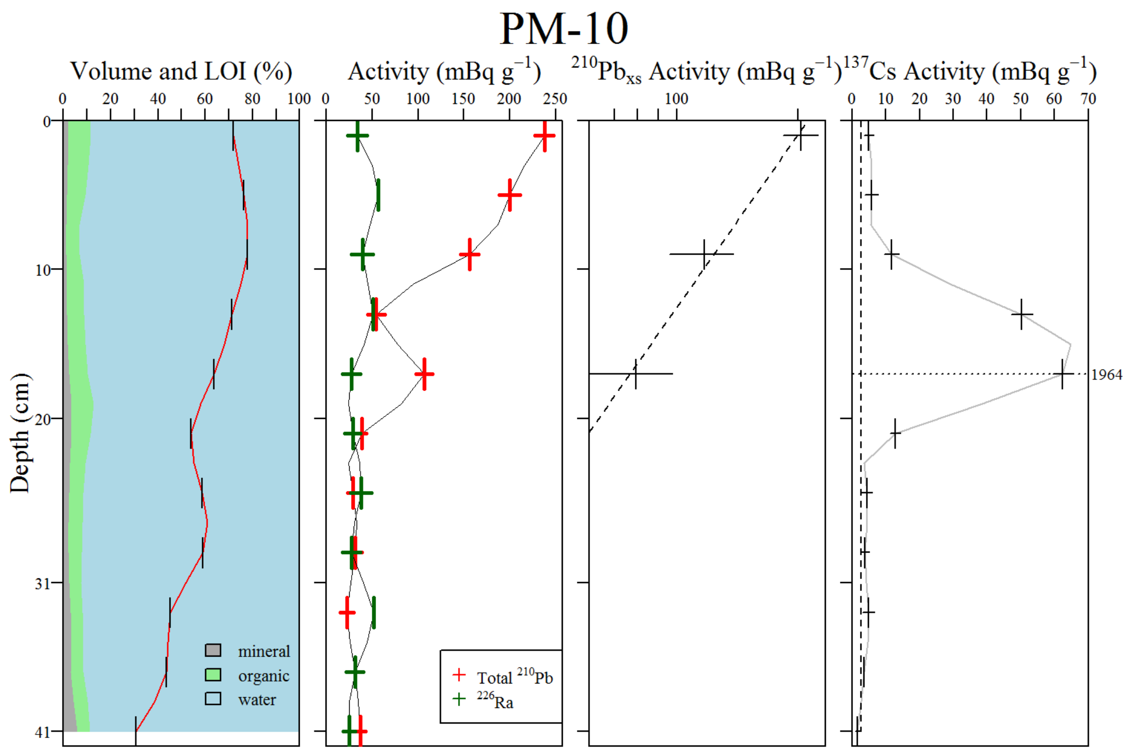

Figure 22: Profiles of volume composition, LOI, and, $^{210}Pb_{xs}$ and ^{137}Cs activity for core PM-10 from the Prime Hook NWR Unit IV unimpounded marsh.

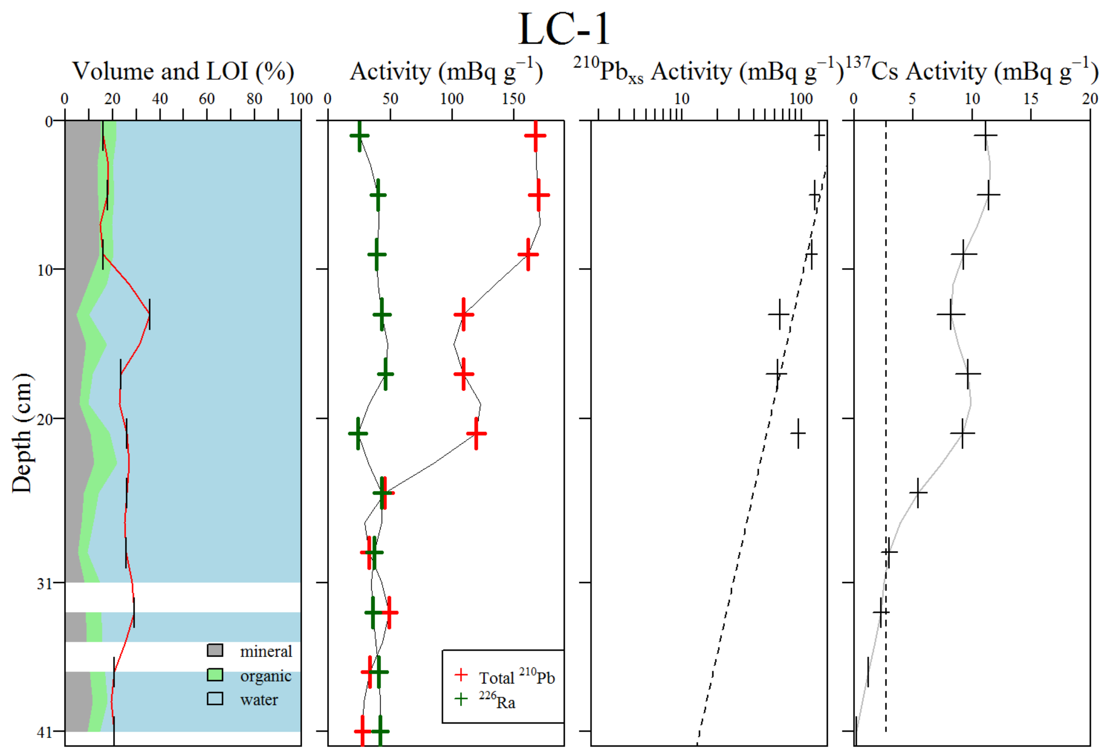

Figure 23: Profiles of volume composition, LOI, and, $^{210}Pb_{xs}$ and ^{137}Cs activity for core LC-1 from the Little Creek impounded marsh.

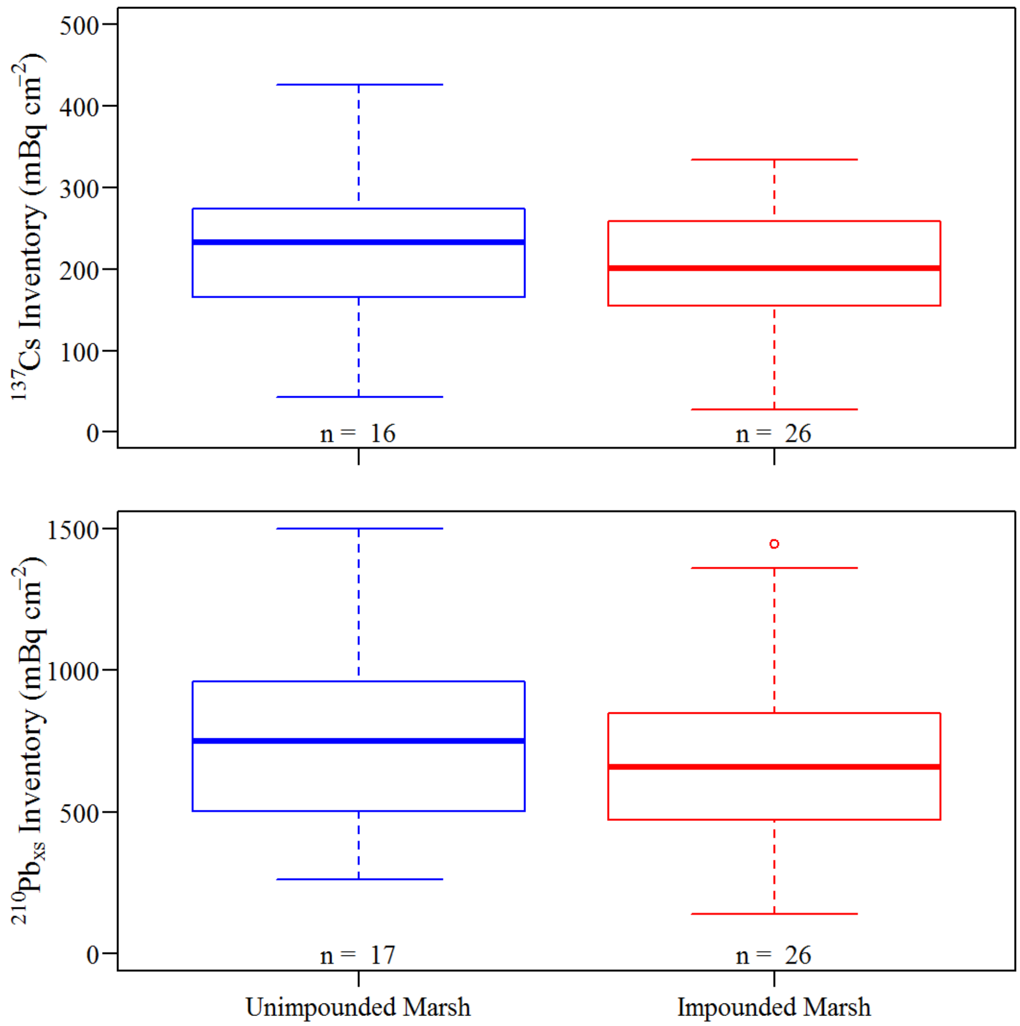

Figure 24: **Box plots of ^{137}Cs and $^{210}Pb_{xs}$ inventories for the unimpounded and impounded marshes. The lower whisker is the minimum value excluding outliers (lower than 1.5 x interquartile range), bottom line of the box is the lower quartile, the solid line inside the box represents the median, the upper line of the box is the upper quartile, the upper whisker is the maximum excluding outliers (larger than 1.5 x the interquartile range), and outliers are represented by open circles. n = the number of observations.**

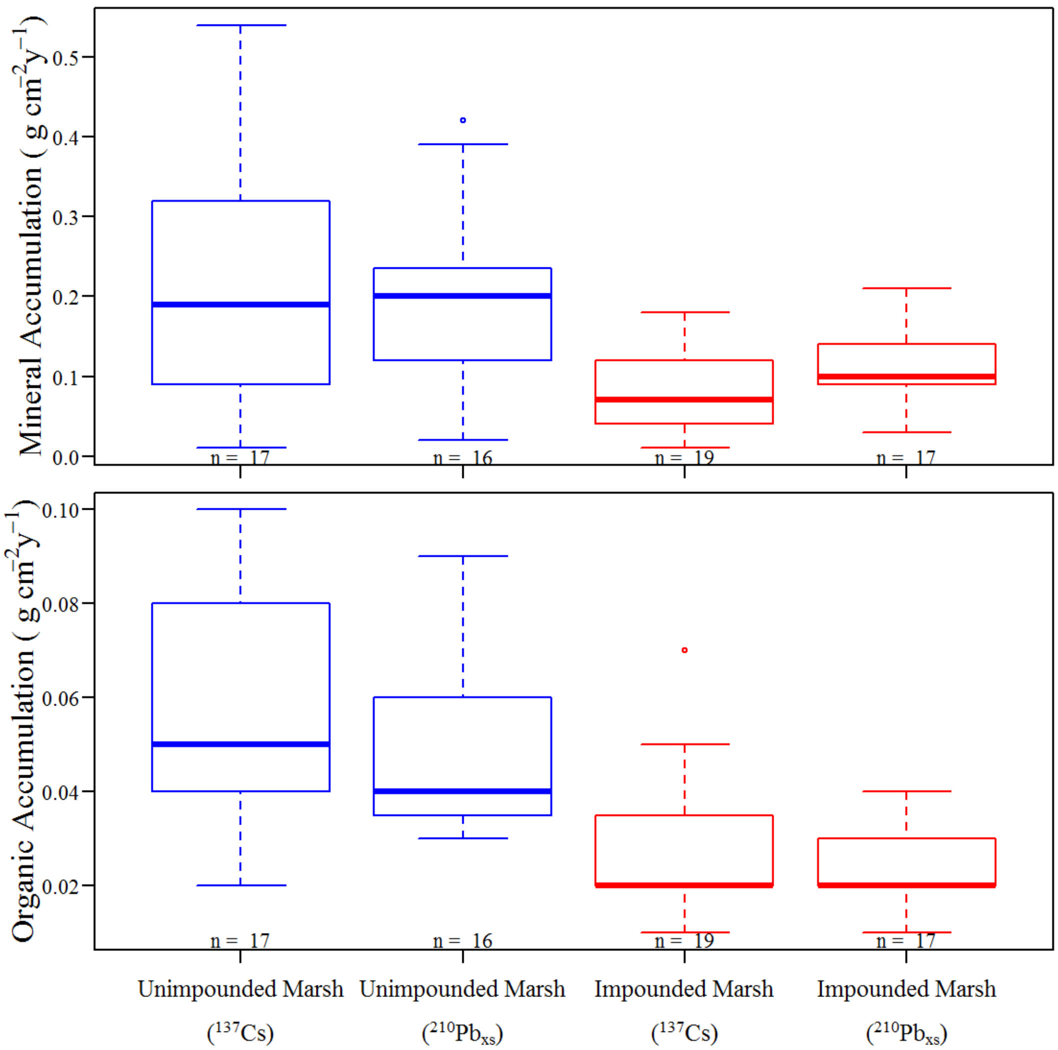

Figure 25: Box plots of mineral (top) and organic (bottom) accumulation rates determined by ^{137}Cs and $^{210}Pb_{xs}$ methods for unimpounded and impounded marshes. See Figure 23 for description of the box plot statistics.

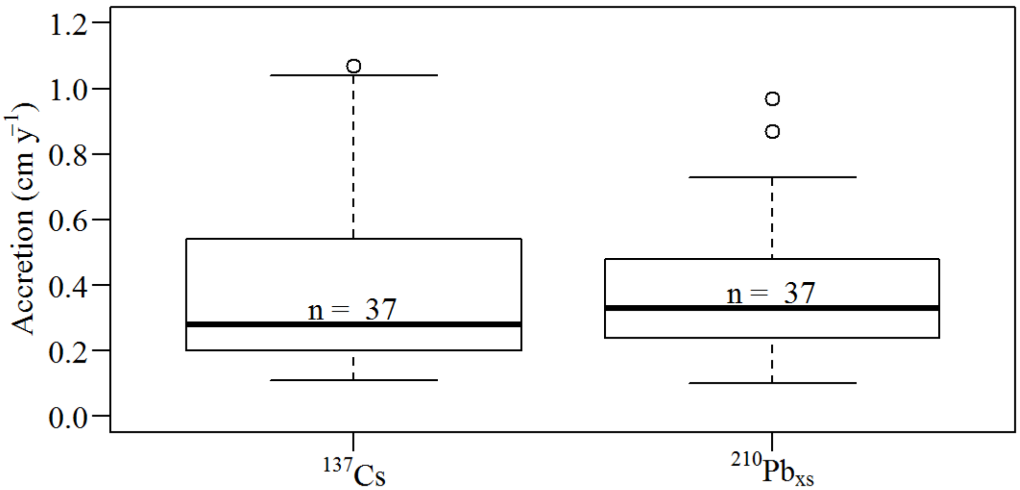

Figure 26: Boxplot of accretion rates determined using ^{137}Cs and $^{210}Pb_{xs}$ for all coring sites. See Figure 23 for description of the box plot statistics.

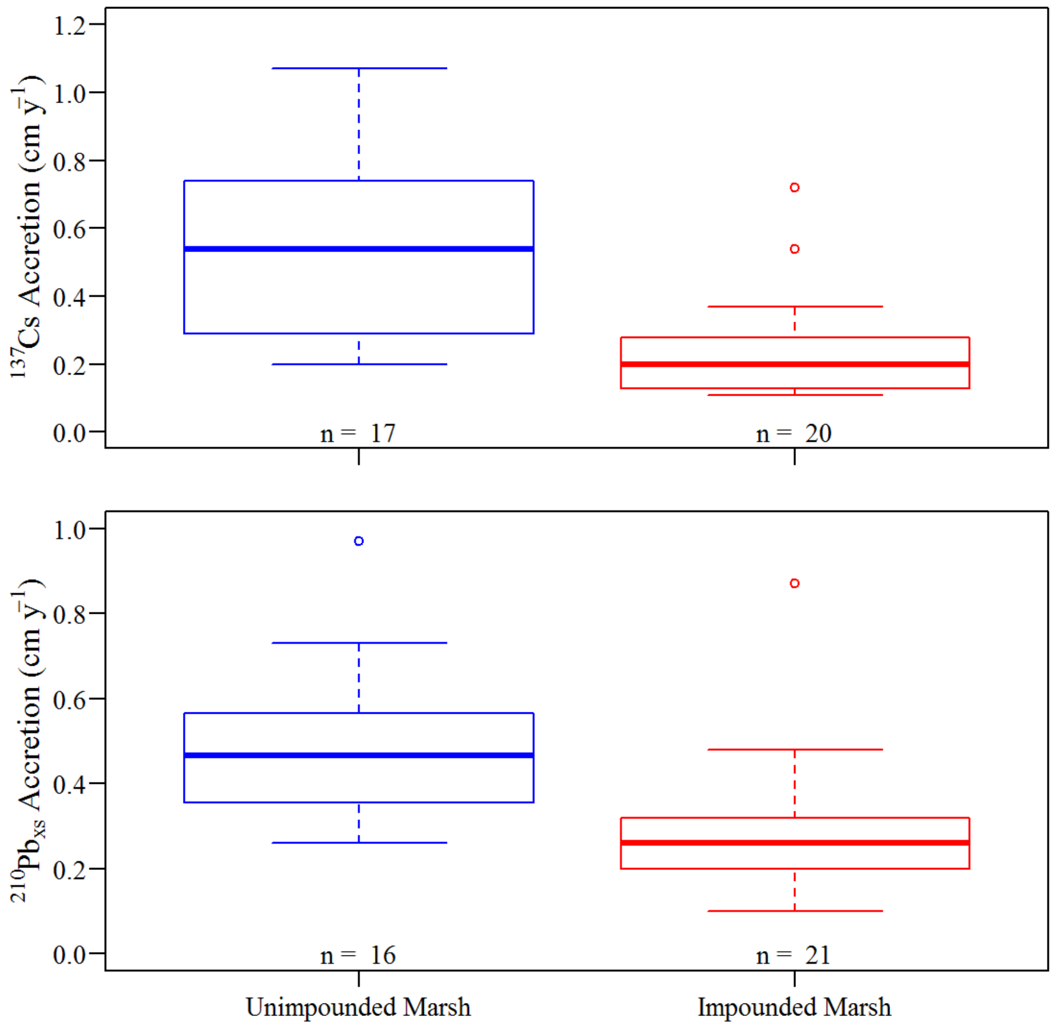

Figure 27: **Box plots of accretion rates determined using ^{137}Cs and ^{210}Pb$_{xs}$ methods separated by marsh type. See Figure 23 for description of the box plot statistics.**

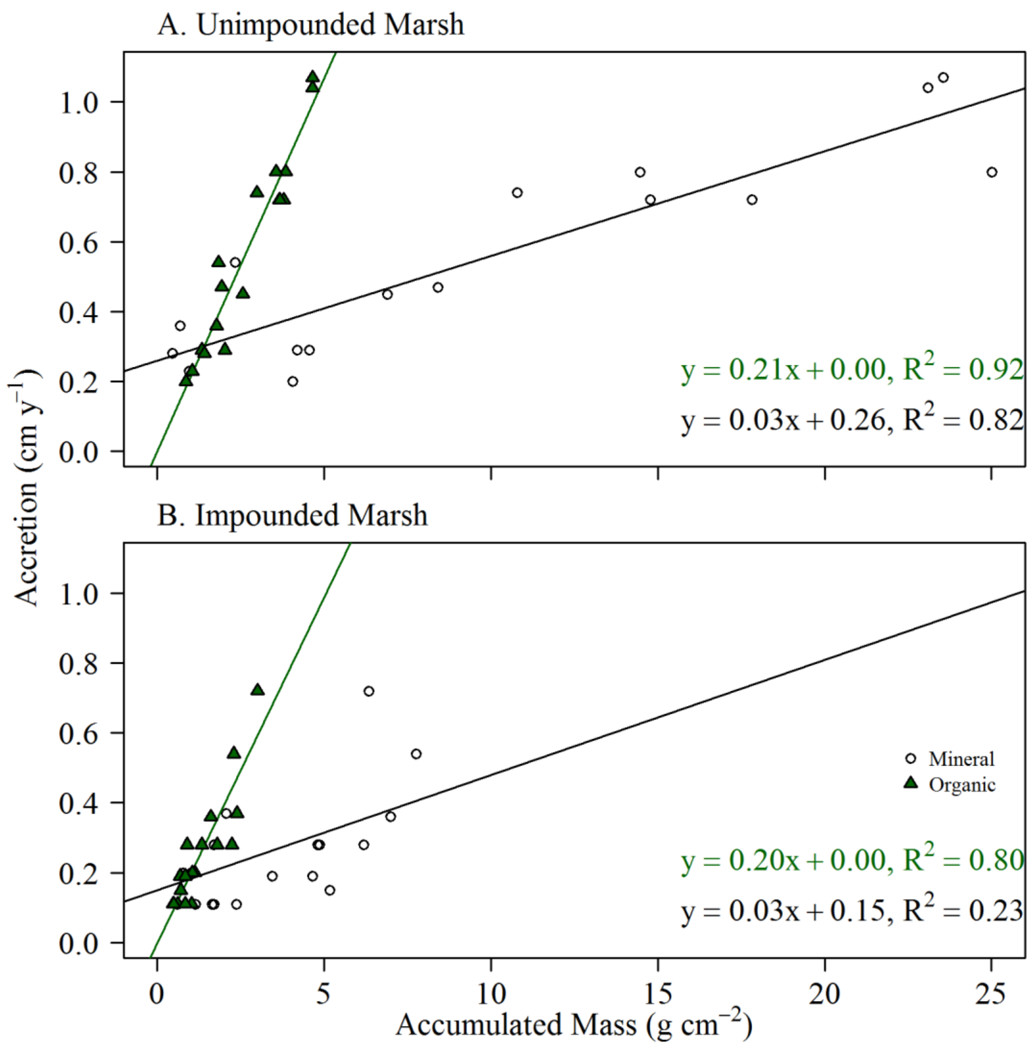

Figure 28: Plot of accumulated mineral and organic mass since 1964 versus accretion rates. Regression lines and equation follow the legend key.

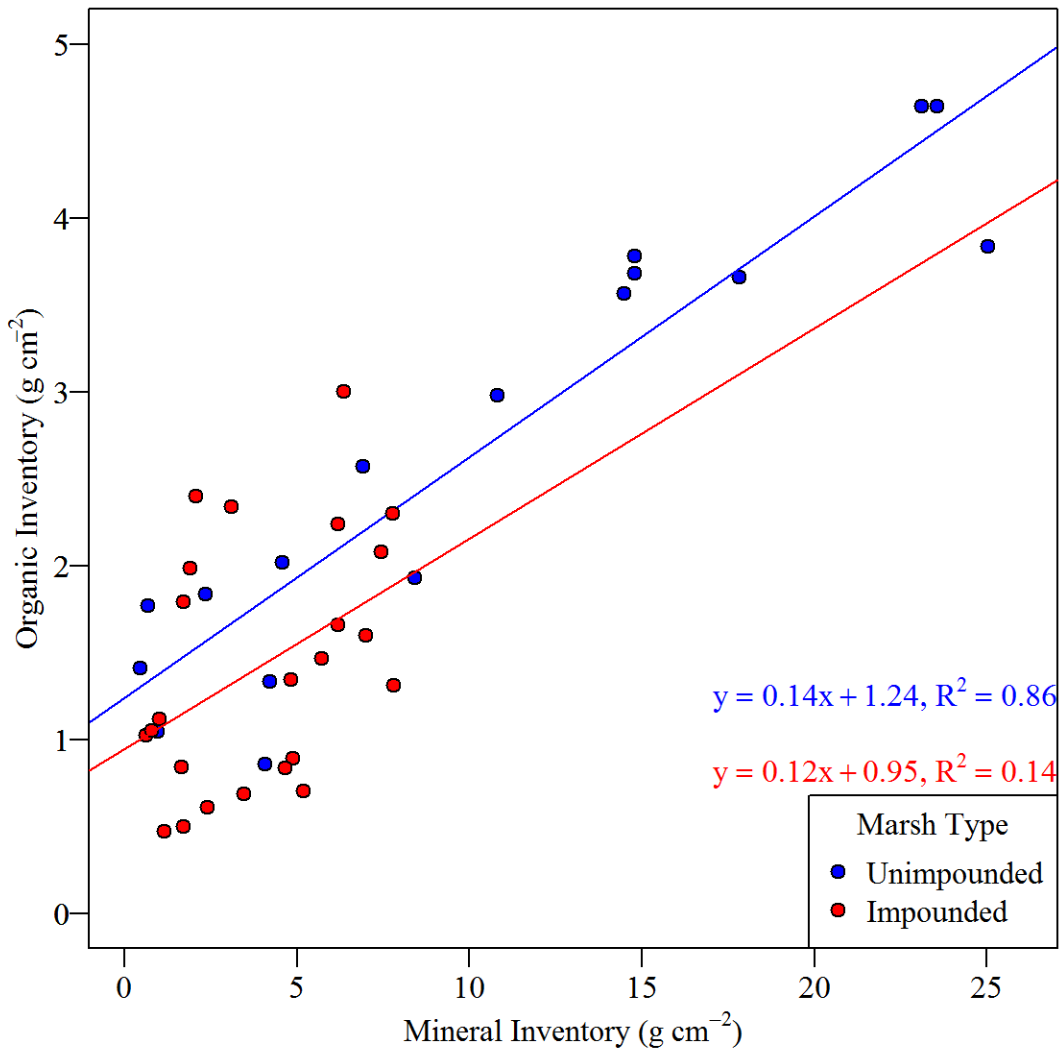

Figure 29: Correlation of mineral and organic inventories for the unimpounded and impounded marsh sites examined in this study. The linear regression lines and regression equations follow the legend color key. Note the similar trends for unimpounded and impounded data.

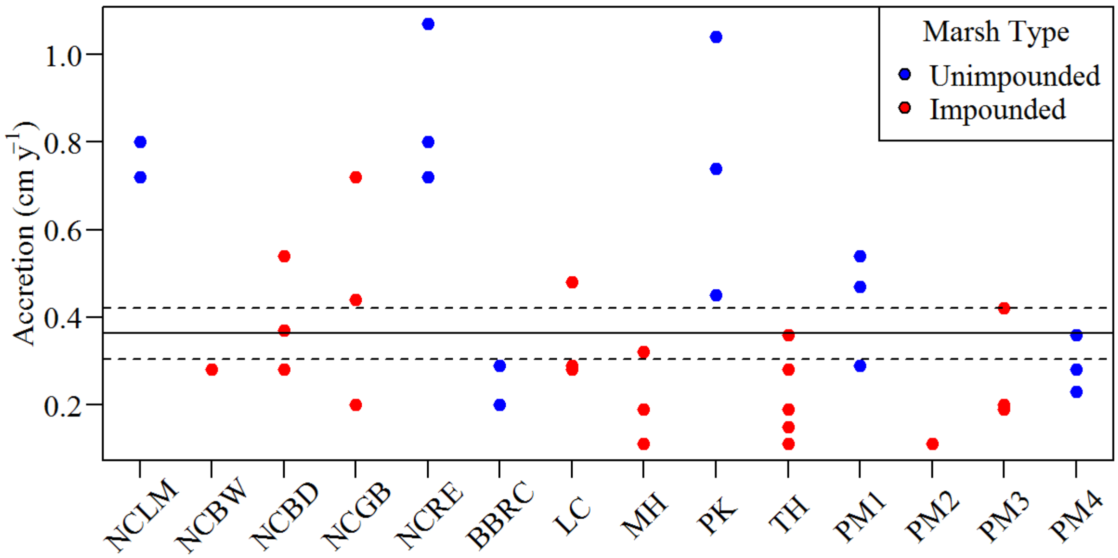

Figure 30: **Strip plot of ^{137}Cs-based accretion rates determined for each site (refer to Table 1 for sites names; PM sites are listed with the corresponding unit number). Accretion rates for unimpounded marshes are shown in blue and impounded marshes in red. The horizontal black line represents the 1956-2011 averaged rate of sea-level rise from NOAA's Reedy Point tide gauge, and the dashed lines are the uncertainty. Sites are ordered left to right corresponding to north to south location of sites. Accretion rates falling above and below the dashed lines reflect accretionary surplus and deficit, respectively. See text for further discussion.**

REFERENCES

Anisfeld, S. C., M. J. Tobin, G. Benoit, and N. Haven. 1999. Sedimentation rates in flow-restricted and restored salt marshes in Long Island Sound. Estuaries **22**: 231, doi:10.2307/1352980

Appleby, P. G. 2008. Three decades of dating recent sediments by fallout radionuclides: a review. The Holocene **18**: 83-93, doi:10.1177/0959683607085598

Appleby, P. G., and F. Oldfield. 1992. Application of lead-210 to sedimentation studies, p. 731-778. *In* M. Ivanovich and R.S. Harmon [eds.], Uranium-series disequilibrium; applications to Earth, marine and environmental sciences. Clarendon Press.

Bennett, R. H., and D. N. Lambert. 1971. Rapid and reliable technique for determining unit weight and porosity of deep-sea sediments. Marine Geology **11**: 201-207, doi:10.1016/0025-3227(71)90007-7

Boumans, R. M., and J. W. Day. 1994. Effects of two Louisiana marsh management plans on water and materials flux and short-term sedimentation. Wetlands **14**: 247–261.

Bricker-Urso, S., S. W. Nixon, J. K. Cochran, D. J. Hirschberg, and C. Hunt. 1989. Accretion rates and sediment accumulation in Rhode Island salt marshes. Estuaries **12**: 300, doi:10.2307/1351908

Bryant, J. C., and R. H. Chabreck. 1998. Effects of impoundment on vertical accretion of coastal marsh. Estuaries **21**: 416, doi:10.2307/1352840

Cahoon, D. 1994. Recent accretion in two managed marsh impoundments in coastal Louisiana. Ecological Applications **4**: 166–176.

Cahoon, D. R., and C. G. Groat. 1990. A study of marsh management practice in coastal Louisiana volume I: executive summary, Minerals Management Service.

Cahoon, D., D. Reed, J. Day Jr, G. Steyer, R. Boumans, J. Lynch, D. McNally, and N. Latif. 1995. The influence of Hurricane Andrew on sediment distribution in Louisiana coastal marshes. Journal of Coastal Research **Special Issue**: 280-294.

Cahoon, D., and R. Turner. 1989. Accretion and canal impacts in a rapidly subsiding wetland II. feldspar marker horizon Technique. Estuaries **12**: 260, doi:10.2307/1351905

Chmura, G. L., and G. A. Hung. 2004. Controls on salt marsh accretion: A test in salt marshes of Eastern Canada. Estuaries **27**: 70-81, doi:10.1007/BF02803561

Crain, C., K. Gedan, and M. Dionne. 2009. Tidal restrictions and mosquito ditching in New England marshes, p. 149-169. *In* B.R. Silliman, E.D. Grosholz, and M.D. Bertness [eds.], Human impacts on salt marshes: A Global Perspective. University of California Press.

Delaware National Estuarine Research Reserve.1999. Delaware National Estuarine Research Estuarine Profile, Delaware Department of Natural Resources and Environmental Control, Dover. DE.

Delaware Coastal Programs. 2011. Preparing for sea level rise: Sea Level Rise Initiative Project Compendium September 2011, Delaware Department of Natural Resources and Environmental Control, Dover, DE.

Daiber, F. 1986. Conservation of tidal marshes, Van Nostrand Rienhold Company Inc.

Daiber, F. C., and C. T. Roman. 1988. Tidal marshes, p. 95-123. *In* T. Bryant and J. Pennock [eds.], The Delaware Estuary: Rediscovering a forgotten resource. University of Delaware SeaGrant College Program.

Day, R., and R. Holz. 1990. An inventory of wetland impoundments in the coastal zone of Louisiana, USA: historical trends. Environmental Management **14**: 229-240.

Davis, G. H. 1987. Land subsidence and sea level rise on the Atlantic Coastal Plain of the United States. Environmental Geology and Water Sciences **10**: 67-80, doi:10.1007/BF02574663

DeLaune, R., W. Patrick, and R. Buresh. 1978. Sedimentation rates determined by ^{137}Cs dating in a rapidly accreting salt marsh. Nature **275**: 532–533.

DeLaune, R., J. H. Whitcomb, W. Patrick, J. H. Pardue, and S. Pezeshki. 1989. Accretion and canal impacts in a rapidly subsiding wetland I: ^{137}Cs and ^{210}Pb techniques. Estuaries **12**: 247–259.

Delaware Division of Fish & Wildlife. 2001. Northern Delaware Wetland Rehabilitation Program Brochure, Delaware Department of Natural Resources and Environmental Control, Dover, DE.

Drexler, J. Z. 2011. Peat formation processes through the millennia in tidal marshes of the Sacramento–San Joaquin Delta, California, USA. Estuaries and Coasts **34**: 900-911, doi:10.1007/s12237-011-9393-7

Fletcher, C. H., H. J. Knebel, and J. C. Craft. 1990. Holocene evolution of an estuarine coast and tidal wetlands. Geological Society of America Bulletin **102**: 283-297.

Friedrichs, C. T., and J. E. Perry. 2001. Tidal salt marsh morphodynamics: a synthesis. Journal of Coastal Research **81**: 7–37.

Gilmore, G. 2008. Practical gamma-ray spectrometry, 2nd ed. John Wiley and Sons.

Gleason, M. L., D. A. Elmer, N. C. Pien, and J. S. Fisher. 1979. Effects of stem density upon sediment retention by salt marsh cord grass, *Spartina alterniflora Loisel*. Estuaries **2**: 271, doi:10.2307/1351574

Graustein, C., and K. K. Turekian. 1986. Vertical profile of aerosol scavenging profiles. Geology **91**: 14,355-14,366.

Heiri, O., A. Lotter, and G. Lemcke. 2001. Loss on ignition as a method for estimating organic and carbonate content in sediments: reproducibility and comparability of results. Journal of Paleolimnology **25**: 101-110.

Inn, K., Z. Lin, W. Liggett, F. Schima, P. Krey, M. Feiner, C. Liu, R. Holloway, J. Harvey, I. L. Larsen, T. Beasley, C. A. Huh, D. McCurdy, P. Germain, M. Yamamoto, J. Handl, D. S. Popplewell, M. J. Woods, S. Jerome, T. H. Bates, A. Holms, B. R. Harvey, K. J. Odell, B. B. Warren, and P. Young. 1996. Low-level radioactivity ocean sediment standard reference material. Applied Radiation and Isotopes **47**: 967-970.

Kearney, M., J. Stevenson, and L. Ward. 1994. Spatial and temporal changes in marsh vertical accretion rates at Monie Bay: Implications for sea-level rise. Journal of Coastal Research **10**: 1010-1020.

Kennish, M. 2001. Coastal salt marsh systems in the US: a review of anthropogenic impacts. Journal of Coastal Research **17**: 731-748.

Kim, G., N. Hussain, T. M. Church, and W. L. Carey. 1997. The fallout isotope ^{207}Bi in a Delaware salt marsh : a comparison with ^{210}Pb and ^{137}Cs as a geochronological tool. The Science of the Total Environment **196**: 31-41.

Knaus, R. M., and D. L. van Gent. 1989. Accretion and canal impacts in a rapidly subsiding wetland. III. A new soil horizon marker method for measuring recent accretion. Estuaries **12**: 269, doi:10.2307/1351906

Knebel, H. J., C. H. Fletcher III, and J. C. Kraft. 1988. Late Wisconsinan-Holocene paleogeography of Delaware Bay; a large coastal plain estuary. Marine Geology **83**: 115–133.

Kraft, J. C. 1979. The coastal environment, p. 31-66. *In* J. Kraft and W. Carey [eds.], Transactions of the Delaware Academy of Science. The Delaware Academy of Science, Wilmington, DE.

Krishnaswamy, S., D. Lal, J. Martin, and M. Meybeck. 1971. Geochronology of lake sediments. Earth and Planetary Science Letters **11**: 407-414.

Leonard, L. A., and M. E. Luther. 1995. Flow hydrodynamics in tidal marsh canopies. Limnology and Oceanography **40**: 1474–1484.

Leonard, L. A., D. J. Reed, and A. Lynn. 2002. Hydrodynamics and sediment transport through tidal marsh canopies. Journal of Coastal Research **36**: 459–469.

Logan, M. 2010. Nested ANOVA, p. 283-312. *In* Biostatistical Design and Analysis Using R. Wiley-Blackwell., doi:10.1002/9781444319620.ch11

Montague, C. L., A. V. Zale, and H. F. Percival. 1987. Ecological effects of coastal marsh impoundments: A review. Environmental Management **11**: 743-756, doi:10.1007/BF01867242

Moskalski, S. 2010. Mechanisms of sediment transport and deposition in marshes of the St. Jones River, Delaware. Ph. D. thesis. University of Delaware.

Moskalski, S. M., and C. K. Sommerfield. 2012. Suspended sediment deposition and trapping efficiency in a Delaware salt marsh. Geomorphology **139-140**: 195-204, doi:10.1016/j.geomorph.2011.10.018

Mudd, S. M., A. D'Alpaos, and J. T. Morris. 2010. How does vegetation affect sedimentation on tidal marshes? Investigating particle capture and hydrodynamic controls on biologically mediated sedimentation. Journal of Geophysical Research **115**: 1-14, doi:10.1029/2009JF001566

Nepf, H. 1999. Drag, turbulence, and diffusion in flow through emergent vegetation. Water Resources Research **35**: 479–489.

Neubauer, S. 2008. Contributions of mineral and organic components to tidal freshwater marsh accretion. Estuarine, Coastal and Shelf Science **78**: 78-88, doi:10.1016/j.ecss.2007.11.011

Nikitina, D. L., J. E. Pizzuto, R. a Schwimmer, and K. W. Ramsey. 2000. An updated Holocene sea-level curve for the Delaware coast. Marine Geology **171**: 7-20, doi:10.1016/S0025-3227(00)00104-3

Nyman, J. A., R. DeLaune, H. Roberts, and W. Patrick Jr. 1993. Relationship between vegetation and soil formation in a rapidly submerging coastal marsh. Marine Ecology Progress Series **96**: 269–279.

Olsen, C., H. Simpson, T. Peng, R. Bopp, and R. Trier. 1981. Sediment mixing and accumulation rate effects on radionuclide depth profiles in Hudson Estuary sediments. Journal of Geophysical Research **86**: 11020-11028.

Philipp, K. 2005. History of Delaware and New Jersey salt marsh restoration sites. Ecological Engineering **25**: 214-230, doi:10.1016/j.ecoleng.2005.04.010

Plater, A. J., M. R. Wright, B. P. Horton, Y. Zong, M. M. Rutherford, E. Y. Haworth, and P. G. Appleby. 2000. Holocene tidal levels and sedimentation rates using a diatom-based palaeo-environmental reconstruction: the Tees estuary, northeastern England. The Holocene **10**: 441-452, doi:10.1191/095968300673546360

Portnoy, J., and A. Giblin. 1997. Effects of historic tidal restrictions on salt marsh sediment chemistry. Biogeochemistry **36**: 275–303.

Prime Hook National Wildlife Refuge. 2010. Final environmental assessment for Dune Work at Prime Hook National Wildlife Refuge, U.S. FWS-DOI. 77pp.

Prime Hook National Wildlife Refuge. 2012. Draft comprehensive conservation plan and environmental impact statement May 2012 volume I, U.S. FWS-DOI. 656 pp.

Ray, G. L. 2007. Thin layer placement of dredged material on coastal wetlands : A review of the technical and scientific literature,.

Reed, D. J. 1989. Patterns of sediment deposition in subsiding coastal salt marshes, Terrebonne Bay, Louisiana: The role of winter storms. Estuaries **12**: 222, doi:10.2307/1351901

Reed, D. J. 1992. Effect of weirs on sediment deposition in Louisiana coastal marshes. Environmental Management **16**: 55–65.

Reed, D. J. 1995. The response of coastal marshes to sea-level rise: Survival or submergence? Earth Surface Processes and Landforms **20**: 39-48, doi:10.1002/esp.3290200105

Reed, D. J., D. A. Bishara, D. R. Cahoon, J. Donnelly, M. Kearney, A. S. Kolker, L. L. Leonard, R. A. Orson, and J. C. Stevenson. 2008. Site-specific scenarios for wetlands accretion as sea level rises in the Mid-Atlantic region, *In* Background documents supporting climate change science program synthesis and assessment Product 4.q.

Reed, D. J., N. de Luca, and A. L. Foote. 1997. Effect of hydrologic management on marsh surface sediment deposition in Coastal Louisiana. Estuaries **20**: 301-311, doi:10.2307/1352345

Reed, D. J., T. Spencer, A. L. Murray, J. R. French, and L. Leonard. 1999. Marsh surface sediment deposition and the role of tidal creeks: Implications for created and managed coastal marshes. Journal of Coastal Conservation **5**: 81-90, doi:10.1007/BF02802742

Richard, G. A. 1978. Seasonal and Environmental Variations in Sediment Accretion in a Long Island Salt Marsh. Estuaries **1**: 29, doi:10.2307/1351647

Ritchie, J. C., and J. R. McHenry. 1990. Application of radioactive fallout cesium-137 for measuring soil erosion and sediment accumulation rates and patterns: a review. Journal of Environmental Quality **19**: 215-233.

Robbins, J. A. 1978. Geochemical and geophysical applications of radioactive lead, p. 285-393. *In* J.O. Nriagu [ed.], The Biogeochemistry of Lead in the Environment. Elsevier.

Roman, C., J. Peck, J. Allen, and J. King. 1997. Accretion of a New England (USA) salt marsh in response to inlet migration, storms, and sea-level rise. Estuarine, Coastal and Shelf Science **45**: 717-727, doi:10.1006/ecss.1997.0236

Rooth, J., and J. Stevenson. 2000. Sediment deposition patterns in *Phragmites australis* communities: Implications for coastal areas threatened by rising sea-level. Wetlands Ecology and Management **8**: 173–183.

Stocks, K. I., and J. F. Grassle. 2003. Benthic macrofaunal communities in partially impounded salt marshes in Delaware: Comparisons with natural marshes and responses to sediment exposure. Estuaries **26**: 777-789, doi:10.1007/BF02711988

Stuart, D. G. 2010. Accumulation of sediment and radionuclides in tidal marshes of the Murderkill River Estuary, Delaware. M.S. thesis. University of Delaware.

Stumpf, R. 1983. The process of sedimentation on the surface of a salt marsh. Estuarine, Coastal and Shelf Science **17**: 495-508.

Sturdevant, A. 2003. Ecological functions of an impounded marsh and three natural estuarine marshes along Woodbridge River , NY / NJ Harbor. Urban Ecosystems **6**: 163-181.

Taylor, N. 1988. Ecological characterization of Jean Lafitte National Historical Park, Louisiana: basis for a management plan. M.S. thesis. Louisiana State University.

Temmerman, S., T. J. Bouma, G. Govers, and D. Lauwaet. 2005. Flow paths of water and sediment in a tidal marsh: Relations with marsh developmental stage and tidal inundation height. Estuaries **28**: 338-352, doi:10.1007/BF02693917

Tiner, R. W. 1985. Wetlands of Delaware, U.S. Fish and Wildlife Service, National Wetlands Inventory, Newton Corner, MA and Delaware Department of Natural Resources and Environmental Control, Wetlands Section, Dover, DE. Cooperative Publication. 77 pp.

Tiner, R. W. 2001. Delaware's wetlands: Status and recent trends, National Wetlands Inventory, Newton Corner, MA and Delaware Department of Natural Resources and Environmental Control, Wetlands Section, Dover, DE. Cooperative Publication. 19 pp., doi:10.1016/B978-0-444-53839-0.00023-5

Tufford, D. L. 2005. State of knowledge report: South Carolina wetland impoundments, South Carolina SeaGrant Consortium, doi:10.1177/0047287598036004134

Turner, R. E., E. M. Swenson, C. S. Milan, and J. M. Lee. 2007. Hurricane signals in salt marsh sediments: Inorganic sources and soil volume. Limnology and Oceanography **52**: 1231–1238.

Turner, R., E. Swenson, and C. Milan. 2000. Organic and inorganic contributions to vertical accretion in salt marsh sediments, p. 583–595. *In* M.P. Weinstien and D.A. Kreeger [eds.], Concepts and controversies in tidal marsh ecology. Springer.

van Proosdij, D., R. Davidson-Arnott, and J. Ollerhead. 2006. Controls on spatial patterns of sediment deposition across a macro-tidal salt marsh surface over single tidal cycles. Estuarine, Coastal and Shelf Science **69**: 64-86, doi:10.1016/j.ecss.2006.04.022

Wetlands Research Associates Inc. 1995. Tidal wetlands characterization - Then and now, Delaware River Basin Commission, 84 pp.

Windham, L. 2001. Comparison of biomass production and decomposition between *Phragmites australis* (common reed) and *Spartina patens* (salt hay grass) in brackish tidal marshes of New Jersey, USA. Wetlands **21**: 179-188, doi:10.1672/0277-5212(2001)021[0179:COBPAD]2.0.CO;2

Yang, S. 1999. Tidal wetland sedimentation in the Yangtze Delta. Journal of Coastal Research **15**: 1091-1099.

Zhang, W., K. Ungar, J. Chen, N. St-Amant, and B. L. Tracy. 2009. An accurate method for the determination of ^{226}Ra activity concentrations in soil. Journal of Radioanalytical and Nuclear Chemistry **280**: 561-567, doi:10.1007/s10967-009-7452-3

Appendix A

PHYSCIAL PROPERTY DATA

Appendix A contains the physical property data for each core sample interval.

Core	Depth Interval (cm)	LOI (%)	Water Content (% weight)	Porosity (ϕ)	Dry Bulk Density (g cm^{-3})	Wet Bulk Density (g cm^{-3})
BBRC-1	0-2	28	76.4	0.88	0.28	1.17
BBRC-1	4-6	23	67.2	0.82	0.41	1.25
BBRC-1	8-10	27	67.7	0.82	0.40	1.24
BBRC-1	12-14	20	63.1	0.80	0.48	1.29
BBRC-1	16-18	18	59.6	0.77	0.54	1.33
BBRC-1	20-22	16	56.7	0.76	0.59	1.36
BBRC-1	24-26	18	58.1	0.76	0.56	1.35
BBRC-1	28-30	20	64.6	0.81	0.45	1.28
BBRC-1	32-34	24	69.7	0.84	0.37	1.23
BBRC-1	36-38	27	70.2	0.84	0.36	1.22
BBRC-1	40-42	24	70.5	0.84	0.36	1.23
BBRC-1	44-46	25	69.9	0.84	0.37	1.23
BBRC-1	48-50	28	69.5	0.83	0.38	1.23
BBRC-1	52-54	26	67.5	0.82	0.41	1.25
BBRC-1	56-58	23	64.6	0.80	0.45	1.27
BBRC-1	60-62	25	69.5	0.83	0.38	1.23
BBRC-1	64-66	29	73.3	0.86	0.32	1.20
BBRC-1	68-70	31	74.0	0.86	0.31	1.19
BBRC-1	72-74	32	73.4	0.85	0.32	1.19
BBRC-1	76-78	32	74.0	0.86	0.31	1.19
BBRC-2	0-2	17	61.8	0.79	0.50	1.31
BBRC-2	4-6	15	60.8	0.79	0.52	1.32
BBRC-2	8-10	23	67.4	0.82	0.41	1.25

Core	Depth Interval (cm)	LOI (%)	Water Content (% weight)	Porosity (ϕ)	Dry Bulk Density (g cm^{-3})	Wet Bulk Density (g cm^{-3})
BBRC-2	12-14	22	64.9	0.81	0.45	1.27
BBRC-2	16-18	29	67.9	0.82	0.40	1.24
BBRC-2	20-22	27	65.2	0.80	0.44	1.26
BBRC-2	24-26	31	74.8	0.86	0.30	1.18
BBRC-2	28-30	32	69.9	0.83	0.37	1.22
BBRC-2	32-34	29	67.6	0.82	0.40	1.24
BBRC-2	36-38	39	74.1	0.85	0.31	1.18
BBRC-2	40-42	46	76.7	0.86	0.27	1.15
BBRC-2	44-46	37	73.1	0.85	0.32	1.19
BBRC-2	48-50	33	71.3	0.84	0.35	1.21
BBRC-2	52-54	34	74.4	0.86	0.30	1.18
BBRC-2	56-58	34	73.2	0.85	0.32	1.19
BBRC-2	60-62	24	63.2	0.79	0.47	1.29
BBRC-2	64-66	24	63.5	0.79	0.47	1.28
BBRC-2	68-70	26	63.2	0.79	0.47	1.28
BBRC-2	72-74	29	67.3	0.82	0.41	1.24
BBRC-2	76-78	25	64.2	0.80	0.46	1.28
BBRC-2	80-82	22	62.4	0.79	0.49	1.30
BBRC-2	84-86	17	57.4	0.76	0.58	1.36
BBRC-2	88-90	18	55.9	0.75	0.60	1.37
BBRC-2	92-94	17	53.0	0.72	0.66	1.40
BBRC-2	96-98	16	51.2	0.71	0.70	1.43
BBRC-2	100-102	15	49.0	0.69	0.74	1.45
LC-1	0-2	16	61.3	0.79	0.51	1.32
LC-1	4-6	18	62.9	0.80	0.48	1.30
LC-1	8-10	16	62.9	0.80	0.48	1.30
LC-1	12-14	36	82.0	0.90	0.20	1.13
LC-1	16-18	23	77.8	0.89	0.26	1.17
LC-1	20-22	26	66.6	0.81	0.42	1.25
LC-1	24-26	26	74.2	0.86	0.31	1.19
LC-1	28-30	26	82.1	0.91	0.20	1.14
LC-1	32-34	29	0.0			
LC-1	36-38	21	0.0			

Core	Depth Interval (cm)	LOI (%)	Water Content (% weight)	Porosity (ϕ)	Dry Bulk Density (g cm^{-3})	Wet Bulk Density (g cm^{-3})
LC-1	40-42	21	72.6	0.86	0.33	1.21
LC-2	0-2	22	71.7	0.85	0.34	1.22
LC-2	4-6	2	67.1	0.84	0.42	1.28
LC-2	8-10	20	64.8	0.81	0.45	1.28
LC-2	12-14	27	70.7	0.84	0.36	1.22
LC-2	16-18	26	72.3	0.85	0.33	1.21
LC-2	20-22	20	66.4	0.82	0.43	1.26
LC-2	24-26	19	67.3	0.83	0.41	1.26
LC-2	28-30	23	74.2	0.87	0.31	1.20
LC-2	32-34	22	73.0	0.86	0.33	1.21
LC-2	36-38	20	71.4	0.85	0.35	1.22
LC-2	40-42	18	66.8	0.82	0.42	1.26
LC-3	0-2	42	76.0	0.86	0.28	1.16
LC-3	4-6	26	67.6	0.82	0.40	1.24
LC-3	8-10	16	57.0	0.76	0.59	1.36
LC-3	12-14	17	55.0	0.74	0.62	1.38
LC-3	16-18	17	59.3	0.77	0.54	1.34
LC-3	20-22	16	74.9	0.88	0.30	1.20
LC-3	24-26	22	58.0	0.76	0.56	1.34
LC-3	28-30	28	78.5	0.89	0.25	1.16
LC-3	32-34	31	79.9	0.89	0.23	1.15
LC-3	36-38	28	76.1	0.87	0.28	1.18
LC-3	40-42	43	82.5	0.90	0.20	1.12
MH-1	0-2	19	52.8	0.72	0.66	1.40
MH-1	4-6	19	59.5	0.77	0.54	1.33
MH-1	8-10	19	67.6	0.83	0.41	1.26
MH-1	12-14	27	76.0	0.87	0.28	1.18
MH-1	16-18	28	73.7	0.86	0.31	1.19
MH-1	20-22	30	76.3	0.87	0.28	1.17
MH-1	24-26	28	74.0	0.86	0.31	1.19
MH-1	28-30	30	74.2	0.86	0.31	1.19
MH-1	32-34	31	78.6	0.89	0.25	1.16
MH-1	36-38	26	72.9	0.86	0.33	1.20
MH-1	40-42	22	70.8	0.85	0.36	1.22

Core	Depth Interval (cm)	LOI (%)	Water Content (% weight)	Porosity (ϕ)	Dry Bulk Density (g cm^{-3})	Wet Bulk Density (g cm^{-3})
MH-2	0-2	19	42.8	0.63	0.87	1.52
MH-2	4-6	13	39.8	0.61	0.95	1.58
MH-2	8-10	12	39.4	0.61	0.96	1.59
MH-2	12-14	9	35.4	0.57	1.07	1.66
MH-2	16-18	9	38.8	0.61	0.98	1.61
MH-2	20-22	11	39.5	0.61	0.96	1.59
MH-2	24-26	13	43.5	0.65	0.86	1.53
MH-2	28-30	10	42.1	0.64	0.90	1.56
MH-2	32-34	10	42.2	0.64	0.90	1.55
MH-2	36-38	11	43.5	0.65	0.87	1.54
MH-2	40-42	12	47.0	0.68	0.79	1.49
MH-3	0-2	29	78.5	0.89	0.25	1.16
MH-3	4-6	29	78.9	0.89	0.24	1.16
MH-3	8-10	33	82.1	0.91	0.20	1.13
MH-3	12-14	46	87.5	0.93	0.14	1.09
MH-3	16-18	33	82.1	0.91	0.20	1.13
MH-3	20-22	37	84.6	0.92	0.17	1.11
MH-3	24-26	39	86.7	0.93	0.15	1.10
MH-3	28-30	31	83.7	0.92	0.18	1.12
MH-3	32-34	29	81.8	0.91	0.21	1.14
MH-3	36-38	24	76.4	0.88	0.28	1.18
MH-3	40-42	19	69.5	0.84	0.38	1.24
NCBD-1	0-2	77	84.9	0.89	0.16	1.08
NCBD-1	4-6	67	85.1	0.90	0.16	1.09
NCBD-1	8-10	54	68.4	0.79	0.38	1.19
NCBD-1	12-14	28	65.9	0.81	0.43	1.26
NCBD-1	16-18	23	61.4	0.78	0.50	1.30
NCBD-1	20-22	21	63.9	0.80	0.46	1.29
NCBD-1	24-26	13	52.7	0.73	0.67	1.41
NCBD-1	28-30	6	33.1	0.55	1.14	1.71
NCBD-1	32-34	5	32.0	0.54	1.18	1.73
NCBD-1	36-38	7	37.4	0.60	1.02	1.64
NCBD-1	40-42	8	40.2	0.62	0.95	1.59
NCBD-1	44-46	9	44.7	0.66	0.84	1.52

Core	Depth Interval (cm)	LOI (%)	Water Content (% weight)	Porosity (ϕ)	Dry Bulk Density (g cm^{-3})	Wet Bulk Density (g cm^{-3})
NCBD-1	48-50	8	43.2	0.65	0.88	1.55
NCBD-2	0-2	53	80.8	0.88	0.21	1.12
NCBD-2	4-6	46	82.6	0.90	0.19	1.12
NCBD-2	8-10	21	70.0	0.84	0.37	1.23
NCBD-2	12-14	28	70.8	0.84	0.36	1.22
NCBD-2	16-18	21	70.9	0.85	0.36	1.22
NCBD-2	20-22	12	52.8	0.73	0.67	1.42
NCBD-2	24-26	17	63.1	0.80	0.48	1.30
NCBD-2	28-30	17	60.7	0.78	0.52	1.32
NCBD-2	32-34	15	55.7	0.75	0.61	1.38
NCBD-2	36-38	15	54.3	0.74	0.64	1.39
NCBD-2	40-42	16	54.4	0.74	0.63	1.39
NCBD-2	44-46	16	54.4	0.74	0.63	1.39
NCBD-2	48-50	13	47.8	0.69	0.77	1.47
NCBD-2	52-54	12	44.8	0.66	0.84	1.51
NCBD-2	56-58	12	46.3	0.68	0.80	1.49
NCBD-2	60-62	13	45.8	0.67	0.81	1.50
NCBD-2	64-66	12	46.0	0.67	0.81	1.50
NCBD-2	68-70	12	43.9	0.65	0.86	1.53
NCBD-3	0-2	70	83.7	0.89	0.18	1.09
NCBD-3	4-6	75	84.5	0.89	0.17	1.08
NCBD-3	8-10	58	82.4	0.89	0.20	1.11
NCBD-3	12-14	47	70.3	0.82	0.35	1.19
NCBD-3	16-18	36	74.8	0.86	0.30	1.18
NCBD-3	20-22	26	66.7	0.82	0.42	1.25
NCBD-3	24-26	28	72.2	0.85	0.33	1.21
NCBD-3	28-30	24	62.0	0.79	0.49	1.30
NCBD-3	32-34	12	45.3	0.67	0.83	1.51
NCBD-3	36-38	11	42.9	0.65	0.88	1.54
NCBD-3	40-42	9	40.5	0.63	0.94	1.58
NCBD-3	44-46	8	37.6	0.60	1.02	1.63
NCBD-3	48-50	11	43.5	0.65	0.87	1.54
NCBW-1	0-2	29	71.1	0.84	0.35	1.21
NCBW-1	4-6	23	63.3	0.80	0.47	1.29

Core	Depth Interval (cm)	LOI (%)	Water Content (% weight)	Porosity (ϕ)	Dry Bulk Density (g cm^{-3})	Wet Bulk Density (g cm^{-3})
NCBW-1	8-10	40	47.4	0.64	0.73	1.39
NCBW-1	12-14	13	43.0	0.64	0.87	1.54
NCBW-1	16-18	13	43.4	0.65	0.87	1.53
NCBW-1	20-22	12	42.5	0.64	0.89	1.55
NCBW-1	24-26	10	38.8	0.61	0.98	1.60
NCBW-1	28-30	11	40.3	0.62	0.94	1.58
NCBW-1	32-34	10	40.1	0.62	0.95	1.58
NCBW-1	36-38	9	39.8	0.62	0.96	1.59
NCBW-1	40-42	10	41.6	0.63	0.91	1.56
NCBW-1	44-46	10	38.3	0.60	0.99	1.61
NCBW-1	48-50	9	34.1	0.56	1.11	1.68
NCBW-1	52-54	8	33.1	0.55	1.14	1.70
NCBW-1	56-58	8	33.8	0.56	1.12	1.69
NCBW-1	60-62	9	35.0	0.57	1.09	1.67
NCBW-1	64-66	8	33.5	0.55	1.13	1.69
NCBW-2	0-2	14	43.4	0.65	0.86	1.53
NCBW-2	4-6	13	42.1	0.63	0.90	1.55
NCBW-2	8-10	12	42.3	0.64	0.89	1.55
NCBW-2	12-14	12	41.0	0.63	0.92	1.57
NCBW-2	16-18	11	37.0	0.59	1.02	1.63
NCBW-2	20-22	8	32.9	0.55	1.15	1.71
NCBW-2	24-26	7	31.1	0.53	1.20	1.74
NCBW-2	28-30	6	28.2	0.50	1.29	1.80
NCBW-2	32-34	6	26.6	0.48	1.34	1.83
NCBW-2	36-38	5	27.1	0.48	1.33	1.82
NCBW-3	0-2	27	66.3	0.81	0.42	1.26
NCBW-3	4-6	16	49.4	0.70	0.73	1.44
NCBW-3	8-10	13	41.6	0.63	0.91	1.55
NCBW-3	12-14	13	40.6	0.62	0.93	1.57
NCBW-3	16-18	11	38.6	0.60	0.98	1.60
NCBW-3	20-22	11	38.5	0.60	0.99	1.61
NCBW-3	24-26	11	39.6	0.61	0.96	1.59
NCBW-3	28-30	9	40.3	0.62	0.95	1.58
NCBW-3	32-34	11	41.3	0.63	0.92	1.56

Core	Depth Interval (cm)	LOI (%)	Water Content (% weight)	Porosity (ϕ)	Dry Bulk Density (g cm^{-3})	Wet Bulk Density (g cm^{-3})
NCBW-3	36-38	10	37.0	0.59	1.03	1.63
NCBW-3	40-42	9	34.2	0.56	1.10	1.68
NCBW-3	44-46	8	34.4	0.56	1.10	1.68
NCBW-3	48-50	9	35.0	0.57	1.08	1.67
NCGB-1	0-2	22	65.3	0.81	0.44	1.27
NCGB-1	4-6	29	74.0	0.86	0.31	1.19
NCGB-1	8-10	29	75.4	0.87	0.29	1.18
NCGB-1	12-14	32	78.0	0.88	0.26	1.16
NCGB-1	16-18	34	79.4	0.89	0.24	1.15
NCGB-1	20-22	40	79.6	0.89	0.23	1.14
NCGB-1	24-26	39	81.1	0.90	0.21	1.13
NCGB-1	28-30	34	79.3	0.89	0.24	1.15
NCGB-1	32-34	34	78.1	0.88	0.25	1.16
NCGB-1	36-38	28	75.3	0.87	0.29	1.18
NCGB-1	40-42	33	79.4	0.89	0.24	1.15
NCGB-1	44-46	32	76.1	0.87	0.28	1.17
NCGB-2	0-2	62	73.4	0.82	0.31	1.15
NCGB-2	4-6	46	81.4	0.89	0.21	1.13
NCGB-2	8-10	49	86.5	0.92	0.15	1.09
NCGB-2	12-14	7	43.8	0.66	0.87	1.54
NCGB-2	16-18	4	27.9	0.49	1.31	1.82
NCGB-2	20-22	3	28.8	0.51	1.28	1.80
NCGB-2	24-26	16	58.7	0.77	0.55	1.34
NCGB-2	28-30	14	57.9	0.77	0.57	1.36
NCGB-2	32-34	16	58.8	0.77	0.55	1.34
NCGB-2	36-38	12	50.3	0.71	0.72	1.44
NCGB-2	40-42	17	61.5	0.79	0.51	1.31
NCGB-2	44-46	19	66.8	0.82	0.42	1.26
NCGB-2	48-50	19	65.8	0.82	0.44	1.27
NCGB-2	52-54	16	60.5	0.78	0.52	1.33
NCGB-2	56-58	15	57.0	0.76	0.59	1.36
NCGB-2	60-62	13	55.8	0.75	0.61	1.38
NCGB-2	64-66	14	54.3	0.74	0.64	1.39
NCGB-2	68-70	10	44.1	0.66	0.85	1.53

Core	Depth Interval (cm)	LOI (%)	Water Content (% weight)	Porosity (ϕ)	Dry Bulk Density (g cm^{-3})	Wet Bulk Density (g cm^{-3})
NCGB-3	0-2	84	77.0	0.82	0.25	1.09
NCGB-3	4-6	50	81.3	0.89	0.21	1.12
NCGB-3	8-10	32	76.2	0.87	0.28	1.17
NCGB-3	12-14	57	87.4	0.92	0.14	1.08
NCGB-3	16-18	29	72.9	0.85	0.33	1.20
NCGB-3	20-22	27	75.9	0.87	0.28	1.18
NCGB-3	24-26	29	77.9	0.88	0.26	1.16
NCGB-3	28-30	30	78.6	0.89	0.25	1.16
NCGB-3	32-34	24	69.8	0.84	0.37	1.23
NCGB-3	36-38	22	67.3	0.82	0.41	1.25
NCGB-3	40-42	18	68.0	0.83	0.40	1.25
NCGB-3	44-46	18	63.9	0.80	0.46	1.29
NCGB-3	48-50	27	70.2	0.84	0.36	1.22
NCGB-3	52-54	29	72.6	0.85	0.33	1.20
NCGB-3	56-58	26	74.3	0.86	0.31	1.19
NCGB-3	60-62	22	77.5	0.89	0.26	1.17
NCGB-3	64-66	18	66.1	0.82	0.43	1.27
NCGB-3	68-70	14	47.4	0.68	0.78	1.48
NCLM-1	0-2	23	59.2	0.77	0.54	1.32
NCLM-1	4-6	18	55.0	0.74	0.62	1.38
NCLM-1	8-10	18	54.5	0.74	0.63	1.38
NCLM-1	12-14	16	52.0	0.72	0.68	1.42
NCLM-1	16-18	14	50.3	0.71	0.72	1.44
NCLM-1	20-22	18	54.6	0.74	0.63	1.38
NCLM-1	24-26	17	53.4	0.73	0.65	1.40
NCLM-1	28-30	17	55.5	0.74	0.61	1.37
NCLM-1	32-34	17	54.9	0.74	0.62	1.38
NCLM-1	36-38	18	52.3	0.72	0.67	1.41
NCLM-1	40-42	21	57.4	0.75	0.57	1.35
NCLM-1	44-46	21	60.6	0.78	0.52	1.32
NCLM-1	48-50	18	53.0	0.72	0.66	1.40
NCLM-2	0-2	16	52.3	0.72	0.67	1.41
NCLM-2	4-6	14	47.6	0.68	0.77	1.47
NCLM-2	8-10	12	47.4	0.68	0.78	1.48

Core	Depth Interval (cm)	LOI (%)	Water Content (% weight)	Porosity (ϕ)	Dry Bulk Density (g cm^{-3})	Wet Bulk Density (g cm^{-3})
NCLM-2	12-14	12	47.4	0.68	0.78	1.48
NCLM-2	16-18	12	47.1	0.68	0.79	1.48
NCLM-2	20-22	13	47.9	0.69	0.77	1.47
NCLM-2	24-26	13	48.0	0.69	0.77	1.47
NCLM-2	28-30	13	48.3	0.69	0.76	1.47
NCLM-2	32-34	14	48.4	0.69	0.75	1.46
NCLM-2	36-38	14	49.7	0.70	0.73	1.45
NCLM-2	40-42	16	51.1	0.71	0.70	1.43
NCLM-2	44-46	17	55.2	0.74	0.62	1.38
NCLM-2	48-50	15	50.7	0.71	0.71	1.43
NCLM-2	52-54	17	51.1	0.71	0.70	1.42
NCLM-2	56-58	15	51.6	0.72	0.69	1.42
NCLM-2	60-62	13	44.3	0.66	0.85	1.52
NCLM-2	64-66	11	41.7	0.63	0.91	1.56
NCLM-2	68-70	26	40.8	0.60	0.90	1.51
NCLM-3	0-2	20	57.1	0.75	0.58	1.35
NCLM-3	4-6	18	57.6	0.76	0.57	1.35
NCLM-3	8-10	25	68.0	0.82	0.40	1.24
NCLM-3	12-14	22	66.4	0.82	0.42	1.26
NCLM-3	16-18	18	58.4	0.76	0.56	1.34
NCLM-3	20-22	23	62.1	0.79	0.49	1.30
NCLM-3	24-26	20	56.6	0.75	0.59	1.36
NCLM-3	28-30	20	58.5	0.76	0.55	1.34
NCLM-3	32-34	18	55.0	0.74	0.62	1.38
NCLM-3	36-38	18	53.6	0.73	0.65	1.39
NCLM-3	40-42	20	56.1	0.75	0.60	1.36
NCLM-3	44-46	21	55.8	0.74	0.60	1.36
NCLM-3	48-50	21	56.4	0.75	0.59	1.36
NCRE-1	0-2	19	58.2	0.76	0.56	1.34
NCRE-1	4-6	18	58.8	0.77	0.55	1.34
NCRE-1	8-10	19	61.3	0.78	0.51	1.31
NCRE-1	12-14	19	63.1	0.80	0.48	1.30
NCRE-1	16-18	20	64.3	0.81	0.46	1.28
NCRE-1	20-22	19	62.2	0.79	0.49	1.31

Core	Depth Interval (cm)	LOI (%)	Water Content (% weight)	Porosity (ϕ)	Dry Bulk Density (g cm^{-3})	Wet Bulk Density (g cm^{-3})
NCRE-1	24-26	15	59.0	0.77	0.55	1.34
NCRE-1	28-30	17	62.1	0.79	0.50	1.31
NCRE-1	32-34	15	57.0	0.76	0.59	1.36
NCRE-1	36-38	14	57.1	0.76	0.59	1.36
NCRE-1	40-42	14	52.9	0.73	0.66	1.41
NCRE-1	44-46	14	50.7	0.71	0.71	1.44
NCRE-1	48-50	14	52.1	0.72	0.68	1.42
NCRE-1	52-54	13	52.1	0.72	0.68	1.42
NCRE-1	56-58	14	52.1	0.72	0.68	1.42
NCRE-1	60-62	12	47.2	0.68	0.78	1.48
NCRE-1	64-66	14	48.8	0.69	0.75	1.46
NCRE-1	68-70	13	49.8	0.70	0.73	1.45
NCRE-1	72-74	12	47.4	0.68	0.78	1.48
NCRE-1	76-78	12	48.7	0.70	0.75	1.46
NCRE-1	80-82	14	50.5	0.71	0.71	1.44
NCRE-1	84-86	16	55.3	0.74	0.62	1.38
NCRE-1	88-90	14	52.2	0.72	0.68	1.42
NCRE-1	92-94	13	52.2	0.72	0.68	1.42
NCRE-2	0-2	19	64.1	0.80	0.46	1.29
NCRE-2	4-6	24	68.5	0.83	0.39	1.24
NCRE-2	8-10	25	69.7	0.84	0.37	1.23
NCRE-2	12-14	24	68.9	0.83	0.38	1.24
NCRE-2	16-18	24	66.0	0.81	0.43	1.26
NCRE-2	20-22	18	62.1	0.79	0.50	1.31
NCRE-2	24-26	19	60.7	0.78	0.52	1.32
NCRE-2	28-30	17	59.1	0.77	0.55	1.34
NCRE-2	32-34	17	57.4	0.76	0.58	1.36
NCRE-2	36-38	15	52.1	0.72	0.68	1.42
NCRE-2	40-42	15	51.4	0.71	0.69	1.42
NCRE-2	44-46	17	57.2	0.76	0.58	1.36
NCRE-2	48-50	19	58.1	0.76	0.56	1.34
NCRE-2	52-54	15	54.3	0.74	0.64	1.39
NCRE-2	56-58	14	51.0	0.71	0.70	1.43
NCRE-2	60-62	12	46.6	0.68	0.80	1.49

Core	Depth Interval (cm)	LOI (%)	Water Content (% weight)	Porosity (ϕ)	Dry Bulk Density (g cm^{-3})	Wet Bulk Density (g cm^{-3})
NCRE-2	64-66	11	45.7	0.67	0.82	1.51
NCRE-2	68-70	10	43.8	0.65	0.86	1.53
NCRE-2	72-74	9	46.9	0.68	0.79	1.49
NCRE-2	76-78	10	45.3	0.67	0.83	1.52
NCRE-2	80-82	9	46.7	0.68	0.80	1.50
NCRE-2	84-86	9	47.6	0.69	0.78	1.49
NCRE-2	88-90	9	47.3	0.69	0.79	1.49
NCRE-3	0-2	30	69.5	0.83	0.37	1.22
NCRE-3	4-6	22	61.9	0.79	0.50	1.30
NCRE-3	8-10	25	60.8	0.77	0.51	1.31
NCRE-3	12-14	23	66.6	0.82	0.42	1.26
NCRE-3	16-18	19	58.8	0.77	0.55	1.34
NCRE-3	20-22	21	62.4	0.79	0.49	1.30
NCRE-3	24-26	16	53.4	0.73	0.65	1.40
NCRE-3	28-30	16	52.3	0.72	0.67	1.41
NCRE-3	32-34	17	52.7	0.72	0.67	1.41
NCRE-3	36-38	18	52.7	0.72	0.66	1.40
NCRE-3	40-42	18	53.5	0.73	0.65	1.40
NCRE-3	44-46	21	58.7	0.76	0.55	1.33
NCRE-3	48-50	21	61.1	0.78	0.51	1.31
NCRE-3	52-54	16	52.6	0.72	0.67	1.41
NCRE-3	56-58	16	52.4	0.72	0.67	1.41
NCRE-3	60-62	10	42.6	0.64	0.89	1.55
NCRE-3	64-66	9	37.2	0.59	1.03	1.63
NCRE-3	68-70	9	35.6	0.58	1.07	1.66
PK-1	0-2	37	69.8	0.82	0.37	1.21
PK-1	4-6	20	59.8	0.77	0.53	1.33
PK-1	8-10	27	57.0	0.74	0.57	1.34
PK-1	12-14	31	69.7	0.83	0.37	1.22
PK-1	16-18	25	66.1	0.81	0.43	1.26
PK-1	20-22	30	70.7	0.84	0.36	1.22
PK-1	24-26	27	68.2	0.82	0.39	1.24
PK-1	28-30	39	76.1	0.87	0.28	1.17
PK-1	32-34	34	73.5	0.85	0.32	1.19

Core	Depth Interval (cm)	LOI (%)	Water Content (% weight)	Porosity (ϕ)	Dry Bulk Density (g cm^{-3})	Wet Bulk Density (g cm^{-3})
PK-1	36-38	29	73.1	0.85	0.32	1.20
PK-1	40-42	24	68.5	0.83	0.39	1.24
PK-1	44-46	17	61.7	0.79	0.50	1.31
PK-1	48-50	25	69.4	0.83	0.38	1.23
PK-1	52-54	21	65.9	0.81	0.43	1.27
PK-1	56-58	15	55.4	0.75	0.62	1.38
PK-2	0-2	43	76.9	0.87	0.27	1.16
PK-2	4-6	20	60.0	0.78	0.53	1.32
PK-2	8-10	17	60.8	0.78	0.52	1.32
PK-2	12-14	18	59.9	0.78	0.53	1.33
PK-2	16-18	17	61.0	0.79	0.52	1.32
PK-2	20-22	21	62.4	0.79	0.49	1.30
PK-2	24-26	15	55.4	0.75	0.61	1.38
PK-2	28-30	16	58.7	0.77	0.56	1.34
PK-2	32-34	15	57.3	0.76	0.58	1.36
PK-2	36-38	14	55.2	0.75	0.62	1.38
PK-2	40-42	14	54.8	0.74	0.63	1.39
PK-2	44-46	12	53.3	0.73	0.66	1.41
PK-2	48-50	15	56.9	0.76	0.59	1.36
PK-2	52-54	22	66.4	0.82	0.42	1.26
PK-2	56-58	29	73.5	0.86	0.32	1.20
PK-2	60-62	22	65.5	0.81	0.44	1.27
PK-3	0-2	23	74.9	0.87	0.30	1.19
PK-3	4-6	22	69.1	0.83	0.38	1.24
PK-3	8-10	22	67.6	0.83	0.41	1.25
PK-3	12-14	19	64.6	0.81	0.45	1.28
PK-3	16-18	25	69.3	0.83	0.38	1.23
PK-3	20-22	24	73.6	0.86	0.32	1.20
PK-3	24-26	20	67.5	0.83	0.41	1.26
PK-3	28-30	19	67.0	0.82	0.42	1.26
PK-3	32-34	20	69.4	0.84	0.38	1.24
PK-3	36-38	26	75.2	0.87	0.29	1.19
PK-3	40-42	19	68.0	0.83	0.40	1.25
PK-3	44-46	19	69.9	0.84	0.37	1.24

Core	Depth Interval (cm)	LOI (%)	Water Content (% weight)	Porosity (ϕ)	Dry Bulk Density (g cm^{-3})	Wet Bulk Density (g cm^{-3})
PK-3	48-50	17	67.2	0.83	0.41	1.26
PK-3	52-54	18	68.7	0.84	0.39	1.25
PK-3	56-58	15	64.8	0.81	0.45	1.29
PK-3	60-62	17	69.1	0.84	0.38	1.24
PM-1	0-2	52	77.5	0.86	0.26	1.14
PM-1	4-6	10	42.1	0.64	0.90	1.56
PM-1	8-10	8	44.0	0.66	0.86	1.54
PM-1	12-14	39	76.7	0.87	0.27	1.16
PM-1	16-18	34	77.3	0.88	0.26	1.16
PM-1	20-22	28	71.8	0.85	0.34	1.21
PM-1	24-26	22	64.6	0.81	0.45	1.28
PM-1	28-30	14	51.4	0.72	0.69	1.43
PM-1	32-34	12	40.5	0.62	0.93	1.57
PM-1	36-38	10	32.9	0.55	1.14	1.70
PM-1	38-40	8	28.0	0.49	1.29	1.79
PM-10	0-2	72	84.0	0.89	0.17	1.09
PM-10	4-6	76	87.2	0.91	0.14	1.07
PM-10	8-10	78	90.9	0.94	0.10	1.05
PM-10	12-14	71	87.8	0.92	0.13	1.07
PM-10	16-18	64	84.7	0.90	0.17	1.09
PM-10	20-22	54	81.5	0.89	0.21	1.12
PM-10	24-26	59	86.7	0.92	0.14	1.09
PM-10	28-30	59	88.0	0.93	0.13	1.08
PM-10	32-34	45	86.3	0.92	0.15	1.10
PM-10	36-38	44	85.7	0.92	0.16	1.10
PM-10	40-42	31	79.1	0.89	0.24	1.15
PM-11	0-2	75	87.3	0.91	0.14	1.07
PM-11	4-6	74	88.1	0.92	0.13	1.07
PM-11	8-10	75	87.2	0.91	0.14	1.07
PM-11	12-14	79	86.8	0.90	0.14	1.07
PM-11	16-18	64	87.5	0.92	0.13	1.08
PM-11	20-22	52	84.0	0.91	0.18	1.11
PM-11	24-26	46	83.8	0.91	0.18	1.11
PM-11	28-30	60	87.0	0.92	0.14	1.08

Core	Depth Interval (cm)	LOI (%)	Water Content (% weight)	Porosity (ϕ)	Dry Bulk Density (g cm^{-3})	Wet Bulk Density (g cm^{-3})
PM-11	32-34	61	87.2	0.92	0.14	1.08
PM-11	36-38	47	86.5	0.92	0.15	1.10
PM-11	40-42	39	84.7	0.92	0.17	1.11
PM-12	0-2	41	78.5	0.88	0.25	1.15
PM-12	4-6	62	86.7	0.92	0.14	1.08
PM-12	8-10	54	85.9	0.92	0.15	1.09
PM-12	12-14	32	76.8	0.88	0.27	1.17
PM-12	16-18	27	75.0	0.87	0.30	1.19
PM-12	20-22	16	85.0	0.93	0.17	1.12
PM-12	24-26	37	83.5	0.91	0.19	1.12
PM-12	28-30	19	73.4	0.86	0.32	1.21
PM-12	32-34	18	69.5	0.84	0.38	1.24
PM-12	36-38	23	76.9	0.88	0.27	1.18
PM-12	40-42	16	71.1	0.85	0.35	1.23
PM-2	0-2	36	65.9	0.80	0.42	1.24
PM-2	4-6	27	62.1	0.78	0.49	1.29
PM-2	8-10	37	68.2	0.81	0.39	1.22
PM-2	12-14	22	62.5	0.79	0.49	1.30
PM-2	16-18	11	48.3	0.69	0.76	1.47
PM-2	20-22	19	57.9	0.76	0.57	1.35
PM-2	24-26	20	57.2	0.75	0.58	1.35
PM-2	28-30	8	36.2	0.58	1.05	1.65
PM-2	32-34	6	32.3	0.54	1.17	1.72
PM-2	36-38	6	33.3	0.55	1.14	1.71
PM-2	40-42	7	37.1	0.59	1.03	1.64
PM-2	44-46	7	35.9	0.58	1.06	1.66
PM-2	48-50	7	38.0	0.60	1.01	1.63
PM-2	52-54	9	41.2	0.63	0.93	1.57
PM-2	56-58	6	38.9	0.61	0.99	1.62
PM-2	60-62	7	40.5	0.63	0.95	1.59
PM-2	64-66	9	44.5	0.66	0.85	1.53
PM-2	68-70	9	47.3	0.69	0.78	1.49
PM-2	72-74	9	47.6	0.69	0.78	1.49
PM-2	76-78	10	45.8	0.67	0.82	1.51

Core	Depth Interval (cm)	LOI (%)	Water Content (% weight)	Porosity (ϕ)	Dry Bulk Density (g cm^{-3})	Wet Bulk Density (g cm^{-3})
PM-2	80-82	10	47.6	0.69	0.78	1.49
PM-2	84-86	10	45.4	0.67	0.83	1.51
PM-2	88-90	10	47.7	0.69	0.78	1.48
PM-2	92-94	10	48.8	0.70	0.75	1.47
PM-3	0-2	34	76.8	0.87	0.27	1.17
PM-3	4-6	14	49.2	0.70	0.74	1.45
PM-3	8-10	8	34.5	0.56	1.10	1.68
PM-3	12-14	7	28.0	0.49	1.30	1.80
PM-3	16-18	6	30.5	0.52	1.22	1.76
PM-3	20-22	5	26.8	0.48	1.34	1.83
PM-3	24-26	4	27.0	0.48	1.34	1.83
PM-3	28-30	3	19.6	0.38	1.61	2.00
PM-3	32-34	3	17.9	0.36	1.68	2.04
PM-3	36-38	3	18.0	0.36	1.68	2.04
PM-3	40-42	3	18.8	0.37	1.64	2.02
PM-3	44-46	3	19.9	0.39	1.59	1.99
PM-3	48-50	3	19.0	0.37	1.63	2.02
PM-4	0-2	60	82.5	0.89	0.19	1.11
PM-4	4-6	61	69.4	0.79	0.36	1.17
PM-4	8-10	9	34.4	0.56	1.10	1.68
PM-4	12-14	5	26.5	0.48	1.35	1.84
PM-4	16-18	3	18.4	0.36	1.65	2.03
PM-4	20-22	3	17.2	0.35	1.71	2.06
PM-4	24-26	2	15.9	0.33	1.77	2.10
PM-4	28-30	2	15.0	0.31	1.80	2.12
PM-4	32-34	2	14.6	0.30	1.82	2.13
PM-4	36-38	2	14.5	0.30	1.83	2.14
PM-4	40-42	2	13.4	0.28	1.88	2.17
PM-4	44-46	2	12.6	0.27	1.92	2.19
PM-4	48-50	1	12.8	0.27	1.91	2.19
PM-5	0-2	58	89.6	0.94	0.11	1.07
PM-5	4-6	59	87.3	0.92	0.14	1.08
PM-5	8-10	55	81.9	0.89	0.20	1.11
PM-5	12-14	32	74.1	0.86	0.31	1.19

Core	Depth Interval (cm)	LOI (%)	Water Content (% weight)	Porosity (ϕ)	Dry Bulk Density (g cm^{-3})	Wet Bulk Density (g cm^{-3})
PM-5	16-18	16	57.9	0.76	0.57	1.35
PM-5	20-22	15	57.1	0.76	0.58	1.36
PM-5	24-26	10	43.4	0.65	0.87	1.54
PM-5	28-30	8	43.7	0.66	0.87	1.54
PM-5	32-34	8	45.7	0.68	0.82	1.52
PM-5	36-38	7	46.4	0.68	0.81	1.51
PM-5	40-42	7	47.5	0.69	0.78	1.49
PM-5	44-46	7	49.6	0.71	0.74	1.47
PM-5	48-50	8	49.8	0.71	0.73	1.46
PM-5	52-54	8	50.7	0.72	0.71	1.45
PM-5	56-58	8	52.3	0.73	0.68	1.43
PM-5	60-62	9	53.9	0.74	0.65	1.41
PM-5	64-66	11	54.1	0.74	0.64	1.40
PM-5	68-70	11	56.3	0.76	0.60	1.38
PM-5	72-74	13	50.1	0.71	0.72	1.45
PM-5	76-78	12	56.6	0.76	0.60	1.37
PM-5	80-82	14	53.9	0.74	0.64	1.40
PM-5	84-86	13	49.4	0.70	0.74	1.45
PM-5	88-90	12	51.6	0.72	0.69	1.43
PM-5	92-94	11	45.4	0.67	0.82	1.51
PM-6	0-2	61	88.0	0.93	0.13	1.08
PM-6	4-6	55	83.2	0.90	0.19	1.11
PM-6	8-10	56	85.6	0.91	0.16	1.09
PM-6	12-14	75	87.0	0.91	0.14	1.07
PM-6	16-18	55	84.6	0.91	0.17	1.10
PM-6	20-22	22	71.2	0.85	0.35	1.22
PM-6	24-26	17	63.1	0.80	0.48	1.30
PM-6	28-30	25	72.4	0.85	0.33	1.21
PM-6	32-34	13	53.7	0.74	0.65	1.40
PM-6	36-38	10	49.0	0.70	0.75	1.47
PM-6	40-42	9	49.4	0.70	0.74	1.46
PM-6	44-46	9	50.5	0.71	0.72	1.45
PM-6	48-50	9	49.7	0.71	0.74	1.46
PM-6	52-54	9	49.5	0.71	0.74	1.46

Core	Depth Interval (cm)	LOI (%)	Water Content (% weight)	Porosity (ϕ)	Dry Bulk Density (g cm^{-3})	Wet Bulk Density (g cm^{-3})
PM-6	56-58	8	52.2	0.73	0.69	1.43
PM-6	60-62	9	52.3	0.73	0.68	1.43
PM-6	64-66	9	52.6	0.73	0.68	1.43
PM-6	68-70	9	52.1	0.73	0.68	1.43
PM-6	72-74	10	51.3	0.72	0.70	1.44
PM-6	76-78	10	53.0	0.73	0.67	1.42
PM-7	0-2	40	82.1	0.90	0.20	1.13
PM-7	4-6	41	82.6	0.90	0.20	1.12
PM-7	8-10	38	83.5	0.91	0.18	1.12
PM-7	12-14	52	88.3	0.93	0.13	1.08
PM-7	16-18	50	87.0	0.93	0.14	1.09
PM-7	20-22	49	88.5	0.94	0.12	1.08
PM-7	24-26	38	83.4	0.91	0.19	1.12
PM-7	28-30	25	77.8	0.89	0.26	1.17
PM-7	32-34	30	81.9	0.91	0.21	1.14
PM-7	36-38	27	80.2	0.90	0.23	1.15
PM-7	40-42	44	84.8	0.92	0.17	1.11
PM-7	44-46	28	75.7	0.87	0.29	1.18
PM-7	48-50	25	69.9	0.84	0.37	1.23
PM-7	52-54	35	77.9	0.88	0.26	1.16
PM-7	56-58	33	79.2	0.89	0.24	1.15
PM-8	0-2	41	72.6	0.84	0.33	1.19
PM-8	4-6	28	61.5	0.78	0.50	1.29
PM-8	8-10	13	42.2	0.64	0.89	1.55
PM-8	12-14	6	25.9	0.47	1.37	1.84
PM-8	16-18	6	26.3	0.47	1.35	1.83
PM-8	20-22	5	24.9	0.45	1.40	1.87
PM-8	24-26	4	24.8	0.45	1.41	1.88
PM-8	28-30	3	24.4	0.45	1.43	1.89
PM-8	32-34	3	22.0	0.42	1.52	1.95
PM-9	0-2	69	0.0			
PM-9	4-6	62	0.0			
PM-9	8-10	45	0.0			
PM-9	12-14	8	0.0			

Core	Depth Interval (cm)	LOI (%)	Water Content (% weight)	Porosity (ϕ)	Dry Bulk Density (g cm^{-3})	Wet Bulk Density (g cm^{-3})
PM-9	16-18	7	0.0			
PM-9	20-22	7	36.1	0.58	1.06	1.66
PM-9	24-26	4	32.4	0.55	1.17	1.73
PM-9	28-30	5	31.9	0.54	1.18	1.74
PM-9	32-34	5	36.8	0.59	1.04	1.65
PM-9	36-38	6	37.8	0.60	1.02	1.64
PM-9	40-42	6	35.6	0.58	1.08	1.67
PM-9	44-46	5	35.8	0.58	1.07	1.67
PM-9	48-50	6	38.1	0.61	1.01	1.63
TH-1	0-2	22	77.3	0.89	0.27	1.17
TH-1	4-6	15	63.2	0.80	0.48	1.30
TH-1	8-10	16	64.5	0.81	0.46	1.29
TH-1	12-14	27	77.3	0.88	0.27	1.17
TH-1	16-18	32	82.7	0.91	0.20	1.13
TH-1	20-22	36	82.7	0.91	0.19	1.12
TH-1	24-26	29	70.9	0.84	0.35	1.22
TH-1	28-30	30	75.3	0.87	0.29	1.18
TH-1	32-34	44	84.9	0.92	0.17	1.11
TH-1	36-38	38	82.6	0.91	0.20	1.12
TH-1	40-42	45	84.1	0.91	0.18	1.11
TH-1	44-46	50	84.8	0.91	0.17	1.10
TH-1	48-50	53	85.2	0.91	0.16	1.10
TH-2	0-2	12	48.3	0.69	0.76	1.47
TH-2	4-6	12	50.9	0.71	0.70	1.44
TH-2	8-10	11	47.3	0.69	0.78	1.48
TH-2	12-14	10	45.8	0.67	0.82	1.51
TH-2	16-18	11	45.4	0.67	0.82	1.51
TH-2	20-22	10	47.1	0.68	0.79	1.49
TH-2	24-26	11	50.3	0.71	0.72	1.45
TH-2	28-30	11	50.0	0.71	0.73	1.45
TH-2	32-34	14	56.0	0.75	0.61	1.38
TH-2	36-38	15	57.9	0.77	0.57	1.35
TH-2	40-42	16	54.9	0.74	0.62	1.38
TH-3	0-2	23	71.0	0.85	0.35	1.22

Core	Depth Interval (cm)	LOI (%)	Water Content (% weight)	Porosity (ϕ)	Dry Bulk Density (g cm^{-3})	Wet Bulk Density (g cm^{-3})
TH-3	4-6	18	56.7	0.75	0.59	1.36
TH-3	8-10	31	71.2	0.84	0.35	1.21
TH-3	12-14	18	64.3	0.81	0.46	1.29
TH-3	16-18	27	75.0	0.87	0.30	1.19
TH-3	20-22	27	77.0	0.88	0.27	1.17
TH-3	24-26	35	79.6	0.89	0.23	1.15
TH-3	28-30	23	75.8	0.88	0.29	1.18
TH-3	32-34	26	77.1	0.88	0.27	1.17
TH-3	36-38	34	78.3	0.88	0.25	1.16
TH-3	40-42	39	81.4	0.90	0.21	1.13
TH-4	0-2	35	76.5	0.87	0.27	1.17
TH-4	4-6	14	56.8	0.76	0.59	1.37
TH-4	8-10	10	47.4	0.69	0.78	1.49
TH-4	12-14	13	54.8	0.74	0.63	1.39
TH-4	16-18	9	47.8	0.69	0.77	1.48
TH-4	20-22	7	38.4	0.61	1.00	1.62
TH-4	24-26	6	31.8	0.54	1.18	1.74
TH-4	28-30	7	31.3	0.53	1.20	1.74
TH-4	32-34	5	27.5	0.49	1.32	1.82
TH-4	36-38	4	22.2	0.42	1.51	1.94
TH-4	40-42	3	19.1	0.37	1.63	2.02
TH-4	44-46	2	16.8	0.34	1.73	2.07
TH-4	48-50	2	15.7	0.32	1.77	2.10
TH-5	0-2	21	72.8	0.86	0.33	1.21
TH-5	4-6	18	37.2	0.58	1.00	1.60
TH-5	8-10	22	68.5	0.83	0.39	1.24
TH-5	12-14	16	63.0	0.80	0.48	1.30
TH-5	16-18	19	68.0	0.83	0.40	1.25
TH-5	20-22	17	63.2	0.80	0.48	1.30
TH-5	24-26	19	67.4	0.83	0.41	1.26
TH-5	28-30	16	62.9	0.80	0.48	1.30
TH-5	32-34	18	66.0	0.82	0.43	1.27
TH-5	36-38	23	71.7	0.85	0.34	1.22
TH-5	40-42	24	72.6	0.86	0.33	1.21

Core	Depth Interval (cm)	LOI (%)	Water Content (% weight)	Porosity (ϕ)	Dry Bulk Density (g cm^{-3})	Wet Bulk Density (g cm^{-3})
TH-5	44-46	20	70.7	0.85	0.36	1.23
TH-5	48-50	19	68.1	0.83	0.40	1.25
TH-6	0-2	25	71.5	0.85	0.35	1.22
TH-6	4-6	20	69.9	0.84	0.37	1.23
TH-6	8-10	16	61.3	0.79	0.51	1.32
TH-6	12-14	12	52.8	0.73	0.67	1.42
TH-6	16-18	12	52.3	0.73	0.68	1.42
TH-6	20-22	13	58.2	0.77	0.57	1.35
TH-6	24-26	12	64.6	0.81	0.46	1.29
TH-6	28-30	13	58.4	0.77	0.56	1.35
TH-6	32-34	12	54.7	0.74	0.63	1.39
TH-6	36-38	16	47.4	0.68	0.77	1.47
TH-6	40-42	16	61.9	0.79	0.50	1.31

Appendix B

RADIONUCLIDE DATA

Appendix B contains the activities of ^{226}Ra, ^{210}Pb and ^{137}Cs for each core sample interval.

Core	Depth Interval (cm)	Sample Mass (g)	^{210}Pb Activity	^{210}Pb Uncertainty	^{226}Ra Activity	^{226}Ra Uncertainty	^{137}Cs Activity	^{137}Cs Activity Uncertainty
BBRC-1	0-2	24.29	181.31	8.23	63.27	5.87	10.04	1.33
BBRC-1	4-6	25.76	175.84	7.92	54.68	5.39	17.03	1.44
BBRC-1	8-10	31.35	169.72	7.70	48.65	5.18	22.65	1.38
BBRC-1	12-14	33.23	119.16	6.53	62.07	7.00	43.54	1.60
BBRC-1	16-18	30.15	100.99	7.23	65.42	6.76	18.62	1.27
BBRC-1	20-22	34.41	88.20	6.20	56.11	4.50	0.54	0.41
BBRC-1	24-26	32.95	104.48	6.44	57.11	5.98	0.91	0.42
BBRC-1	28-30	29.79	89.22	6.02	54.50	4.85	4.38	0.75
BBRC-1	32-34	32.85	86.95	6.09	49.87	5.41	0.63	0.39
BBRC-1	36-38	28.16	74.20	6.60	48.55	6.77	1.34	
BBRC-1	40-42	29.8	74.90	6.02	42.62	5.16	0.24	
BBRC-1	44-46	23.93	71.35	6.02	56.97	6.91	0.88	
BBRC-1	48-50	26.07	58.18	5.56	43.74	7.27	0.66	

Core	Depth Interval (cm)	Sample Mass (g)	^{210}Pb Activity	^{210}Pb Uncertainty	^{226}Ra Activity	^{226}Ra Uncertainty	^{137}Cs Activity	^{137}Cs Activity Uncertainty
BBRC-2	0-2	27.24	96.59	4.58	34.76	4.07	6.60	0.80
BBRC-2	4-6	27.5	107.32	4.66	52.11	4.26	13.10	1.02
BBRC-2	8-10	25.83	72.28	4.09	32.83	4.00	51.57	1.81
BBRC-2	12-14	23.77	64.91	4.22	35.82	4.75	38.14	1.54
BBRC-2	16-18	24.16	64.74	4.17	32.25	4.21	11.83	1.03
BBRC-2	20-22	23.65	60.45	4.12	38.28	4.16	1.17	
BBRC-2	24-26	24.11	63.68	3.94	30.37	4.34	0.97	
BBRC-2	28-30	23.46	58.32	4.02	39.38	4.31	1.10	
BBRC-2	32-34	22.25	48.45	3.94	36.94	4.36	0.43	
BBRC-2	36-38	21.71	41.33	3.38	29.56	3.79	0.31	
BBRC-2	40-42	21.66	39.27	3.64	24.24	4.32	1.17	
BBRC-2	44-46	21.7	36.33	3.76	28.00	3.66	1.53	
BBRC-2	48-50	20.57	44.23	4.04	38.37	4.37	0.88	
BBRC-2	52-54	23.18	42.60	4.18	27.20	3.85	0.40	
BBRC-2	56-58	22	45.88	4.22	39.73	4.40	0.18	
BBRC-2	60-62	28.2	41.79	3.54	40.56	3.65	0.65	0.26
BBRC-2	64-66	27.61	43.74	3.49	29.09	3.27	0.28	
BBRC-2	68-70	24.94	48.24	3.62	45.92	4.11	0.25	
BBRC-2	72-74	25.8	50.54	3.65	34.01	4.01	0.23	
BBRC-2	76-78	24.57	51.61	3.78	38.49	4.04	0.61	
BBRC-2	80-82	24.23	50.16	4.16	35.06	4.08	0.06	

Core	Depth Interval (cm)	Sample Mass (g)	^{210}Pb Activity	^{210}Pb Uncertainty	^{226}Ra Activity	^{226}Ra Uncertainty	^{137}Cs Activity	^{137}Cs Activity Uncertainty
BBRC-2	84-86	24.96	47.19	3.62	40.85	4.11	0.83	
LC-1	0-2	31.81	166.91	7.64	25.08	6.71	11.13	0.97
LC-1	4-6	31.95	169.58	7.50	39.87	5.32	11.38	0.97
LC-1	8-10	29.03	161.14	7.38	39.00	6.41	9.28	1.12
LC-1	12-14	26.45	109.14	6.72	43.28	6.18	8.17	1.20
LC-1	16-18	29.89	109.23	7.14	45.93	5.56	9.64	1.05
LC-1	20-22	28.67	119.21	6.92	24.07	6.57	9.18	1.05
LC-1	24-26	27.67	45.53	6.28	43.18	6.31	5.44	0.76
LC-1	28-30	29.59	32.75	6.05	37.03	6.22	2.96	0.68
LC-1	32-34	36.1	49.10	5.74	35.98	5.65	2.26	0.69
LC-1	36-38	27.25	33.66	6.47	40.80	6.60	1.20	
LC-1	40-42	31.09	27.73	5.89	41.80	6.12	0.22	
LC-2	0-2	20.66	130.69	5.72	31.16	4.22	6.05	0.83
LC-2	4-6	24.57	97.04	4.58	36.11	4.16	18.43	1.21
LC-2	8-10	30.47	98.86	4.27	33.74	3.76	24.91	1.27
LC-2	12-14	30.43	79.37	4.07	25.13	3.87	34.50	1.40
LC-2	16-18	21.56	78.94	4.78	36.03	4.47	17.79	1.29
LC-2	20-22	28.72	49.44	3.91	34.74	3.71	5.78	0.86
LC-2	24-26	32.88	45.37	3.80	36.42	3.67	3.93	0.74
LC-2	28-30	20.03	55.13	4.53	33.63	4.60	2.16	0.97
LC-2	32-34	26.21	40.15	3.83	34.40	3.85	1.74	0.73

Core	Depth Interval (cm)	Sample Mass (g)	^{210}Pb Activity	^{210}Pb Uncertainty	^{226}Ra Activity	^{226}Ra Uncertainty	^{137}Cs Activity	^{137}Cs Activity Uncertainty
LC-2	36-38	22.08	38.71	3.96	39.36	4.26	2.82	
LC-2	40-42	28.27	23.10	3.54	34.17	3.75	1.10	
LC-3	0-2	12.91	169.23	7.46	35.52	5.89	6.50	1.25
LC-3	4-6	17.2	158.09	6.16	32.77	5.07	7.51	1.10
LC-3	8-10	17.8	122.78	5.85	37.07	5.08	9.05	1.13
LC-3	12-14	21.07	115.04	5.25	37.10	4.69	11.90	1.15
LC-3	16-18	19.57	68.88	4.88	34.55	4.98	11.03	1.22
LC-3	20-22	19.63	40.18	4.60	24.40	4.96	11.17	1.22
LC-3	24-26	17.01	47.77	4.70	28.76	5.27	6.93	1.18
LC-3	28-30	16.41	35.45	4.68	26.85	5.44	0.00	
LC-3	32-34	13.34	33.09	4.65	34.11	5.92	0.71	
LC-3	36-38	13.51	42.29	4.96	22.23	5.07	0.84	
LC-3	40-42	12.04	23.98	4.88	25.49	6.26	0.46	
MH-1	0-2	25.03	120.35	6.54	31.98	5.27	5.29	1.04
MH-1	4-6	31.1	127.22	7.24	46.31	4.81	4.78	0.91
MH-1	8-10	28.61	83.93	7.31	57.24	6.58	3.82	0.74
MH-1	12-14	26.59	84.81	6.56	37.40	6.61	1.29	
MH-1	16-18	27.51	47.26	6.30	42.16	5.90	1.78	
MH-1	20-22	24.54	44.67	5.92	20.09	5.11	0.42	
MH-1	24-26	25.75	30.75	5.06	32.79	5.85	0.73	
MH-1	28-30	29.57	28.35	4.41	23.87	4.25	1.10	

Core	Depth Interval (cm)	Sample Mass (g)	^{210}Pb Activity	^{210}Pb Uncertainty	^{226}Ra Activity	^{226}Ra Uncertainty	^{137}Cs Activity	^{137}Cs Activity Uncertainty
MH-1	32-34	30.76	20.48	5.55	18.88	6.16	0.85	
MH-1	36-38	27.89	25.52	4.43	15.57	3.79	0.58	
MH-1	40-42	27.58	25.17	6.03	22.79	5.89	0.19	
MH-2	0-2	35.55	216.97	8.19	45.79	5.88	19.88	1.32
MH-2	4-6	33.4	147.09	7.47	37.96	6.60	14.37	1.14
MH-2	8-10	34.56	101.11	7.36	37.90	6.18	16.28	1.35
MH-2	12-14	40.04	59.11	5.66	34.34	6.27	3.05	0.67
MH-2	16-18	39.79	39.88	6.22	39.28	6.12	1.44	0.73
MH-2	20-22	36.34	47.01	6.97	33.80	5.09	3.03	0.62
MH-2	24-26	36.19	36.22	5.04	38.57	5.55	1.28	
MH-2	28-30	38.6	33.00	5.50	45.55	5.40	0.45	
MH-2	32-34	37.73	39.97	5.19	49.79	5.41	0.55	
MH-2	36-38	36.93	34.13	6.26	36.40	6.38	0.31	
MH-2	40-42	37.5	34.40	4.64	47.11	5.97	0.94	
MH-3	0-2	13.33	182.30	7.25	47.75	6.31	16.19	1.62
MH-3	4-6	17.91	128.82	6.38	42.67	5.27	40.83	1.89
MH-3	8-10	12.35	55.25	5.37	31.04	6.33	9.89	1.39
MH-3	12-14	9.98	56.88	5.76	26.11	5.12	6.32	1.69
MH-3	16-18	13.79	38.67	4.88	42.32	5.36	2.46	
MH-3	20-22	8.2	12.05	4.59	21.48	8.29	1.72	
MH-3	24-26	7.93	15.68	5.62	29.49		2.61	

Core	Depth Interval (cm)	Sample Mass (g)	^{210}Pb Activity	^{210}Pb Uncertainty	^{226}Ra Activity	^{226}Ra Uncertainty	^{137}Cs Activity	^{137}Cs Activity Uncertainty
MH-3	28-30	8.02	10.25	5.56	20.99	8.46	1.46	
MH-3	32-34	12.51	9.83	5.11	40.50	6.47	1.70	
MH-3	36-38	8.89	13.32	5.33	32.46	8.26	1.44	
MH-3	40-42	15	16.49	4.04	31.85	5.52	0.25	
NCBD-1	0-2	5.08	350.81	14.82	26.07	12.07	8.21	
NCBD-1	4-6	8.48	242.62	9.74	23.80	7.44	7.60	1.72
NCBD-1	8-10	10.76	155.95	7.63	18.17	6.21	14.84	1.87
NCBD-1	12-14	20.94	82.76	4.76	35.67	4.44	44.51	1.87
NCBD-1	16-18	22.95	65.03	4.21	40.69	4.26	25.78	1.43
NCBD-1	20-22	26.45	62.85	3.91	32.48	3.93	6.93	0.91
NCBD-1	24-26	31.74	54.14	3.68	39.25	3.76	2.15	
NCBD-1	28-30	34.98	36.61	3.58	40.30	3.71	1.48	
NCBD-1	32-34	33.45	41.36	3.67	44.52	3.92	1.41	
NCBD-1	36-38	35.11	33.06	3.48	42.34	3.71	1.39	
NCBD-1	40-42	30.1	35.50	3.60	36.08	3.89	0.92	
NCBD-1	44-46	30.73	35.55	3.65	41.13	3.74	0.46	
NCBD-1	48-50	31.1	35.88	3.63	37.79	3.91	0.90	
NCBD-2	0-2	8.75	198.45	8.92	16.76	6.93	5.25	
NCBD-2	4-6	11.42	274.59	8.94	14.27	6.57	4.93	1.30
NCBD-2	8-10	22.99	119.44	5.28	34.01	4.38	7.43	0.92
NCBD-2	12-14	23.85	130.68	5.14	42.05	4.13	11.07	0.99

Core	Depth Interval (cm)	Sample Mass (g)	^{210}Pb Activity	^{210}Pb Uncertainty	^{226}Ra Activity	^{226}Ra Uncertainty	^{137}Cs Activity	^{137}Cs Activity Uncertainty
NCBD-2	16-18	27.64	90.91	4.54	38.97	4.14	16.80	1.10
NCBD-2	20-22	31.15	65.13	4.02	46.26	4.10	13.49	1.05
NCBD-2	24-26	30.6	61.38	3.96	51.38	4.05	20.05	1.15
NCBD-2	28-30	30.49	55.06	4.07	48.46	4.88	15.59	1.11
NCBD-2	32-34	25.61	49.69	4.11	52.96	4.49	10.98	1.07
NCBD-2	36-38	32.04	51.63	3.95	56.00	4.22	10.53	0.95
NCBD-2	40-42	31.11	50.87	3.82	48.10	4.21	2.06	0.65
NCBD-2	44-46	27.42	47.55	3.93	52.88	4.27	0.97	
NCBD-2	48-50	32.88	50.97	3.51	39.60	3.96	0.28	
NCBD-3	0-2	5.24	433.64	21.73	40.77	19.68	5.31	
NCBD-3	4-6	9.45	268.30	14.45	38.09		3.91	1.34
NCBD-3	8-10	8.16	229.81	15.46	58.89	13.26	16.33	2.84
NCBD-3	12-14	8.19	175.64	14.04	59.61	14.44	26.88	3.30
NCBD-3	16-18	17.24	150.42	9.08	40.29	7.11	43.64	2.44
NCBD-3	20-22	24.5	92.54	7.48	66.55	7.14	23.34	1.54
NCBD-3	24-26	19.8	87.03	7.69	70.42	8.59	8.65	1.16
NCBD-3	28-30	23.88	61.40	7.03	43.10	7.16	1.05	
NCBD-3	32-34	34.15	47.88	6.69	52.79	6.13	1.14	
NCBD-3	36-38	32.05	36.62	6.65	46.46	6.68	0.93	
NCBD-3	40-42	32.57	43.41	5.52	47.24	6.61	0.42	0.28
NCBD-3	44-46	29.51	38.98	6.69	48.32	5.20	0.32	

Core	Depth Interval (cm)	Sample Mass (g)	^{210}Pb Activity	^{210}Pb Uncertainty	^{226}Ra Activity	^{226}Ra Uncertainty	^{137}Cs Activity	^{137}Cs Activity Uncertainty
NCBD-3	48-50	36.12	35.44	6.54	45.53	5.92	0.44	
NCBW-1	0-2	17.97	310.91	10.91	54.78	8.24	7.23	1.21
NCBW-1	4-6	22.85	212.36	9.31	37.31	6.66	13.32	1.54
NCBW-1	8-10	32.19	128.68	7.36	61.51	6.27	18.61	1.49
NCBW-1	12-14	32.34	108.42	6.38	54.98	5.08	20.53	1.42
NCBW-1	16-18	29.33	103.27	6.83	44.25	5.11	18.80	1.34
NCBW-1	20-22	33.9	91.84	5.89	57.59	5.11	10.99	1.16
NCBW-1	24-26	29.95	64.69	6.26	51.83	5.35	2.59	0.83
NCBW-1	28-30	28	49.76	5.59	70.85	6.79	0.87	
NCBW-1	32-34	33.35	66.42	6.76	54.84	5.07	0.99	
NCBW-1	36-38	33.63	55.30	5.91	56.26	5.52	0.26	
NCBW-1	40-42	34.33	68.62	6.56	55.63	6.39	1.99	
NCBW-1	44-46	35.23	56.99	6.72	58.80	6.47	0.86	
NCBW-1	48-50	33.65	61.66	6.85	58.05	6.85	0.00	
NCBW-1	52-54	35.95	64.00	7.01	67.12	6.30	1.46	
NCBW-1	56-58	34.36	54.90	6.79	59.16	6.29	1.18	
NCBW-1	60-62	38.88	50.55	6.82	58.72	6.02	0.77	
NCBW-1	64-66	36.84	62.85	6.49	36.09	6.57	1.38	
NCBW-2	0-2	29.3	81.36	4.27	44.59	4.28	21.45	1.18
NCBW-2	4-6	32.66	67.17	4.10	59.86	4.07	12.70	0.94
NCBW-2	8-10	32.67	67.44	4.10	53.16	4.07	9.06	0.94

Core	Depth Interval (cm)	Sample Mass (g)	^{210}Pb Activity	^{210}Pb Uncertainty	^{226}Ra Activity	^{226}Ra Uncertainty	^{137}Cs Activity	^{137}Cs Activity Uncertainty
NCBW-2	12-14	32.78	49.34	3.80	51.01	4.07	6.28	0.82
NCBW-2	16-18	35.94	46.33	3.62	48.14	3.93	2.09	0.70
NCBW-2	20-22	32.42	40.57	3.64	44.26	4.00	2.71	
NCBW-2	24-26	39.91	39.48	3.53	43.86	3.70	2.16	0.55
NCBW-2	28-30	44.95	33.38	3.39	40.12	3.73	0.91	
NCBW-2	32-34	38.76	30.12	3.32	40.55	3.58	2.08	
NCBW-2	36-38	41.32	36.39	3.32	39.68	3.55	1.69	
NCBW-3	0-2	19.28	173.19	7.84	54.56	8.06	7.61	1.30
NCBW-3	4-6	25.66	124.64	8.08	57.83	7.13	7.73	1.06
NCBW-3	8-10	35.03	88.01	7.31	63.56	6.49	5.38	0.94
NCBW-3	12-14	36.48	122.72	7.31	60.20	6.43	27.61	1.33
NCBW-3	16-18	35.05	86.24	6.73	56.49	6.77	22.86	1.40
NCBW-3	20-22	33.07	66.08	7.50	62.74	6.74	7.29	0.94
NCBW-3	24-26	35.27	70.97	6.72	59.13	6.38	1.14	
NCBW-3	28-30	35.27	64.14	5.67	53.31	5.91	0.91	
NCBW-3	32-34	30.06	81.17	7.24	70.58	6.98	0.96	
NCBW-3	36-38	35.93	70.80	6.90	58.01	5.39	0.22	
NCBW-3	40-42	35.29	63.08	6.83	48.58	6.47	0.66	
NCBW-3	44-46	35.58	68.07	6.69	50.54	6.80	0.62	
NCBW-3	48-50	36.62	64.58	6.96	49.40	6.95	0.55	0.36
NCGB-1	0-2	20.08	132.91	5.45	33.84	4.60	6.59	1.02

Core	Depth Interval (cm)	Sample Mass (g)	^{210}Pb Activity	^{210}Pb Uncertainty	^{226}Ra Activity	^{226}Ra Uncertainty	^{137}Cs Activity	^{137}Cs Activity Uncertainty
NCGB-1	4-6	16.36	162.66	6.26	28.74	5.45	8.45	1.15
NCGB-1	8-10	18.1	125.76	5.48	30.64	4.55	13.45	1.24
NCGB-1	12-14	18.5	115.51	5.39	31.28	4.92	18.38	1.46
NCGB-1	16-18	16.29	126.15	5.81	34.31	5.30	18.80	1.43
NCGB-1	20-22	17.93	105.21	5.23	38.98	4.89	29.00	1.69
NCGB-1	24-26	13.82	92.88	5.77	35.74	5.93	38.26	2.04
NCGB-1	28-30	17.43	84.74	5.20	34.60	5.01	37.26	1.86
NCGB-1	32-34	19.6	79.36	4.74	36.22	4.83	47.01	1.91
NCGB-1	36-38	24.12	52.87	4.17	45.30	4.46	26.59	1.37
NCGB-1	40-42	19.19	47.78	4.41	29.05	4.91	7.08	1.06
NCGB-1	44-46	26.42	46.47	3.70	43.54	4.16	2.61	
NCGB-1	48-50	25.58	50.62	3.78	38.14	4.15	2.62	
NCGB-1	52-54	25.46	44.87	3.68	36.43	4.05	2.01	
NCGB-1	56-58	23.5	31.90	3.66	39.82	4.30	1.50	0.75
NCGB-1	60-62	24.28	45.70	3.92	39.44	4.20	2.11	
NCGB-1	64-66	30.42	43.62	3.58	38.26	3.76	2.18	0.58
NCGB-2	0-2	21.25	73.57	4.20	19.69	3.99	15.24	1.08
NCGB-2	4-6	12.45	190.83	7.89	38.78	6.08	61.73	2.58
NCGB-2	8-10	10.31	161.54	7.93	33.55	7.21	62.77	3.07
NCGB-2	12-14	42.79	37.26	3.11	29.20	3.24	10.88	0.76
NCGB-2	16-18	37.57	28.96	3.01	34.96	3.29	1.53	0.57

Core	Depth Interval (cm)	Sample Mass (g)	^{210}Pb Activity	^{210}Pb Uncertainty	^{226}Ra Activity	^{226}Ra Uncertainty	^{137}Cs Activity	^{137}Cs Activity Uncertainty
NCGB-2	20-22	36.35	25.19	2.79	27.03	3.18	1.61	
NCGB-2	24-26	24.66	57.07	4.11	43.83	4.98	2.43	
NCGB-2	28-30	28.82	47.68	4.11	50.82	4.23	1.21	
NCGB-2	32-34	26.82	50.41	3.99	54.85	4.34	1.85	
NCGB-2	36-38	29.9	51.11	3.72	49.01	4.22	1.66	0.67
NCGB-2	40-42	24.1	45.48	4.18	38.33	4.70	1.15	
NCGB-2	44-46	24.68	45.29	3.99	53.39	4.38	1.66	
NCGB-2	48-50	23.21	45.66	4.17	44.92	4.84	2.60	
NCGB-2	52-54	21.53	41.46	4.16	44.50	4.48	2.15	
NCGB-3	0-2	5.98	227.69	18.29	47.10	18.18	5.09	2.39
NCGB-3	4-6	7.83	277.82	14.98	43.58	15.06	9.96	2.09
NCGB-3	8-10	14.69	140.77	9.08	26.64	10.69	21.07	2.20
NCGB-3	12-14	7.62	90.66	13.53	52.59	14.46	14.14	2.65
NCGB-3	16-18	16.99	87.28	7.90	39.99	9.28	73.33	3.08
NCGB-3	20-22	15.9	200.41	9.49	33.85	9.48	10.87	1.73
NCGB-3	24-26	14.31	208.35	10.54	36.89	9.83	12.44	1.55
NCGB-3	28-30	15.77	182.04	10.33	39.03	9.71	18.23	1.48
NCGB-3	32-34	17.77	131.15	8.52	62.53	7.55	21.68	1.97
NCGB-3	36-38	20.63	95.90	7.14	51.91	7.90	41.63	2.04
NCGB-3	40-42	19.73	93.16	7.55	24.58	9.18	24.67	1.80
NCGB-3	44-46	23.37	76.85	6.70	39.01	8.15	7.11	1.28

Core	Depth Interval (cm)	Sample Mass (g)	^{210}Pb Activity	^{210}Pb Uncertainty	^{226}Ra Activity	^{226}Ra Uncertainty	^{137}Cs Activity	^{137}Cs Activity Uncertainty
NCGB-3	48-50	22.45	57.89	6.13	31.33	7.13	5.17	1.00
NCGB-3	52-54	22.12	36.12	5.59	23.07	6.70	2.69	0.72
NCGB-3	56-58	19.1	35.96	7.22	49.76	7.25	1.80	0.98
NCGB-3	60-62	19.81	45.95	7.03	50.12	7.46	2.43	
NCGB-3	64-66	24.22	65.95	6.82	39.63	7.09	2.12	
NCLM-1	0-2	23.62	123.59	5.06	35.99	4.16	2.24	0.90
NCLM-1	4-6	23.96	108.00	5.01	41.78	4.36	3.49	0.74
NCLM-1	8-10	24.86	101.12	4.88	40.97	4.24	3.44	0.86
NCLM-1	12-14	29.7	76.84	4.24	48.41	4.14	6.77	0.84
NCLM-1	16-18	26.16	65.08	4.49	41.14	4.42	6.85	0.92
NCLM-1	20-22	27.6	65.95	4.23	47.62	4.25	9.05	0.97
NCLM-1	24-26	26.17	55.75	4.27	54.61	4.42	20.59	1.19
NCLM-1	28-30	27.64	63.99	4.33	50.83	4.46	28.88	1.41
NCLM-1	32-34	27.76	63.07	4.53	51.00	4.67	29.18	1.41
NCLM-1	36-38	25.31	55.14	4.60	56.45	4.53	7.78	0.85
NCLM-1	40-42	27.1	60.66	4.07	47.81	4.53	1.14	
NCLM-1	44-46	22.01	56.53	4.59	45.93	4.79	0.53	
NCLM-1	48-50	25.56	50.09	4.23	43.58	4.27	0.78	
NCLM-2	0-2	30.05	120.52	4.60	42.58	4.00	2.69	0.79
NCLM-2	4-6	28.11	91.69	4.39	36.24	3.98	2.87	0.74
NCLM-2	8-10	28.65	78.50	4.33	44.77	4.03	5.62	0.82

Core	Depth Interval (cm)	Sample Mass (g)	^{210}Pb Activity	^{210}Pb Uncertainty	^{226}Ra Activity	^{226}Ra Uncertainty	^{137}Cs Activity	^{137}Cs Activity Uncertainty
NCLM-2	12-14	35.5	74.22	3.82	47.03	3.77	6.13	0.70
NCLM-2	16-18	33.33	68.95	4.14	47.97	3.93	5.82	0.85
NCLM-2	20-22	28.56	67.08	4.24	48.81	4.04	6.67	0.86
NCLM-2	24-26	26.14	69.06	4.27	45.24	4.54	12.33	1.01
NCLM-2	28-30	35.19	64.67	3.84	50.70	3.98	14.68	1.04
NCLM-2	32-34	29.04	58.09	4.19	45.08	4.41	13.68	1.10
NCLM-2	36-38	28.57	64.90	4.24	56.77	4.36	20.00	1.25
NCLM-2	40-42	28.06	56.04	4.29	50.61	4.63	18.44	1.18
NCLM-2	44-46	29.89	62.17	4.12	52.73	4.22	10.44	0.96
NCLM-2	48-50	26.93	49.52	3.97	60.01	4.33	0.51	
NCLM-2	52-54	27.41	41.62	4.03	45.23	4.49	0.32	
NCLM-2	56-58	28.95	45.70	4.10	39.39	4.42	0.10	
NCLM-2	60-62	31.56	39.17	3.89	46.45	3.87	0.68	
NCLM-2	64-66	28.12	40.93	4.28	39.03	4.19	0.35	
NCLM-2	68-70	31.2	40.41	3.62	49.21	4.10	0.46	
NCLM-3	0-2	23.3	169.62	8.46	35.51	8.29	3.40	1.10
NCLM-3	4-6	25.49	162.57	8.25	46.91	7.28	3.16	1.03
NCLM-3	8-10	26.75	150.31	7.88	54.51	6.69	3.12	1.03
NCLM-3	12-14	26.89	119.36	7.72	46.42	7.22	5.32	0.90
NCLM-3	16-18	27.83	107.18	6.78	49.93	5.52	5.45	1.00
NCLM-3	20-22	24.8	95.18	7.84	46.12	7.78	15.73	1.22

Core	Depth Interval (cm)	Sample Mass (g)	^{210}Pb Activity	^{210}Pb Uncertainty	^{226}Ra Activity	^{226}Ra Uncertainty	^{137}Cs Activity	^{137}Cs Activity Uncertainty
NCLM-3	24-26	26.97	86.74	7.31	67.59	6.98	17.35	1.39
NCLM-3	28-30	25.24	85.25	7.61	62.39	7.57	22.91	1.72
NCLM-3	32-34	31.71	80.30	7.29	52.43	7.62	24.76	1.44
NCLM-3	36-38	28.9	75.16	7.40	60.10	7.28	13.87	1.39
NCLM-3	40-42	27.63	72.15	6.68	54.88	7.62	5.00	0.96
NCLM-3	44-46	26.93	61.96	7.18	60.68	6.21	2.41	
NCLM-3	48-50	28.54	66.95	7.45	57.34	6.81	1.37	0.82
NCRE-1	0-2	18.39	117.77	5.55	41.61	4.94	3.85	1.04
NCRE-1	4-6	24.9	101.24	4.76	41.86	4.47	4.97	0.91
NCRE-1	8-10	19.9	76.29	4.95	35.63	5.05	5.32	1.03
NCRE-1	12-14	23.26	80.10	4.64	45.59	4.46	6.45	0.96
NCRE-1	16-18	20.17	76.43	4.90	40.51	4.86	4.81	0.96
NCRE-1	20-22	27.83	66.01	3.99	34.34	4.12	5.75	0.83
NCRE-1	24-26	24.82	64.88	4.32	38.31	4.48	6.94	0.91
NCRE-1	28-30	34.81	57.13	3.86	41.45	3.82	7.15	0.86
NCRE-1	32-34	34.37	57.89	3.80	40.94	3.94	8.83	0.91
NCRE-1	36-38	28.04	61.71	4.08	45.14	4.20	8.55	0.92
NCRE-1	40-42	36.51	64.74	3.59	42.52	3.98	9.43	0.83
NCRE-1	44-46	32.27	53.72	3.84	47.52	3.91	18.80	1.06
NCRE-1	48-50	34.89	46.49	3.77	48.83	3.91	28.36	1.27
NCRE-1	52-54	35.18	54.71	3.66	50.99	3.89	27.61	1.23

Core	Depth Interval (cm)	Sample Mass (g)	^{210}Pb Activity	^{210}Pb Uncertainty	^{226}Ra Activity	^{226}Ra Uncertainty	^{137}Cs Activity	^{137}Cs Activity Uncertainty
NCRE-1	56-58	33.26	52.81	3.77	49.76	4.12	15.01	0.96
NCRE-1	60-62	32.08	50.34	3.75	57.72	4.02	5.34	0.79
NCRE-1	64-66	35.13	46.51	3.75	49.83	3.89	2.64	
NCRE-1	68-70	35.88	51.26	3.71	45.17	3.93	1.56	
NCRE-1	72-74	39.32	53.61	3.73	48.12	3.90	0.47	
NCRE-1	76-78	30.3	44.92	3.78	53.16	3.98	0.14	
NCRE-2	0-2	25.13	147.44	5.18	47.41	4.20	3.13	0.90
NCRE-2	4-6	24.66	138.45	5.14	34.47	4.03	3.37	0.82
NCRE-2	8-10	22.11	119.35	5.19	40.48	4.51	3.10	0.94
NCRE-2	12-14	24.6	111.48	4.80	35.84	4.51	5.50	0.82
NCRE-2	16-18	23.02	114.41	5.04	49.71	4.75	7.06	1.07
NCRE-2	20-22	33.48	72.72	4.04	48.21	3.91	6.45	0.81
NCRE-2	24-26	29.59	65.59	4.24	45.74	4.15	10.94	0.88
NCRE-2	28-30	31.52	67.79	4.08	49.96	4.17	8.73	0.88
NCRE-2	32-34	31.34	63.53	4.00	41.28	4.19	13.11	0.97
NCRE-2	36-38	31.73	52.80	3.97	56.76	4.05	24.68	1.28
NCRE-2	40-42	33.15	54.89	3.78	56.50	4.04	12.26	0.97
NCRE-2	44-46	31.18	44.93	3.92	54.33	4.20	5.29	0.93
NCRE-2	48-50	30.95	49.55	3.74	39.32	4.12	2.78	
NCRE-2	52-54	32.56	43.04	3.63	42.58	3.89	0.67	
NCRE-2	56-58	33.26	30.46	3.58	48.42	3.74	0.46	

Core	Depth Interval (cm)	Sample Mass (g)	^{210}Pb Activity	^{210}Pb Uncertainty	^{226}Ra Activity	^{226}Ra Uncertainty	^{137}Cs Activity	^{137}Cs Activity Uncertainty
NCRE-2	60-62	29.72	41.93	3.73	39.60	4.03	1.27	
NCRE-2	64-66	35.63	43.72	3.64	44.17	3.86	1.36	0.55
NCRE-2	68-70	35.33	44.37	3.65	44.76	3.78	2.02	
NCRE-2	72-74	33.18	37.68	3.68	45.42	3.84	1.02	
NCRE-2	76-78	33.22	41.14	3.49	47.30	3.93	0.63	
NCRE-3	0-2	17.23	153.21	6.30	29.08	5.22	3.30	
NCRE-3	4-6	25.05	135.92	5.08	40.85	4.10	3.18	0.81
NCRE-3	8-10	15.12	93.26	5.68	37.29	5.48	3.11	1.23
NCRE-3	12-14	29.23	90.13	4.28	38.28	4.08	5.79	0.85
NCRE-3	16-18	29.93	66.93	4.01	51.34	4.01	8.90	1.00
NCRE-3	20-22	32.14	60.96	3.94	45.20	3.82	10.12	0.91
NCRE-3	24-26	31.11	61.55	4.02	49.20	4.01	15.36	1.09
NCRE-3	28-30	32.06	56.91	3.95	54.61	4.22	18.76	1.19
NCRE-3	32-34	33.47	56.76	3.76	49.27	4.01	19.83	1.08
NCRE-3	36-38	34.86	52.49	3.68	53.33	4.00	5.83	0.75
NCRE-3	40-42	36.17	47.90	3.52	41.31	3.82	1.28	0.66
NCRE-3	44-46	32.39	48.53	3.64	45.85	3.80	3.77	0.79
NCRE-3	48-50	31.01	44.29	3.54	44.69	3.82	3.81	0.69
NCRE-3	52-54	32.42	47.93	3.83	50.89	3.90	2.18	
NCRE-3	56-58	29.42	49.19	3.85	46.13	4.27	1.20	
PK-1	0-2	20.93	283.00	7.21	21.01	4.31	1.70	0.66

Core	Depth Interval (cm)	Sample Mass (g)	^{210}Pb Activity	^{210}Pb Uncertainty	^{226}Ra Activity	^{226}Ra Uncertainty	^{137}Cs Activity	^{137}Cs Activity Uncertainty
PK-1	4-6	24.95	114.79	4.87	42.97	5.64	3.77	0.72
PK-1	8-10	20.1	69.06	4.91	29.50	4.59	6.47	1.02
PK-1	12-14	18.1	64.32	5.05	32.46	5.01	10.35	1.18
PK-1	16-18	21.96	65.81	4.72	31.49	4.54	16.57	1.27
PK-1	20-22	21.69	89.36	5.01	32.85	4.84	56.73	2.03
PK-1	24-26	26.27	99.41	4.70	28.92	4.07	35.78	1.51
PK-1	28-30	15.73	55.63	5.01	28.53	4.78	17.56	1.54
PK-1	32-34	17.11	49.50	4.38	24.96	4.61	5.79	1.24
PK-1	36-38	20.03	51.14	4.39	18.56	4.60	3.13	0.80
PK-1	40-42	28.65	32.70	3.61	25.25	3.71	1.55	0.52
PK-1	44-46	32.08	34.94	3.37	24.15	3.63	1.64	
PK-1	48-50	28.87	26.69	3.28	34.50	3.90	0.62	
PK-1	52-54	29.48	19.14	3.52	30.48	3.93	0.00	
PK-1	56-58	35.71	29.58	3.43	29.69	3.37	0.21	
PK-2	0-2	13.56	232.25	7.70	13.60	5.64	2.03	
PK-2	4-6	30.23	124.07	4.79	31.37	3.68	3.47	0.87
PK-2	8-10	31.27	116.48	4.69	30.56	3.89	4.27	0.73
PK-2	12-14	31.76	98.37	4.26	39.93	3.76	6.18	0.84
PK-2	16-18	30.09	89.52	4.30	28.70	3.79	6.34	0.83
PK-2	20-22	26.49	92.33	4.45	32.00	4.15	9.70	1.00
PK-2	24-26	28.07	73.27	4.29	32.51	4.09	9.54	0.96

Core	Depth Interval (cm)	Sample Mass (g)	^{210}Pb Activity	^{210}Pb Uncertainty	^{226}Ra Activity	^{226}Ra Uncertainty	^{137}Cs Activity	^{137}Cs Activity Uncertainty
PK-2	28-30	27.09	64.95	4.17	29.93	3.98	9.31	0.98
PK-2	32-34	32.41	69.86	4.11	32.08	3.71	11.71	0.94
PK-2	36-38	28.48	66.79	4.14	29.30	4.05	12.63	1.03
PK-2	40-42	29.57	59.25	4.15	31.23	3.84	14.80	1.01
PK-2	44-46	34.34	60.97	3.61	30.53	3.48	19.22	1.06
PK-2	48-50	30.34	60.41	3.98	37.82	3.87	35.19	1.40
PK-2	52-54	28.91	44.41	3.79	44.80	4.01	27.93	1.32
PK-2	56-58	16.76	40.83	4.76	51.78	5.66	18.87	1.52
PK-2	60-62	22.5	52.32	4.15	33.06	4.32	6.68	0.88
PK-3	0-2	24.17	181.19	5.56	24.42	4.09	2.05	0.83
PK-3	4-6	31.01	160.08	4.91	29.22	3.51	5.19	0.77
PK-3	8-10	28.12	114.64	4.49	27.63	3.66	5.09	0.78
PK-3	12-14	33.23	80.48	3.96	35.69	2.97	3.48	0.77
PK-3	16-18	28.4	96.48	4.36	26.90	3.74	4.71	0.82
PK-3	20-22	28.28	88.11	4.47	27.63	3.96	11.44	0.91
PK-3	24-26	27.87	69.31	4.31	27.48	3.68	15.64	1.10
PK-3	28-30	32.59	62.67	3.91	28.95	3.59	17.61	1.10
PK-3	32-34	32.11	54.93	3.85	41.21	3.83	38.43	1.46
PK-3	36-38	22.87	55.07	4.10	33.14	3.89	37.09	1.69
PK-3	40-42	29.42	42.50	3.65	21.55	3.02	9.93	0.93
PK-3	44-46	32.68	42.57	3.52	33.46	3.69	4.53	0.82

Core	Depth Interval (cm)	Sample Mass (g)	^{210}Pb Activity	^{210}Pb Uncertainty	^{226}Ra Activity	^{226}Ra Uncertainty	^{137}Cs Activity	^{137}Cs Activity Uncertainty
PK-3	48-50	38.06	33.45	3.34	34.88	3.44	2.01	0.57
PK-3	52-54	36.63	31.91	3.23	34.95	3.43	1.41	0.47
PK-3	56-58	32.97	27.96	3.32	26.61	3.76	0.19	
PK-3	60-62	31.5	27.92	3.49	33.39	3.92	0.86	
PM-1	0-2	20.11	197.55	5.97	12.24	3.20	2.20	
PM-1	4-6	46.25	47.30	3.36	27.05	2.80	1.52	0.44
PM-1	8-10	37.86	39.80	3.26	25.86	3.45	4.25	0.71
PM-1	12-14	22.63	102.13	4.74	20.38	3.80	24.06	1.29
PM-1	16-18	25.74	69.90	3.99	24.43	3.78	41.79	1.58
PM-1	20-22	27.83	87.77	4.41	25.45	3.90	69.78	1.93
PM-1	24-26	29.22	74.06	4.07	32.64	3.66	16.41	1.10
PM-1	28-30	33.28	43.36	3.58	38.14	3.55	8.87	0.89
PM-1	32-34	40.91	29.79	3.24	35.99	3.48	4.33	0.71
PM-1	36-38	41.62	25.01	3.22	34.32	3.20	1.11	0.40
PM-1	38-40	48.9	27.53	3.48	33.34	3.13	0.87	
PM-10	0-2	11.87	237.61	9.87	33.91	10.50	4.92	1.42
PM-10	4-6	9.02	199.95	11.30	56.55		5.81	1.94
PM-10	8-10	10.06	156.12	9.69	39.14	11.44	11.76	2.23
PM-10	12-14	9.03	54.25	9.41	51.03		50.32	3.12
PM-10	16-18	13.62	106.55	8.79	27.49	9.68	62.33	2.79
PM-10	20-22	15.48	38.77	5.14	28.92	8.49	12.84	1.51

Core	Depth Interval (cm)	Sample Mass (g)	^{210}Pb Activity	^{210}Pb Uncertainty	^{226}Ra Activity	^{226}Ra Uncertainty	^{137}Cs Activity	^{137}Cs Activity Uncertainty
PM-10	24-26	11.26	28.92	5.68	38.08	11.47	4.38	1.58
PM-10	28-30	11.87	31.58	7.16	27.35	10.06	3.83	1.33
PM-10	32-34	10.6	22.59	7.35	51.44		4.90	1.67
PM-10	36-38	14.33	31.18	7.79	31.11	9.44	3.60	
PM-10	40-42	23.23	36.83	5.85	25.05	6.70	1.61	0.78
PM-11	0-2	10.46	288.57	9.43	37.03	6.38	2.52	1.21
PM-11	4-6	6.93	188.75	9.72	23.36	9.34	4.80	
PM-11	8-10	9.11	162.11	8.08	21.71	7.24	5.50	1.26
PM-11	12-14	10.46	101.71	6.67	41.74		9.08	1.31
PM-11	16-18	13.37	151.77	6.31	25.58	5.51	49.58	2.26
PM-11	20-22	17.19	93.97	5.11	38.64	4.91	50.08	1.94
PM-11	24-26	15.58	36.68	4.40	44.61	5.51	11.64	1.27
PM-11	28-30	12.79	41.64	4.82	49.12	5.94	3.70	1.26
PM-11	32-34	12.47	31.73	4.73	26.59	6.07	3.61	1.20
PM-11	36-38	10.49	22.95	5.28	38.41	6.60	3.82	1.41
PM-11	40-42	18.66	20.97	3.80	31.79	4.44	2.84	0.91
PM-12	0-2	19.21	394.16	10.71	26.13	6.93	7.31	1.35
PM-12	4-6	8.51	64.16	9.92	51.53		4.21	1.93
PM-12	8-10	5.84	94.42	15.89	73.10	16.90	23.77	3.26
PM-12	12-14	21.66	99.99	7.05	34.85	7.34	21.90	1.66
PM-12	16-18	16.77	29.70	5.94	42.53	8.25	7.08	1.28

Core	Depth Interval (cm)	Sample Mass (g)	^{210}Pb Activity	^{210}Pb Uncertainty	^{226}Ra Activity	^{226}Ra Uncertainty	^{137}Cs Activity	^{137}Cs Activity Uncertainty
PM-12	20-22	13.35	39.54	8.49	51.04	8.47	4.72	1.05
PM-12	24-26	11.6	73.74	8.05	19.88	10.94	2.38	1.11
PM-12	28-30	19.16	30.51	6.54	37.76	8.10	2.15	
PM-12	32-34	26.94	30.44	5.72	46.91	5.88	1.59	0.65
PM-12	36-38	21.83	15.56	6.41	28.26	7.55	2.09	0.68
PM-12	40-42	27.75	13.19	6.53	36.25	6.51	1.22	
PM-2	0-2	25.44	201.47	7.99	20.71	6.71	6.67	0.98
PM-2	4-6	29.24	160.62	7.48	17.36	6.69	6.74	1.00
PM-2	8-10	23.1	145.52	7.63	30.89	6.73	31.31	1.48
PM-2	12-14	30.19	109.52	7.23	30.58	4.70	47.86	1.57
PM-2	16-18	30.69	56.45	6.05	32.16	6.47	5.24	0.92
PM-2	20-22	30.81	55.97	6.41	27.13	6.86	1.07	
PM-2	24-26	31.43	51.62	5.37	44.78	5.57	0.80	
PM-2	28-30	30.88	35.71	6.40	31.32	6.85	0.81	
PM-2	32-34	34.81	41.44	5.24	34.19	6.43	0.96	
PM-2	36-38	38.68	36.85	6.16	30.62	6.04	0.97	
PM-2	40-42	39.07	27.36	6.25	35.41	5.92	0.97	
PM-2	44-46	37.75	41.20	6.10	47.64	5.86	0.71	
PM-3	0-2	25.44	285.34	6.48	21.17	3.82	10.94	1.03
PM-3	4-6	29.24	96.73	4.58	28.86	3.97	62.24	1.82
PM-3	8-10	23.1	64.72	5.02	58.92	5.23	4.92	1.01

Core	Depth Interval (cm)	Sample Mass (g)	^{210}Pb Activity	^{210}Pb Uncertainty	^{226}Ra Activity	^{226}Ra Uncertainty	^{137}Cs Activity	^{137}Cs Activity Uncertainty
PM-3	12-14	30.19	50.91	4.19	53.08	4.50	1.61	0.70
PM-3	16-18	30.69	53.76	4.25	56.23	4.45	1.61	
PM-3	20-22	30.81	60.93	4.24	61.53	4.44	1.50	
PM-3	24-26	31.43	53.78	4.19	52.75	4.38	1.15	
PM-3	28-30	30.88	58.19	4.23	62.24	4.63	1.28	
PM-3	32-34	34.81	55.29	4.05	59.34	4.01	2.14	
PM-3	36-38	38.68	50.51	3.76	47.42	3.94	1.70	
PM-3	40-42	39.07	54.46	3.83	48.73	3.92	1.07	
PM-4	0-2	22.5	407.09	7.68	15.00	3.69	21.79	1.29
PM-4	4-6	29.6	178.04	5.15	19.49	3.73	84.65	2.05
PM-4	8-10	46.67	30.67	3.19	26.47	2.95	5.01	0.66
PM-4	12-14	47.84	27.40	2.93	25.49	3.00	1.55	
PM-4	16-18	56.34	27.30	3.05	26.20	3.00	1.23	
PM-4	20-22	53.11	21.50	2.97	23.38	2.97	0.66	
PM-4	24-26	50.85	37.67	3.14	29.18	3.24	0.91	
PM-4	28-30	55.96	23.28	3.13	29.69	2.93	1.22	
PM-5	0-2	16.71	262.86	9.31	12.98	8.44	39.96	2.39
PM-5	4-6	22.77	288.13	8.74	25.57	6.80	63.66	2.30
PM-5	8-10	20.42	243.93	8.80	11.95	7.83	68.26	2.36
PM-5	12-14	31.07	144.59	7.36	42.12	5.72	38.30	1.57
PM-5	16-18	37.71	57.71	6.66	26.63	6.04	14.60	1.02

Core	Depth Interval (cm)	Sample Mass (g)	^{210}Pb Activity	^{210}Pb Uncertainty	^{226}Ra Activity	^{226}Ra Uncertainty	^{137}Cs Activity	^{137}Cs Activity Uncertainty
PM-5	20-22	32.07	46.51	6.40	43.01	6.38	7.32	0.96
PM-5	24-26	34.68	36.26	6.30	42.20	4.95	0.84	0.47
PM-5	28-30	43.94	42.34	6.31	41.77	6.06	0.52	0.34
PM-5	32-34	40.07	35.92	6.54	36.81	6.01	0.36	
PM-5	36-38	38.27	25.17	6.41	55.63	5.72	0.78	
PM-5	40-42	36.87	30.73	6.26	23.48	6.66	0.63	
PM-5	44-46	39.74	20.78	5.11	37.24	4.57	0.55	
PM-6	0-2	16.71	189.70	8.56	16.71	7.62	15.67	1.47
PM-6	4-6	15.89	230.73	9.49	17.78	8.81	34.81	1.79
PM-6	8-10	17.88	171.51	8.30	28.65	7.66	41.63	2.31
PM-6	12-14	15.37	144.25	8.95	21.08	8.89	42.85	2.04
PM-6	16-18	16.21	103.73	7.63	15.75		39.92	2.14
PM-6	20-22	28.25	34.64	6.20	38.47	6.54	2.36	
PM-6	24-26	32.91	27.92	6.09	43.83	6.08	0.33	
PM-6	28-30	30.14	23.44	5.99	30.51	6.76	0.93	
PM-6	32-34	36.84	30.17	6.49	44.46	5.94	0.37	
PM-6	36-38	39.88	29.75	5.00	37.25	5.16	1.07	0.52
PM-7	0-2	12.18	204.17	7.64	27.15	6.41	3.34	1.32
PM-7	4-6	13.6	105.32	5.85	23.84	5.43	4.79	
PM-7	8-10	14.17	135.94	6.18	30.85	5.42	6.98	1.23
PM-7	12-14	8.98	153.42	8.19	16.08	7.62	3.48	1.51

Core	Depth Interval (cm)	Sample Mass (g)	^{210}Pb Activity	^{210}Pb Uncertainty	^{226}Ra Activity	^{226}Ra Uncertainty	^{137}Cs Activity	^{137}Cs Activity Uncertainty
PM-7	16-18	10.13	100.88	6.87	25.00	5.56	11.64	1.56
PM-7	20-22	10.19	75.38	6.12	30.39	7.03	19.63	1.96
PM-7	24-26	11.1	64.83	6.11	18.82	6.97	85.22	3.25
PM-7	28-30	18.96	64.64	4.45	36.78	4.67	34.39	1.67
PM-7	32-34	19.29	34.83	3.98	39.71	4.46	9.16	1.00
PM-7	36-38	22.44	28.59	3.67	30.45	4.20	4.36	0.83
PM-7	40-42	14.35	38.25	4.37	44.20	5.36	3.64	0.99
PM-7	44-46	22.67	16.74	3.40	32.61	4.04	4.22	0.82
PM-7	48-50	25.34	18.48	3.36	50.48	4.29	3.44	0.75
PM-7	52-54	20.3	7.91	3.56	58.94	5.24	2.42	0.84
PM-7	56-58	15.25	8.96	3.98	43.16	5.96	2.42	
PM-8	0-2	18.88	259.69	6.97	25.19	4.25	16.51	1.32
PM-8	4-6	23.61	156.01	5.42	26.45	4.16	55.93	1.89
PM-8	8-10	24.92	63.45	4.19	40.07	4.11	22.77	1.34
PM-8	12-14	36.2	31.83	3.25	36.74	3.46	1.04	
PM-8	16-18	29.11	32.47	3.47	36.61	3.99	0.31	
PM-8	20-22	32.7	38.08	3.43	36.35	3.78	0.68	
PM-8	24-26	37.4	38.07	3.28	39.78	3.66	0.75	
PM-8	28-30	36.79	33.99	3.04	40.08	3.69	0.64	
PM-8	32-34	37.33	37.04	3.46	38.04	3.66	0.43	
PM-9	0-2	11.63	355.06	12.05	18.05	10.92	22.93	2.12

Core	Depth Interval (cm)	Sample Mass (g)	^{210}Pb Activity	^{210}Pb Uncertainty	^{226}Ra Activity	^{226}Ra Uncertainty	^{137}Cs Activity	^{137}Cs Activity Uncertainty
PM-9	4-6	9.48	265.74	13.51	23.62	13.95	61.42	3.39
PM-9	8-10	13.18	191.02	10.61	40.26	10.36	73.46	3.18
PM-9	12-14	38.33	24.94	4.49	50.22	5.45	0.27	
PM-9	16-18	35.11	29.81	6.61	36.69	6.39	0.39	
PM-9	20-22	32.77	35.75	4.42	40.47	6.20	0.81	0.56
PM-9	24-26	37.97	44.62	5.63	31.92	6.01	0.18	
PM-9	28-30	34.47	35.65	5.61	28.49	5.81	0.20	
PM-9	32-34	35.34	30.66	5.09	38.20	6.18	0.38	
PM-9	36-38	33.34	35.59	4.86	36.28	5.94	0.54	
PM-9	40-42	36.75	37.61	5.70	38.12	5.86	0.36	0.26
PM-9	44-46	33.61	31.56	4.73	37.14	4.76	0.69	
PM-9	48-50	33.05	31.44	4.76	34.95	6.07	0.35	
TH-1	0-2	25.55	131.29	7.55	28.95	6.00	3.67	1.24
TH-1	4-6	32.45	134.91	7.21	38.68	6.24	6.26	1.03
TH-1	8-10	35.01	117.52	6.97	27.94	5.29	8.23	1.10
TH-1	12-14	26.63	104.27	6.69	39.48	6.38	4.78	1.07
TH-1	16-18	17.14	106.21	7.30	15.88	8.26	2.69	1.20
TH-1	20-22	21.02	125.48	7.21	28.32	7.38	1.65	0.85
TH-1	24-26	25.91	25.18	4.90	35.27	6.39	1.39	0.55
TH-1	28-30	27.38	26.99	5.00	21.81	6.90	1.27	
TH-1	32-34	15.38	12.53	4.97	23.51	9.06	1.28	

Core	Depth Interval (cm)	Sample Mass (g)	^{210}Pb Activity	^{210}Pb Uncertainty	^{226}Ra Activity	^{226}Ra Uncertainty	^{137}Cs Activity	^{137}Cs Activity Uncertainty
TH-1	36-38	17.19	13.60		24.71	8.08	0.00	
TH-1	40-42	16.78	10.95	4.82	39.58		0.60	
TH-1	44-46	20.16	9.50		21.65	6.66	0.19	
TH-1	48-50	18.51	7.40	3.61	28.29	6.40	0.00	
TH-2	0-2	38.31	115.49	4.48	23.93	3.08	8.09	0.77
TH-2	4-6	33.73	85.90	4.12	38.20	3.71	39.75	1.45
TH-2	8-10	36.7	78.18	3.85	28.05	3.70	34.63	1.27
TH-2	12-14	30.3	57.77	3.78	31.12	3.16	9.19	0.99
TH-2	16-18	28.91	45.43	3.69	34.37	3.79	0.94	0.47
TH-2	20-22	33.88	48.35	3.64	34.02	3.79	2.21	0.50
TH-2	24-26	32.91	37.76	3.79	38.90	3.48	1.48	
TH-2	28-30	36.23	38.58	3.42	32.27	3.45	0.68	
TH-2	32-34	29.12	33.38	3.68	31.57	3.46	0.76	
TH-2	36-38	30.85	27.98	3.45	36.58	3.63	0.80	
TH-2	40-42	32.09	22.52	3.27	24.34	3.63	0.47	
TH-3	0-2	26.97	184.49	5.58	28.70	3.44	5.21	0.85
TH-3	4-6	33.01	134.76	4.83	30.16	3.47	10.59	0.97
TH-3	8-10	25.28	123.39	5.05	29.64	4.07	31.90	1.56
TH-3	12-14	32.89	67.85	4.18	33.99	3.77	99.47	2.14
TH-3	16-18	25.17	55.69	4.73	37.79	4.20	12.93	1.04
TH-3	20-22	25.42	33.63	3.91	35.54	4.05	3.76	0.75

Core	Depth Interval (cm)	Sample Mass (g)	^{210}Pb Activity	^{210}Pb Uncertainty	^{226}Ra Activity	^{226}Ra Uncertainty	^{137}Cs Activity	^{137}Cs Activity Uncertainty
TH-3	24-26	24.49	39.46	3.79	22.27	3.22	1.53	
TH-3	28-30	28.35	30.53	3.43	18.17	3.74	3.68	0.69
TH-3	32-34	32.74	16.36	2.38	22.86	3.29	1.33	0.51
TH-3	36-38	24.54	16.26	3.44	27.23	3.09	1.48	
TH-3	40-42	21.02	15.53	2.95	22.14	4.29	0.38	
TH-4	0-2	24.98	252.30	8.22	28.04	6.57	9.68	1.22
TH-4	4-6	36.66	166.98	7.98	44.68	5.69	19.65	1.42
TH-4	8-10	38.28	124.06	7.08	33.18	6.43	47.18	1.82
TH-4	12-14	33.12	87.10	6.78	49.42	6.25	5.54	0.87
TH-4	16-18	34.16	55.74	5.98	37.51	5.47	1.37	
TH-4	20-22	36.79	43.86	6.83	41.34	6.03	0.69	
TH-4	24-26	42.89	20.97	6.66	40.43	4.81	0.11	
TH-4	28-30	28.3	45.71	6.59	41.85	7.71	0.21	
TH-4	32-34	45.61	44.24	5.20	35.19	4.59	0.32	
TH-4	36-38	49.89	56.04	5.97	33.72	4.51	0.39	
TH-4	40-42	48.43	53.41	5.42	45.24	4.24	0.21	
TH-4	44-46	47.86	58.80	5.74	41.03	6.23	0.12	
TH-4	48-50	48.85	63.85	6.50	43.45	4.78	0.18	
TH-5	0-2	24.22	138.27	5.43	22.94	3.48	8.15	0.93
TH-5	4-6	34.46	102.02	4.35	25.50	3.37	7.80	0.79
TH-5	8-10	32.14	107.60	4.62	31.77	3.14	14.50	1.03

Core	Depth Interval (cm)	Sample Mass (g)	^{210}Pb Activity	^{210}Pb Uncertainty	^{226}Ra Activity	^{226}Ra Uncertainty	^{137}Cs Activity	^{137}Cs Activity Uncertainty
TH-5	12-14	32.79	79.56	3.99	29.61	3.29	42.71	1.52
TH-5	16-18	29.15	63.66	4.39	34.06	4.19	54.16	1.74
TH-5	20-22	33.4	60.21	3.95	29.45	3.73	18.55	1.15
TH-5	24-26	28.66	57.03	3.92	39.67	3.82	3.43	0.69
TH-5	28-30	40.48	33.85	3.26	21.08	3.16	0.75	0.37
TH-5	32-34	37.73	28.37	3.36	34.97	3.19	0.81	
TH-5	36-38	27.84	21.96	3.47	30.54	3.79	0.66	0.35
TH-5	40-42	28.04	23.33	3.45	36.63	3.88	0.47	
TH-5	44-46	25.94	26.67	3.64	33.64	4.11	0.45	
TH-5	48-50	31.05	28.75	3.34	40.44	4.11	0.38	
TH-6	0-2	22.31	186.89	7.66	26.11	7.68	27.99	1.67
TH-6	4-6	28.46	111.98	6.56	39.97	6.72	74.79	1.99
TH-6	8-10	27.92	128.32	7.81	37.39	7.02	46.42	1.83
TH-6	12-14	35.46	84.57	6.59	26.15	6.81	6.73	0.96
TH-6	16-18	36.19	58.80	6.88	43.48	6.19	1.08	0.72
TH-6	20-22	26.49	42.84	6.31	46.26	6.96	1.01	
TH-6	24-26	28.4	42.40	6.31	39.71	6.41	0.62	
TH-6	28-30	27.23	29.58	7.13	38.40	6.93	0.67	
TH-6	32-34	33.34	32.50	6.52	37.91	6.32	0.35	
TH-6	36-38	28.11	32.02	6.35	36.67	6.56	0.00	
TH-6	40-42	29.88	34.20	6.39	39.87	6.70	0.00	

Appendix C

PHYSCIAL PROPERTY AND RADIONUCLIDE DEPTH PROFILES

Appendix C contains plots of the physical and radionuclide profiles for each core. LOI (% mass) is shown by a black bar representing the sampled interval and a red connecting line. For the radionuclide plots, the errors shown are based on the counting statistics (horizontal error bar) and sampled interval (vertical error bars). In the $^{210}Pb_{xs}$ activity profiles, the grey data points were not used for linear regression vertical dashed line presented in the ^{137}Cs plot marks the MDA determined for this study (See Methods), and the horizontal line marks the depth of the 1963-1964 activity peak, if present.

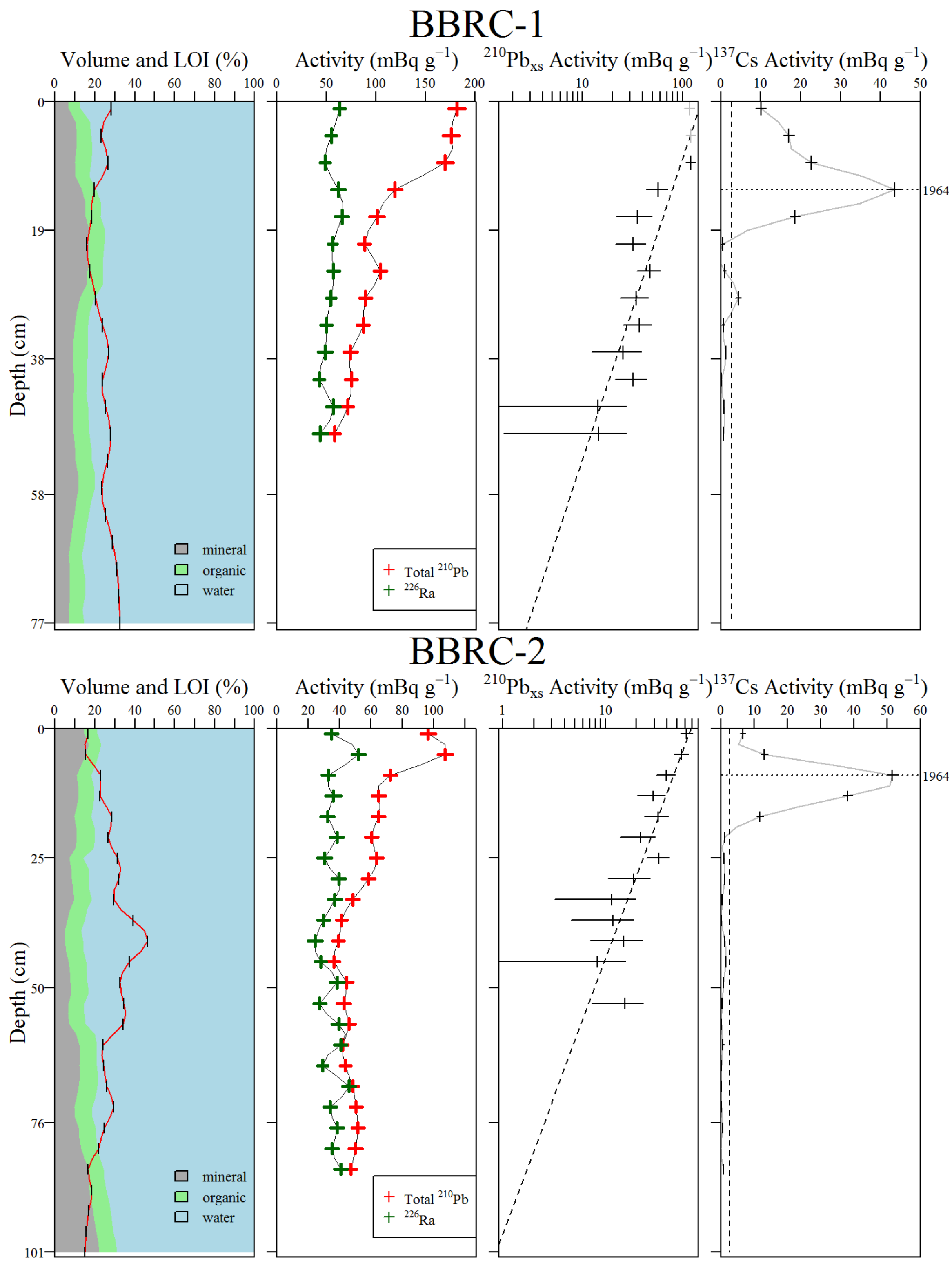
BBRC-1
Volume and LOI (%)
Activity (mBq g⁻¹)
210Pbxs Activity (mBq g⁻¹)
137Cs Activity (mBq g⁻¹)
Depth (cm)
mineral
organic
water
Total 210Pb
226Ra
1964
BBRC-2
Volume and LOI (%)
Activity (mBq g⁻¹)
210Pbxs Activity (mBq g⁻¹)
137Cs Activity (mBq g⁻¹)
Depth (cm)
mineral
organic
water
Total 210Pb
226Ra
1964

LC-1

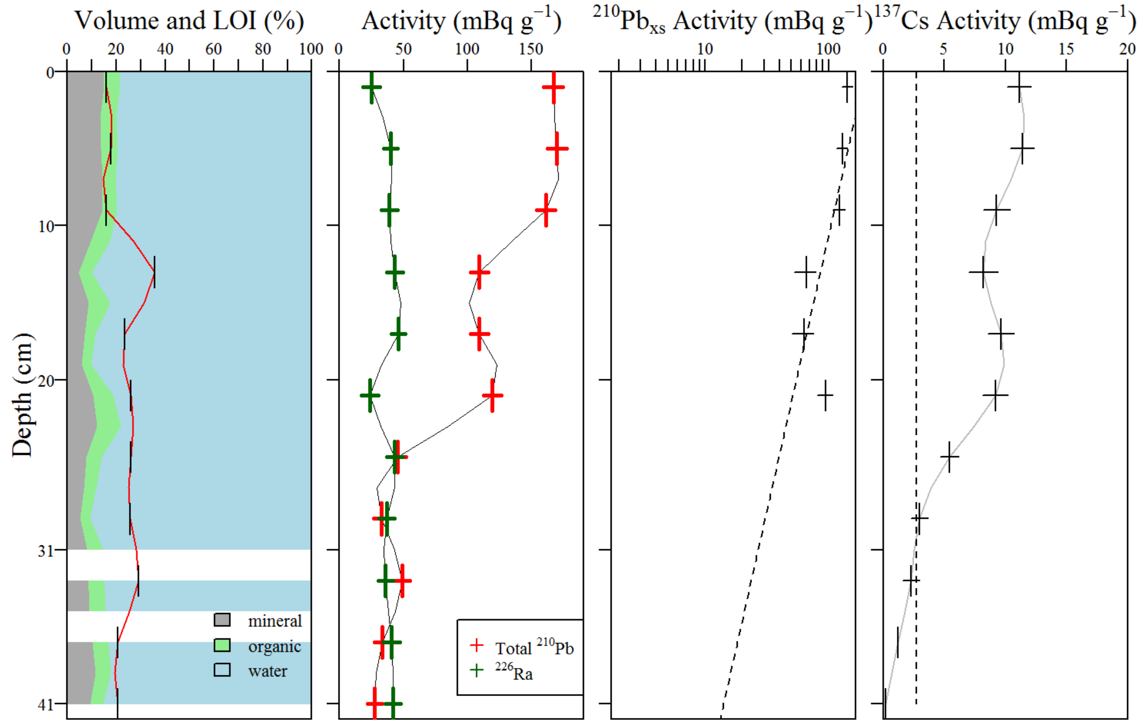

Volume and LOI (%)
Activity (mBq g−1)
210Pbxs Activity (mBq g−1)
137Cs Activity (mBq g−1)
Depth (cm)
mineral
organic
water
Total 210Pb
226Ra

LC-2

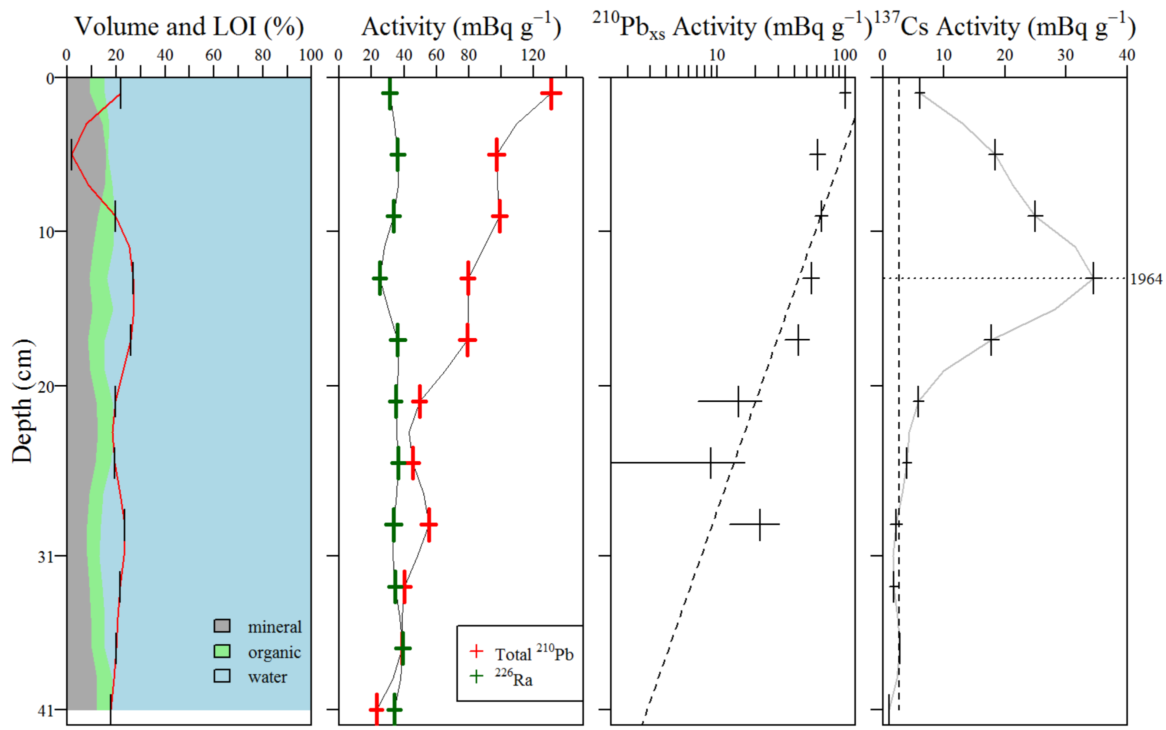

Volume and LOI (%)
Activity (mBq g−1)
210Pbxs Activity (mBq g−1)
137Cs Activity (mBq g−1)
Depth (cm)
1964
mineral
organic
water
Total 210Pb
226Ra

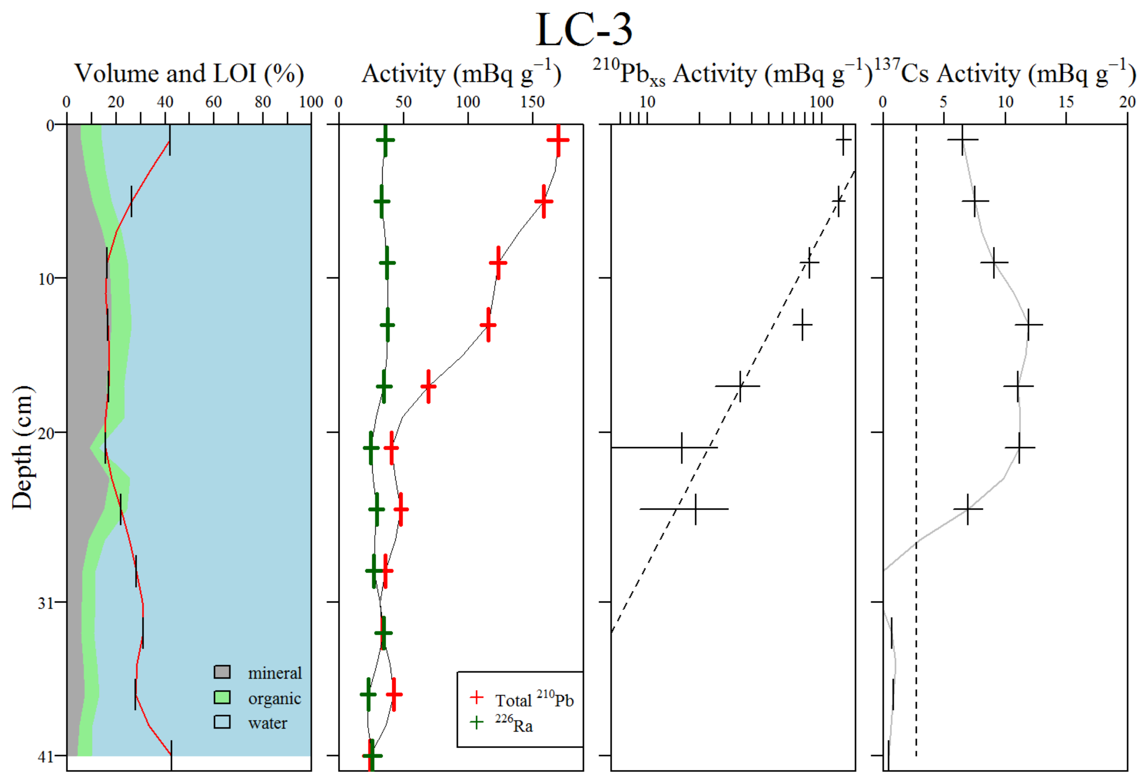
LC-3
Volume and LOI (%)
Activity (mBq g−1)
210Pbxs Activity (mBq g−1)
137Cs Activity (mBq g−1)
Depth (cm)
mineral
organic
water
Total 210Pb
226Ra

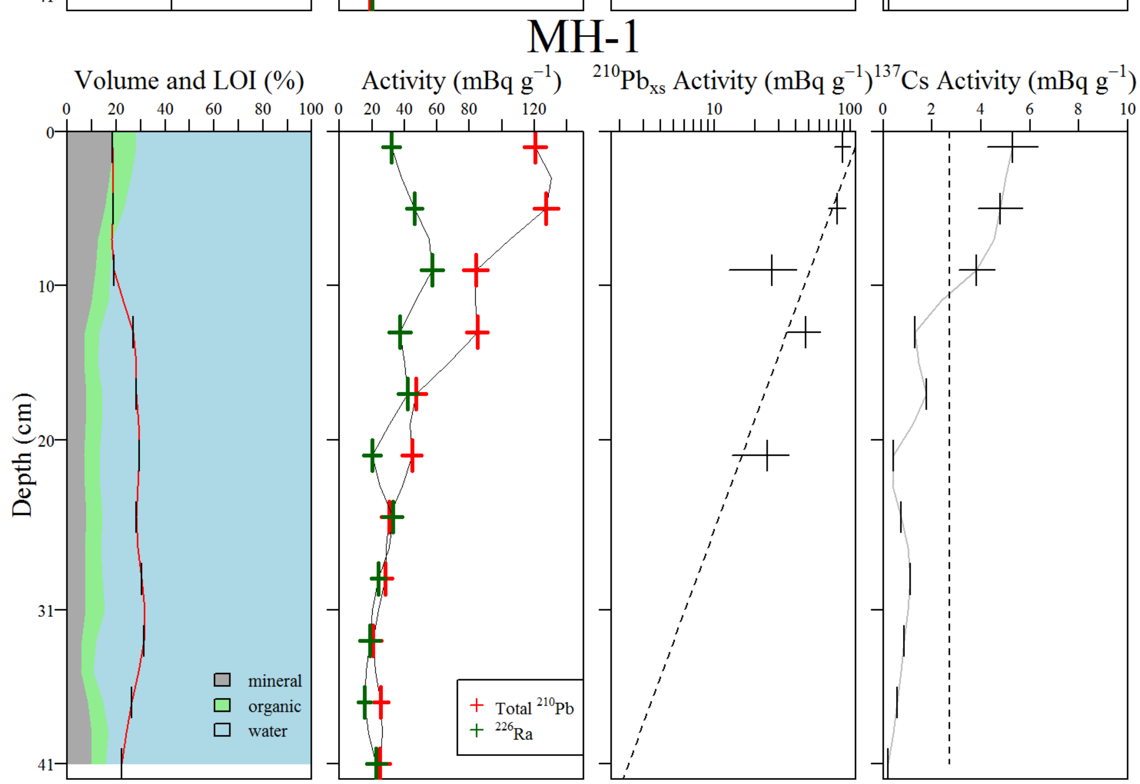
MH-1
Volume and LOI (%)
Activity (mBq g−1)
210Pbxs Activity (mBq g−1)
137Cs Activity (mBq g−1)
Depth (cm)
mineral
organic
water
Total 210Pb
226Ra

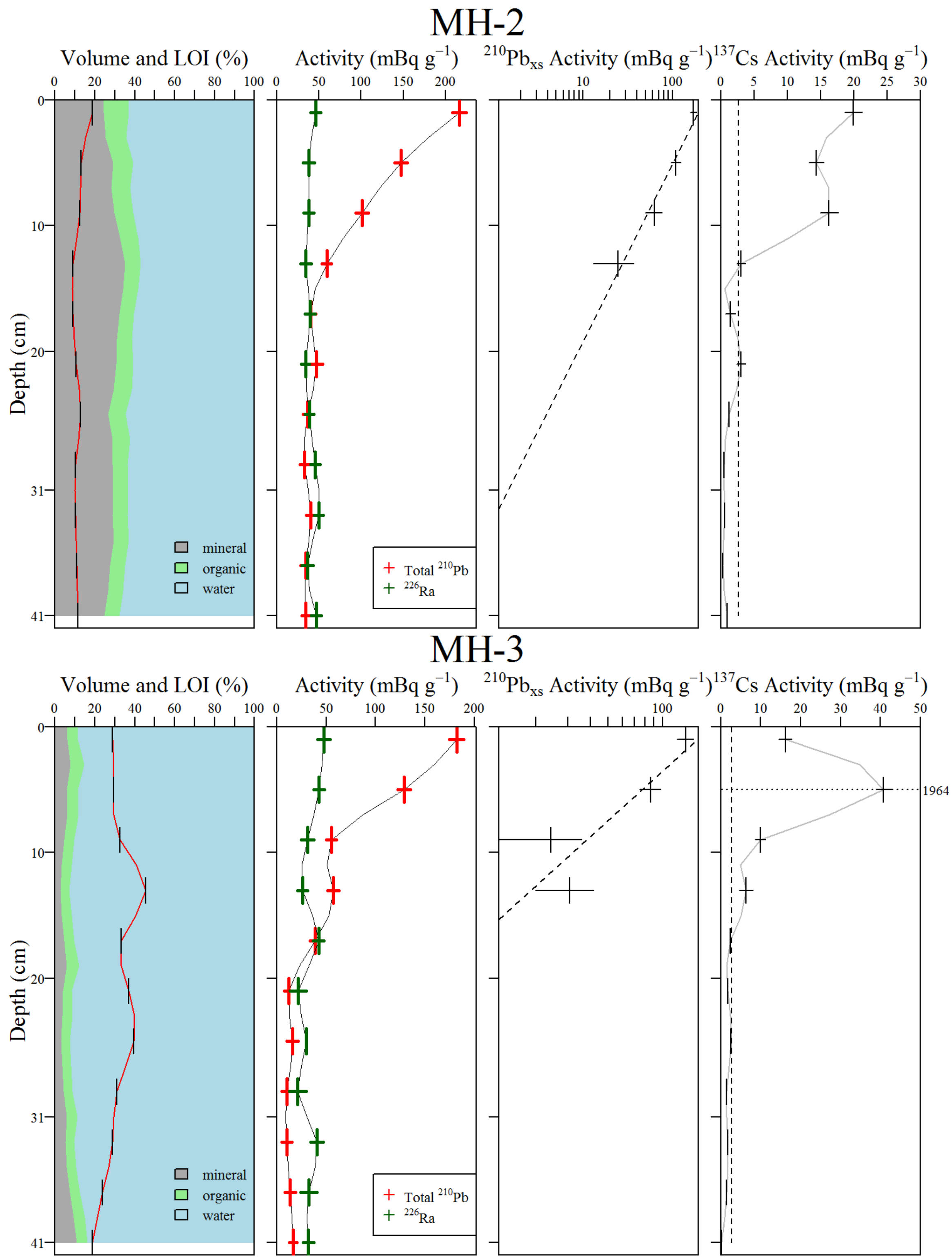
MH-2
Volume and LOI (%)
Activity (mBq g⁻¹)
²¹⁰Pbxs Activity (mBq g⁻¹)
¹³⁷Cs Activity (mBq g⁻¹)
Depth (cm)
mineral
organic
water
Total ²¹⁰Pb
²²⁶Ra
MH-3
Volume and LOI (%)
Activity (mBq g⁻¹)
²¹⁰Pbxs Activity (mBq g⁻¹)
¹³⁷Cs Activity (mBq g⁻¹)
Depth (cm)
1964
mineral
organic
water
Total ²¹⁰Pb
²²⁶Ra

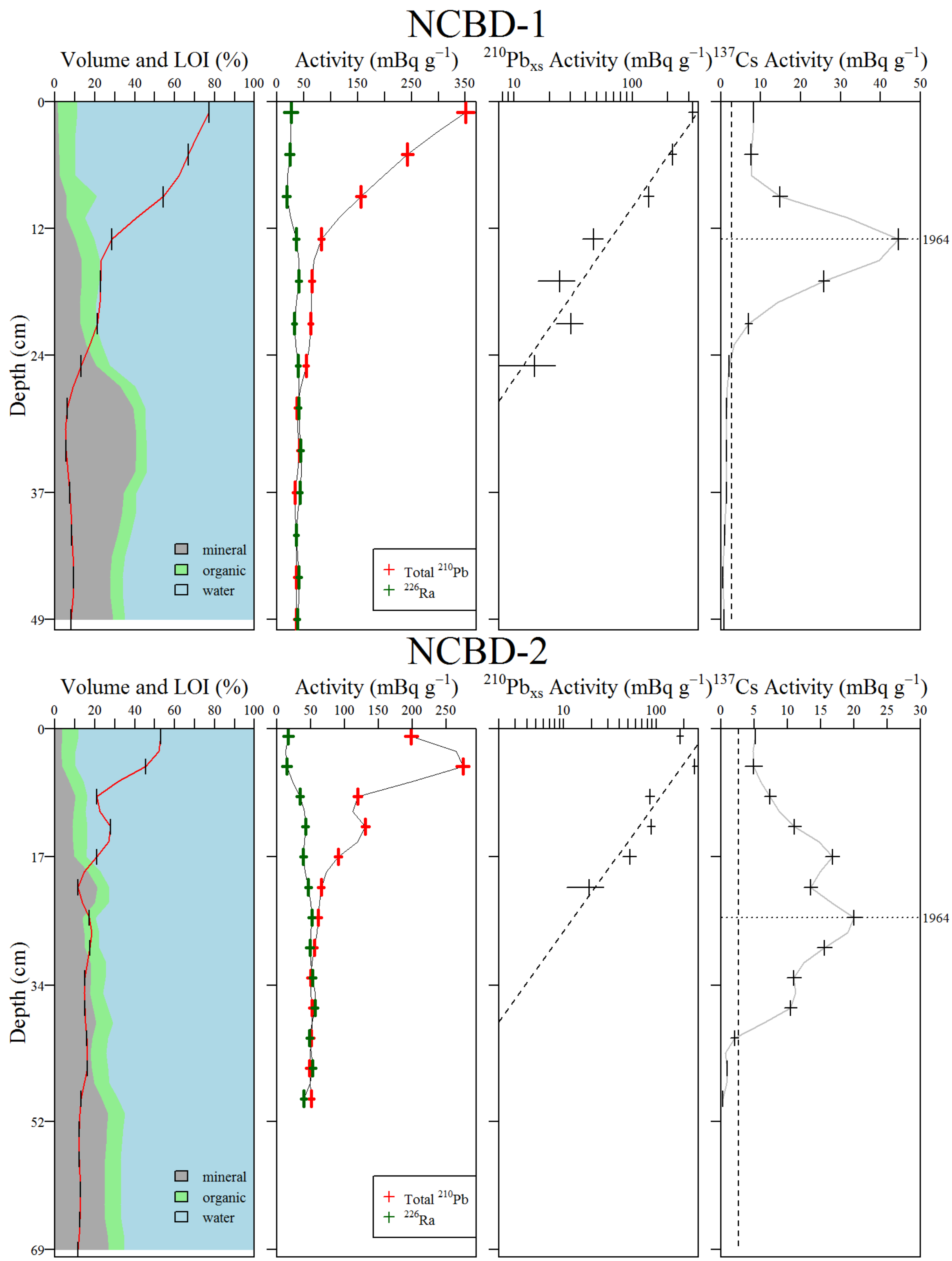

NCBD-1
Volume and LOI (%)
Activity (mBq g−1)
210Pbxs Activity (mBq g−1)
137Cs Activity (mBq g−1)
Depth (cm)
mineral
organic
water
Total 210Pb
226Ra
1964
NCBD-2
Volume and LOI (%)
Activity (mBq g−1)
210Pbxs Activity (mBq g−1)
137Cs Activity (mBq g−1)
Depth (cm)
mineral
organic
water
Total 210Pb
226Ra
1964

NCBD-3

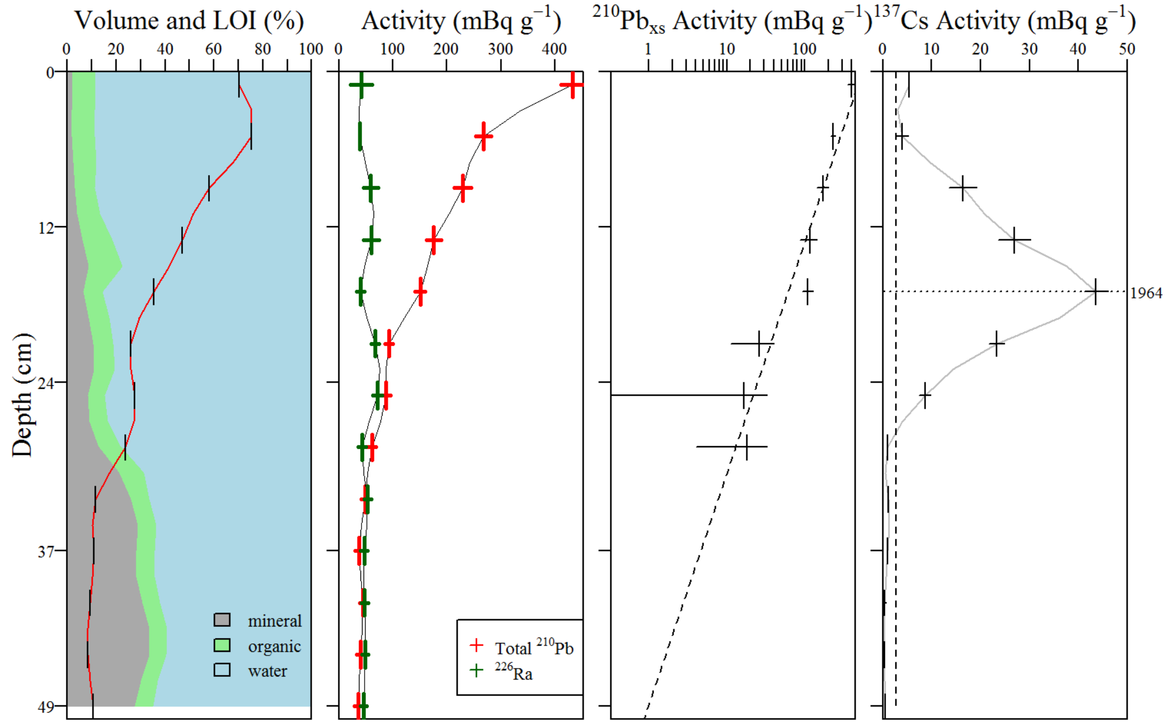
Volume and LOI (%)
Activity (mBq g⁻¹)
210Pbxs Activity (mBq g⁻¹)
137Cs Activity (mBq g⁻¹)
Depth (cm)
mineral
organic
water
Total 210Pb
226Ra
1964

NCBW-1

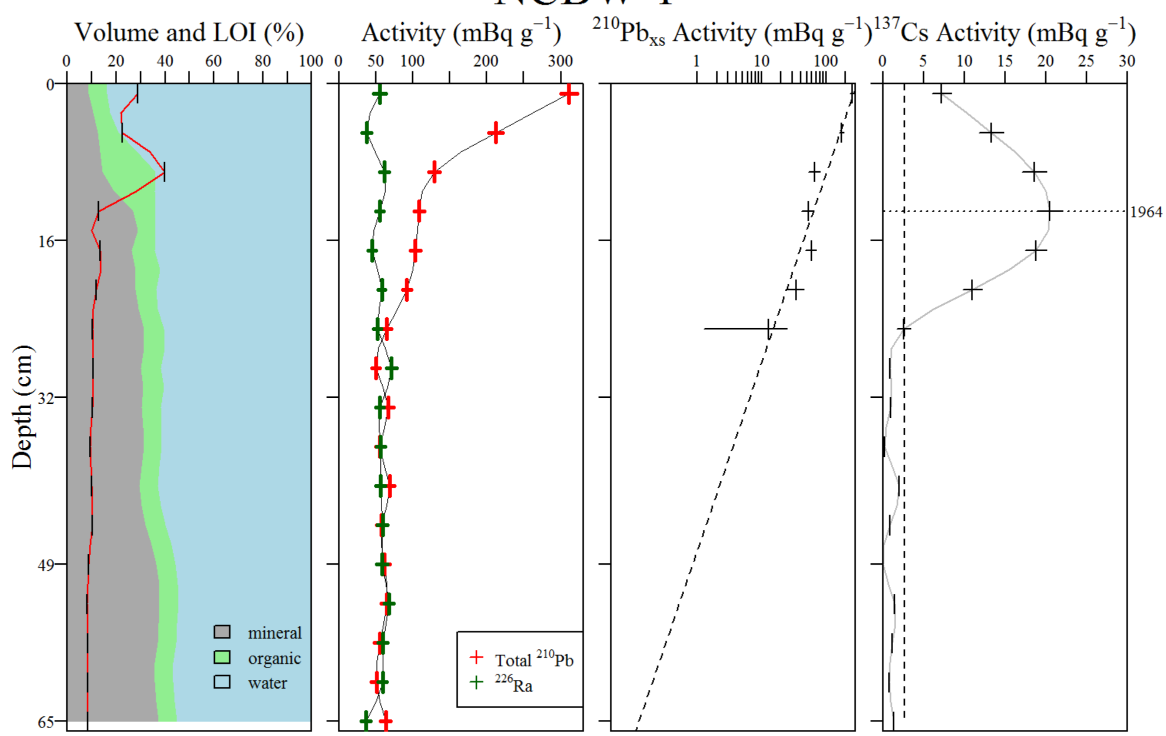
Volume and LOI (%)
Activity (mBq g⁻¹)
210Pbxs Activity (mBq g⁻¹)
137Cs Activity (mBq g⁻¹)
Depth (cm)
mineral
organic
water
Total 210Pb
226Ra
1964

NCBW-2

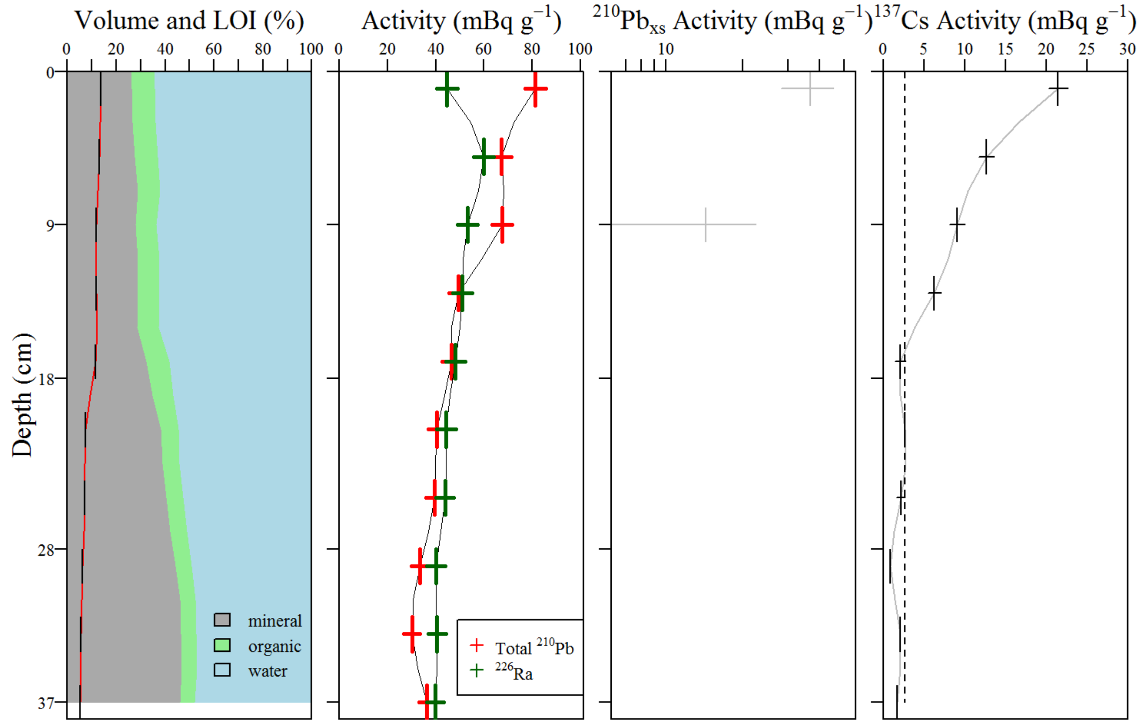
Volume and LOI (%)
Activity (mBq g^{-1})
^{210}Pb$_{xs}$ Activity (mBq g^{-1})
^{137}Cs Activity (mBq g^{-1})
Depth (cm)
mineral
organic
water
Total ^{210}Pb
^{226}Ra

NCBW-3

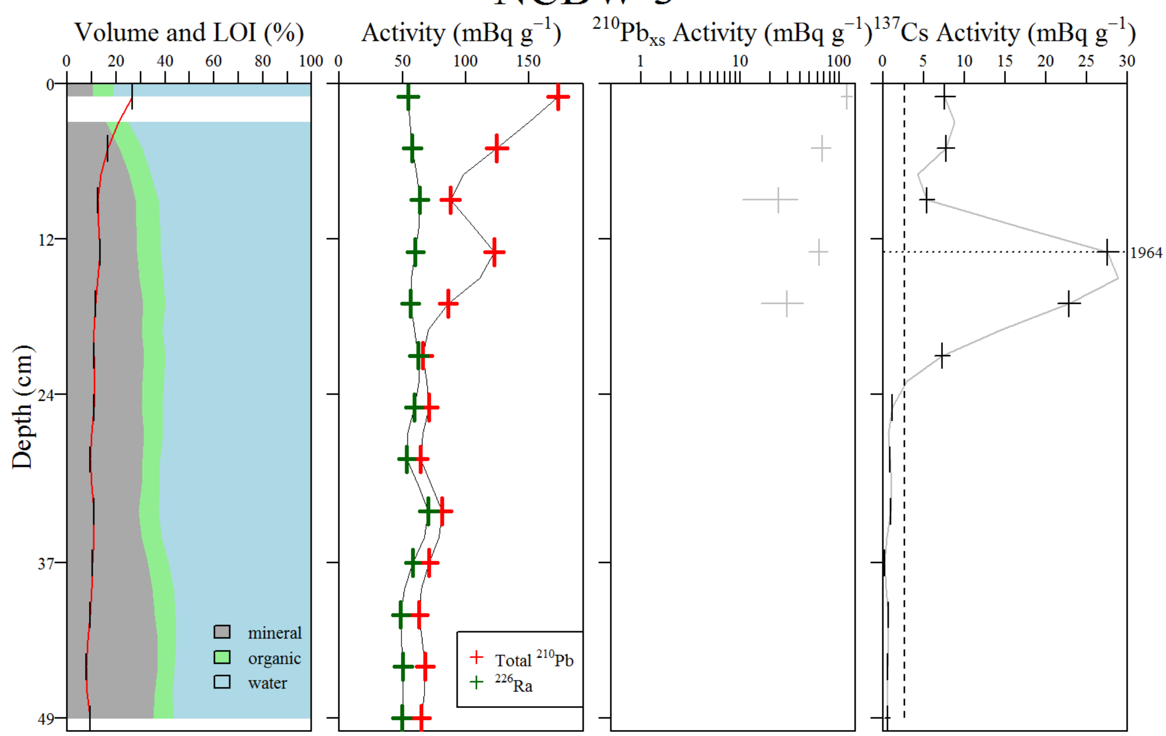
Volume and LOI (%)
Activity (mBq g^{-1})
^{210}Pb$_{xs}$ Activity (mBq g^{-1})
^{137}Cs Activity (mBq g^{-1})
Depth (cm)
mineral
organic
water
Total ^{210}Pb
^{226}Ra
1964

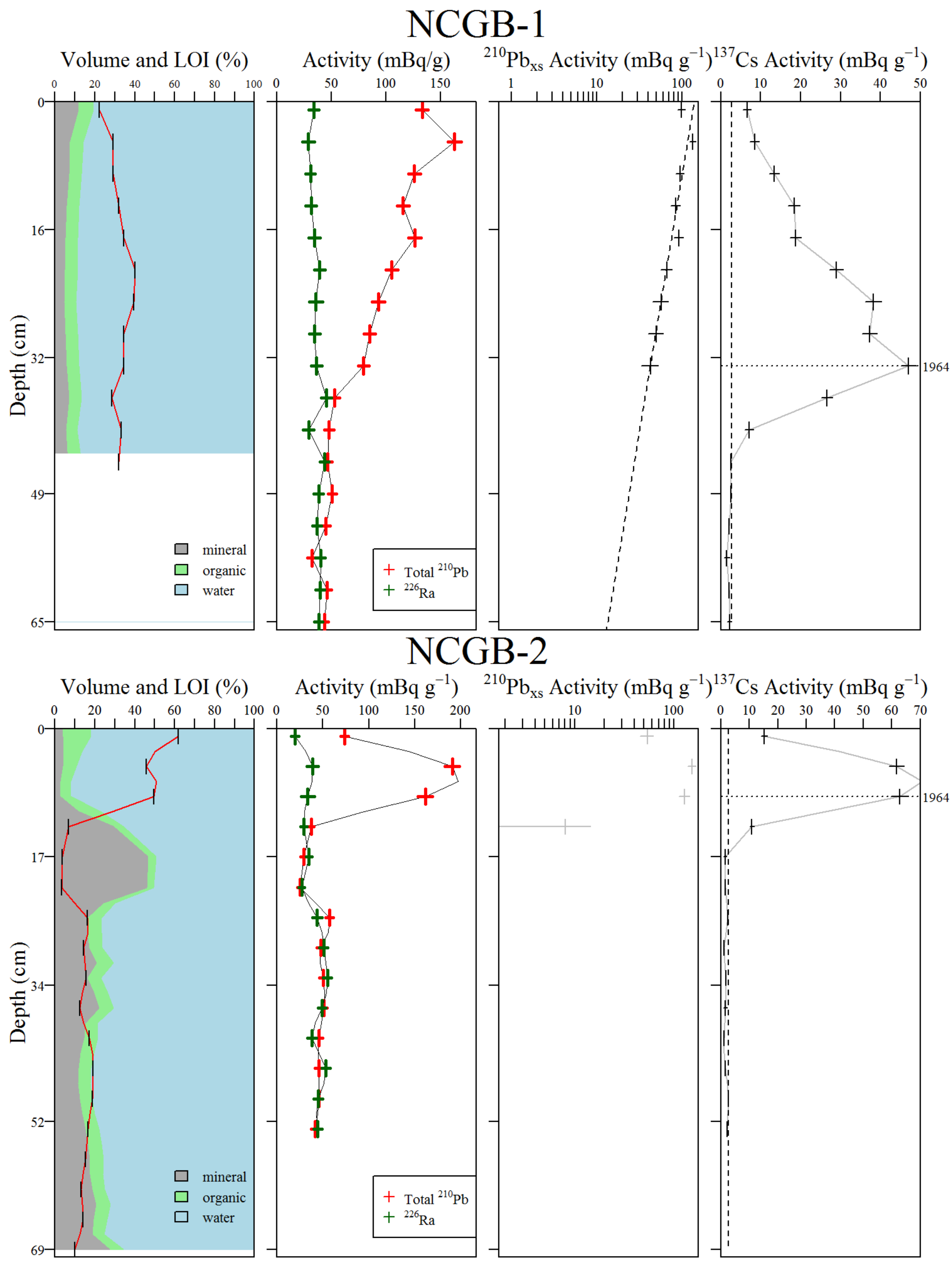
NCGB-1
Volume and LOI (%)
Activity (mBq/g)
$^{210}Pb_{xs}$ Activity (mBq g^{-1})
^{137}Cs Activity (mBq g^{-1})
Depth (cm)
mineral
organic
water
Total ^{210}Pb
^{226}Ra
1964
NCGB-2
Volume and LOI (%)
Activity (mBq g^{-1})
$^{210}Pb_{xs}$ Activity (mBq g^{-1})
^{137}Cs Activity (mBq g^{-1})
Depth (cm)
mineral
organic
water
Total ^{210}Pb
^{226}Ra
1964

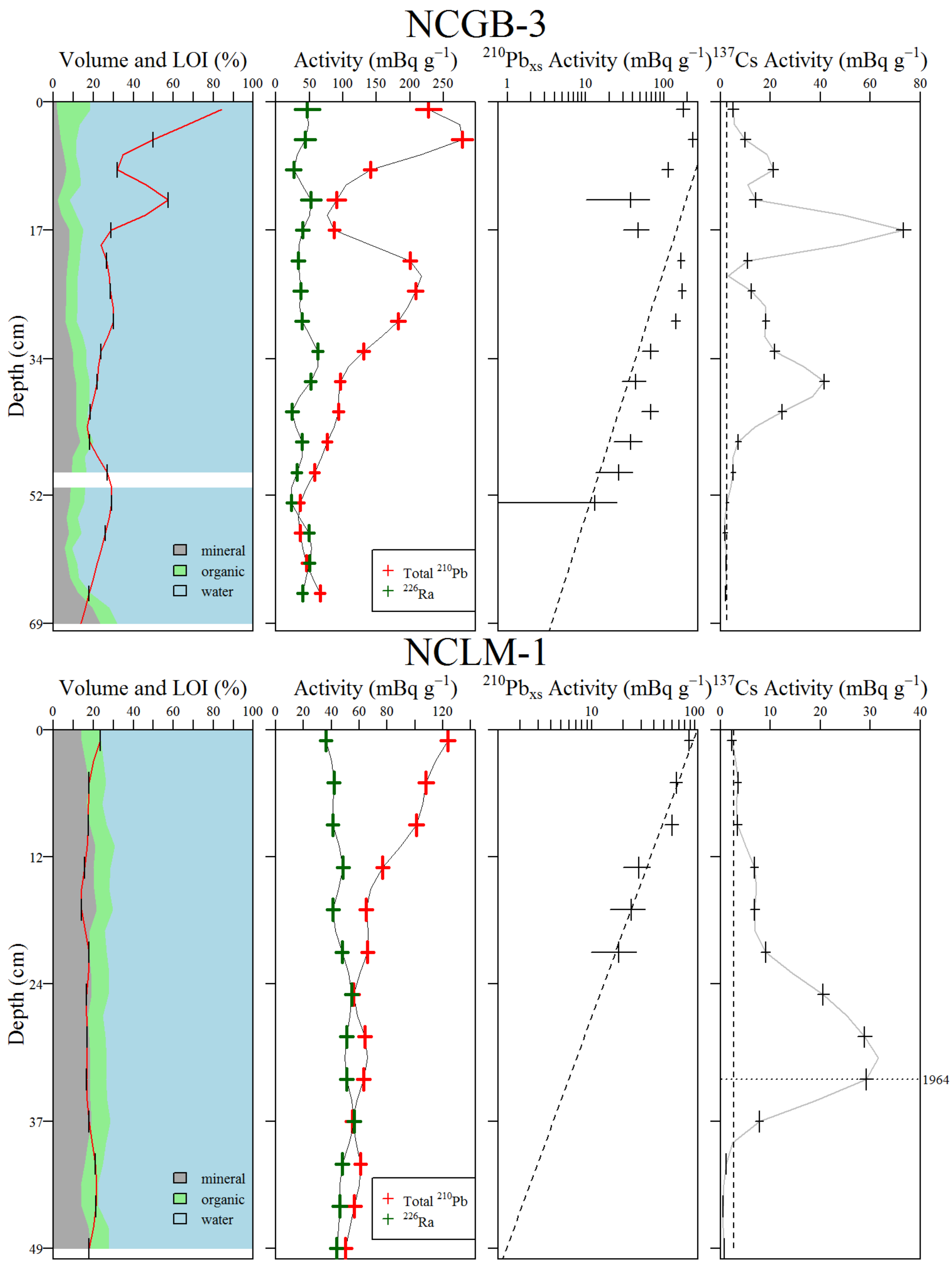
NCGB-3
Volume and LOI (%)
Activity (mBq g−1)
210Pbxs Activity (mBq g−1)
137Cs Activity (mBq g−1)
Depth (cm)
mineral
organic
water
Total 210Pb
226Ra
NCLM-1
Volume and LOI (%)
Activity (mBq g−1)
210Pbxs Activity (mBq g−1)
137Cs Activity (mBq g−1)
Depth (cm)
mineral
organic
water
Total 210Pb
226Ra
1964

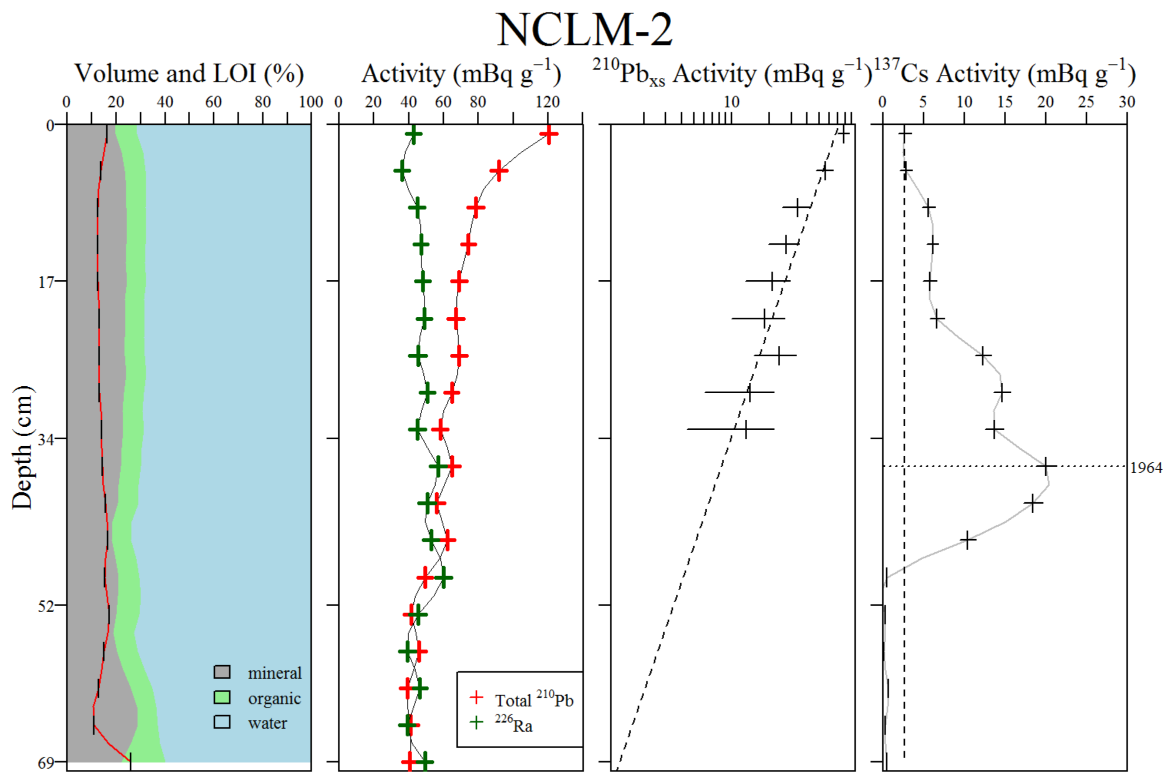
NCLM-2
Volume and LOI (%)
Activity (mBq g^{-1})
^{210}Pb$_{xs}$ Activity (mBq g^{-1})
^{137}Cs Activity (mBq g^{-1})
Depth (cm)
mineral
organic
water
Total ^{210}Pb
^{226}Ra
1964

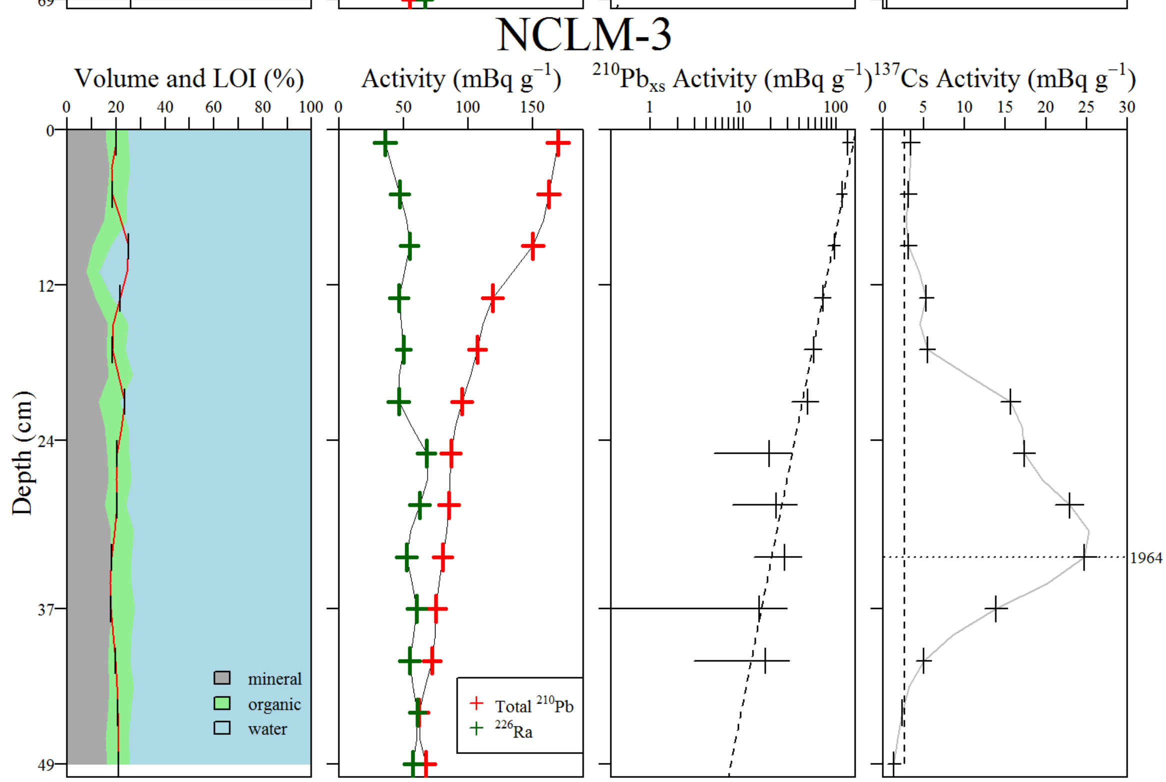
NCLM-3
Volume and LOI (%)
Activity (mBq g^{-1})
^{210}Pb$_{xs}$ Activity (mBq g^{-1})
^{137}Cs Activity (mBq g^{-1})
Depth (cm)
mineral
organic
water
Total ^{210}Pb
^{226}Ra
1964

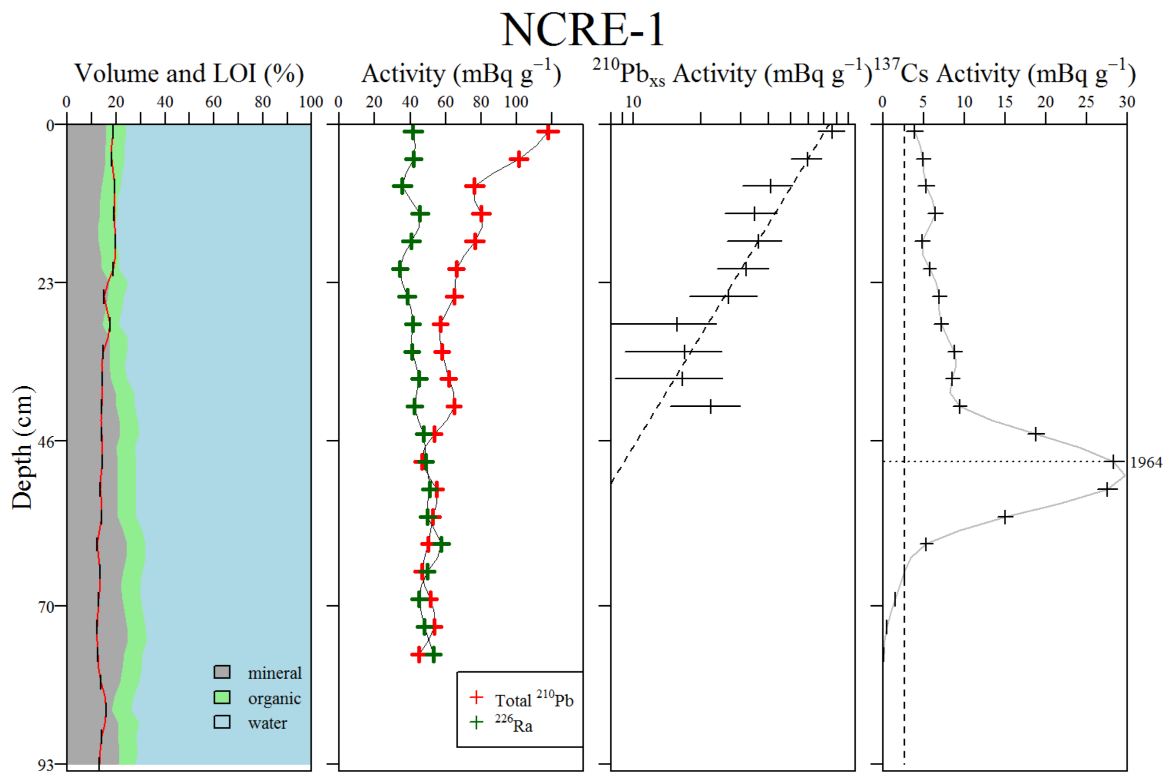
NCRE-1
Volume and LOI (%)
Activity (mBq g^{-1})
^{210}Pb$_{xs}$ Activity (mBq g^{-1})
^{137}Cs Activity (mBq g^{-1})
Depth (cm)
mineral
organic
water
Total ^{210}Pb
^{226}Ra
1964

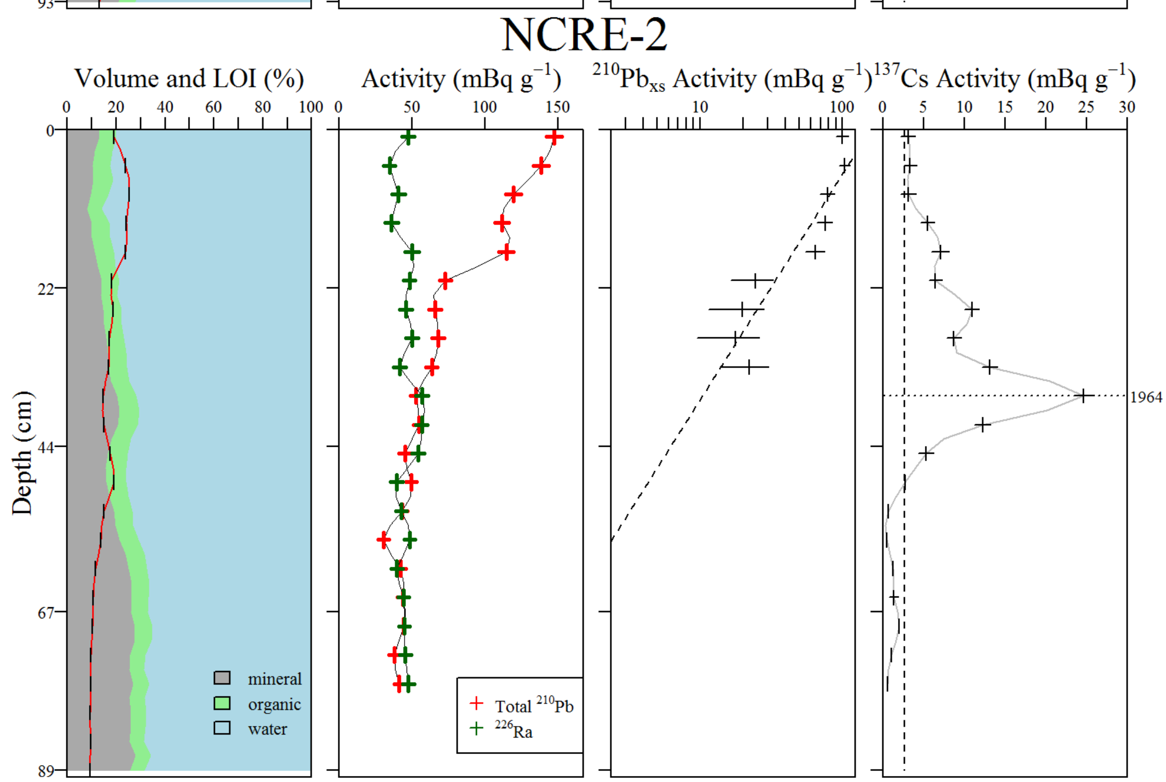
NCRE-2
Volume and LOI (%)
Activity (mBq g^{-1})
^{210}Pb$_{xs}$ Activity (mBq g^{-1})
^{137}Cs Activity (mBq g^{-1})
Depth (cm)
mineral
organic
water
Total ^{210}Pb
^{226}Ra
1964

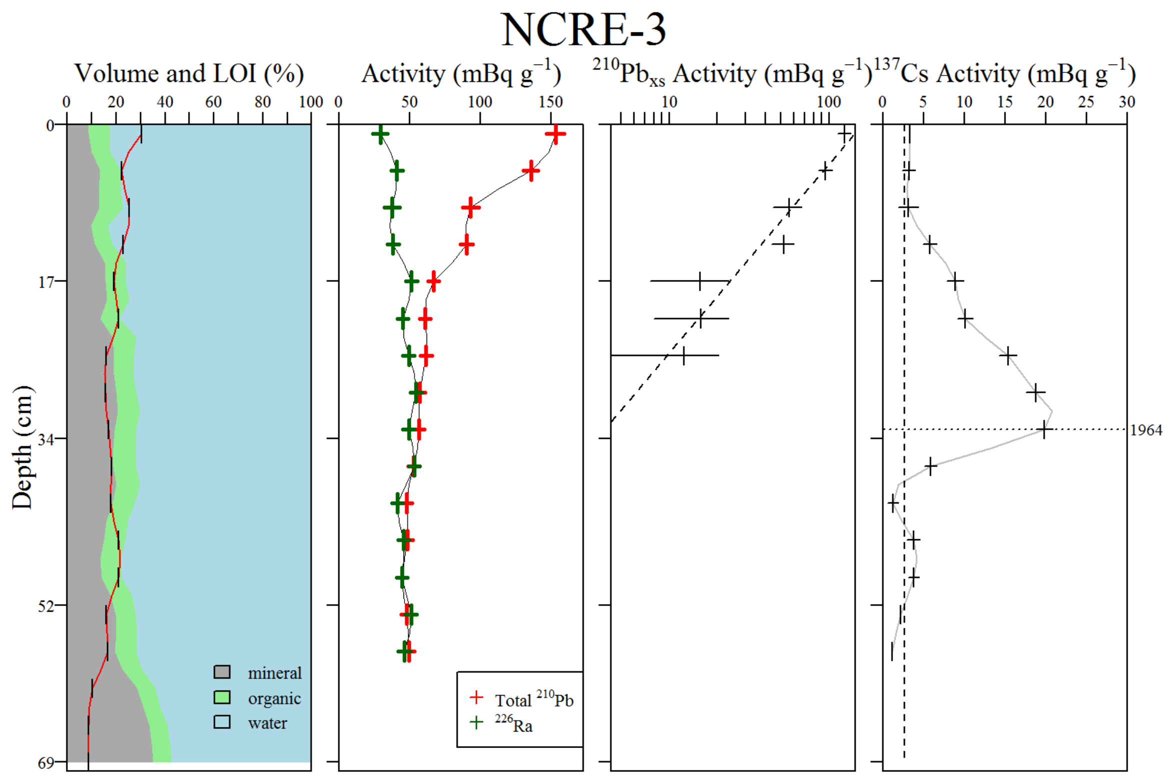
NCRE-3
Volume and LOI (%)
Activity (mBq g−1)
210Pbxs Activity (mBq g−1)
137Cs Activity (mBq g−1)
Depth (cm)
mineral
organic
water
Total 210Pb
226Ra
1964

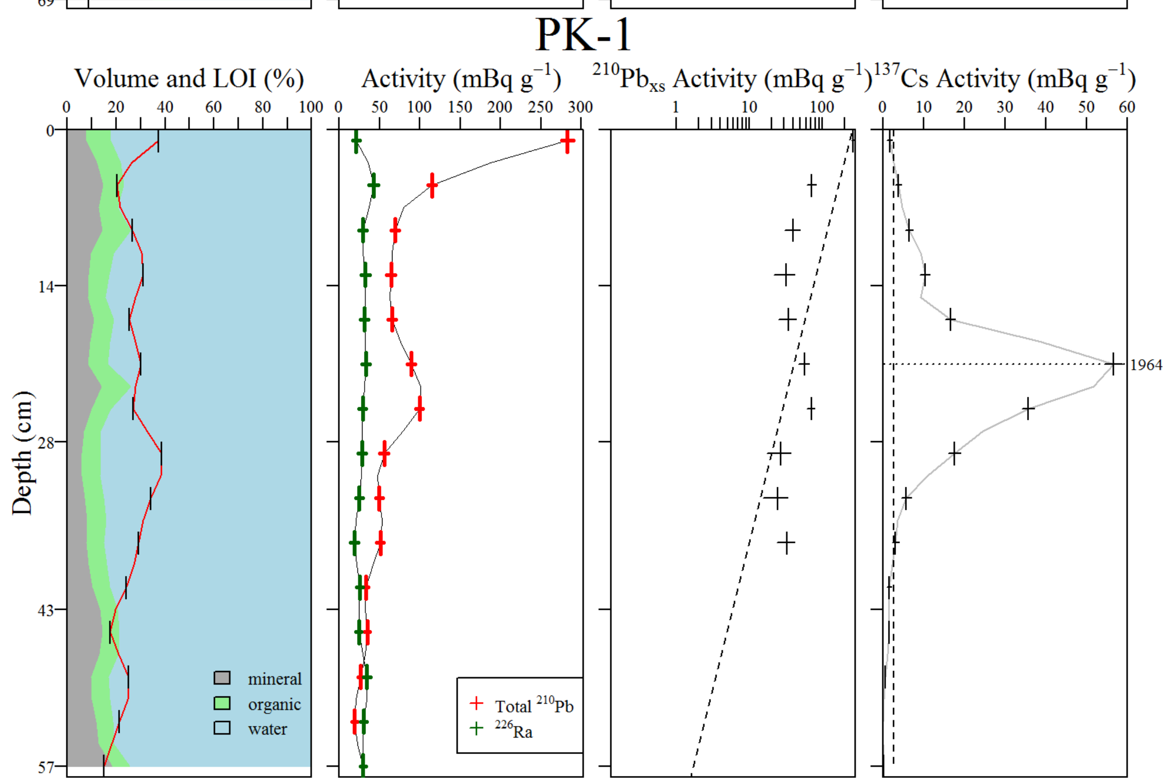
PK-1
Volume and LOI (%)
Activity (mBq g−1)
210Pbxs Activity (mBq g−1)
137Cs Activity (mBq g−1)
Depth (cm)
mineral
organic
water
Total 210Pb
226Ra
1964

PK-2

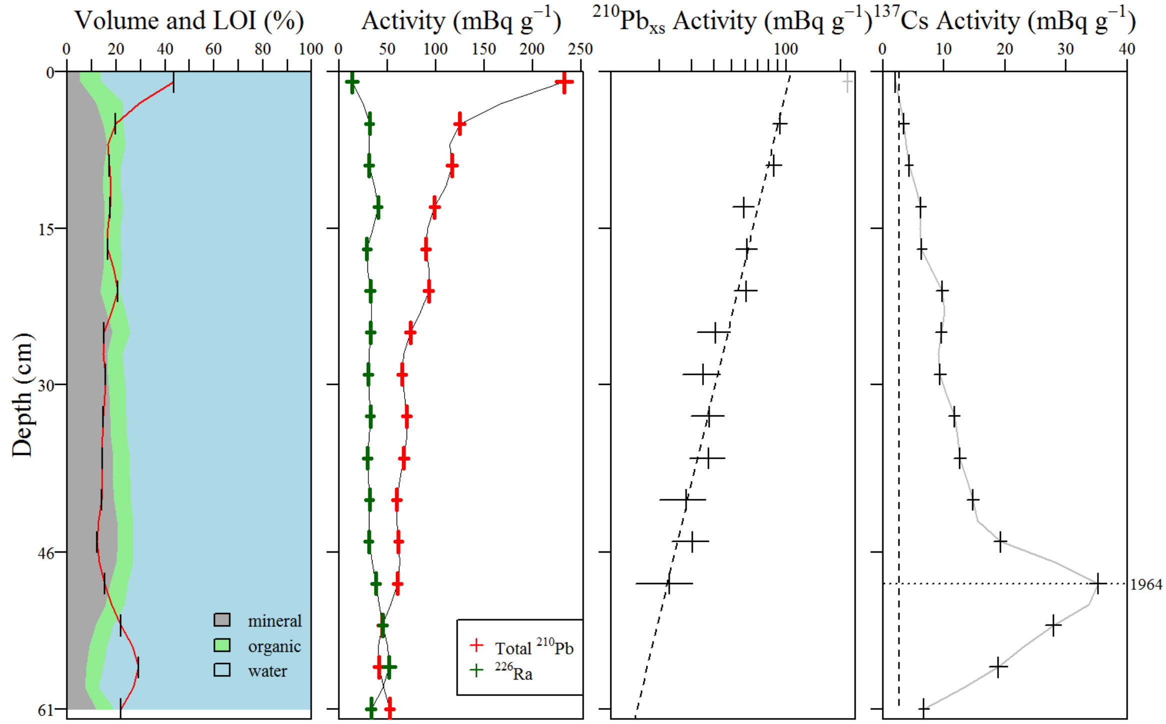

Volume and LOI (%)
Activity (mBq g^{-1})
^{210}Pb$_{xs}$ Activity (mBq g^{-1})
^{137}Cs Activity (mBq g^{-1})
Depth (cm)
mineral
organic
water
Total ^{210}Pb
^{226}Ra
1964

PK-3

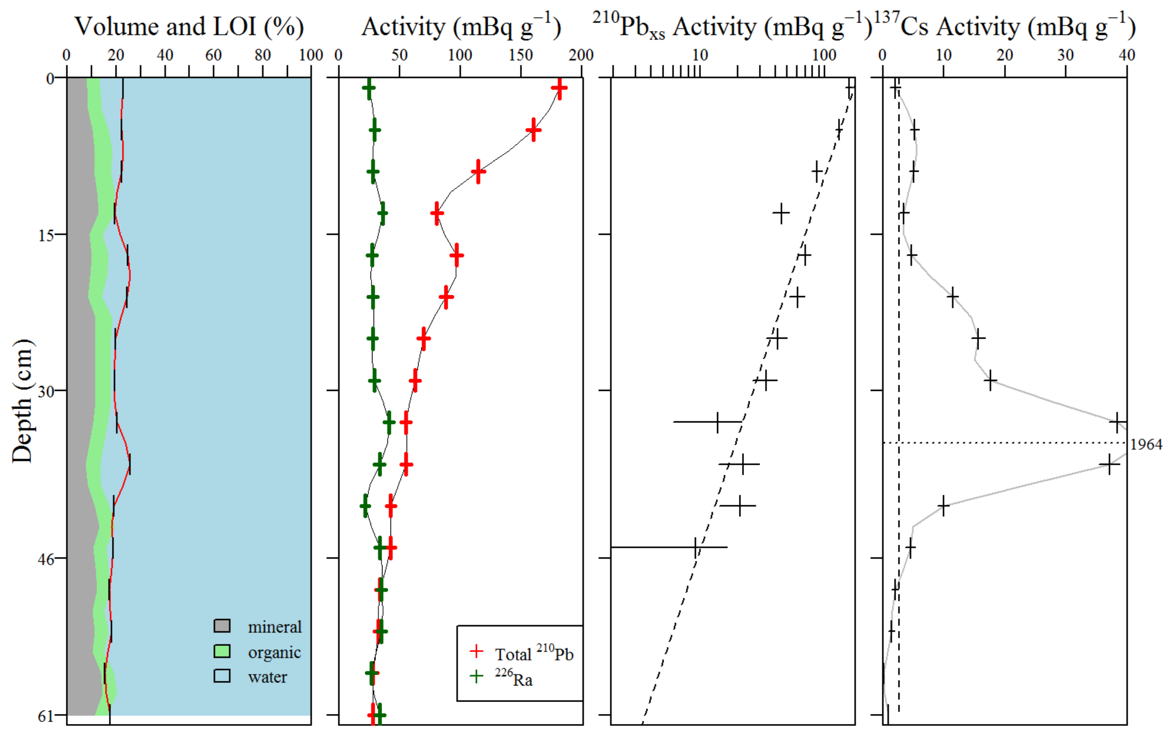

Volume and LOI (%)
Activity (mBq g^{-1})
^{210}Pb$_{xs}$ Activity (mBq g^{-1})
^{137}Cs Activity (mBq g^{-1})
Depth (cm)
mineral
organic
water
Total ^{210}Pb
^{226}Ra
1964

PM-1

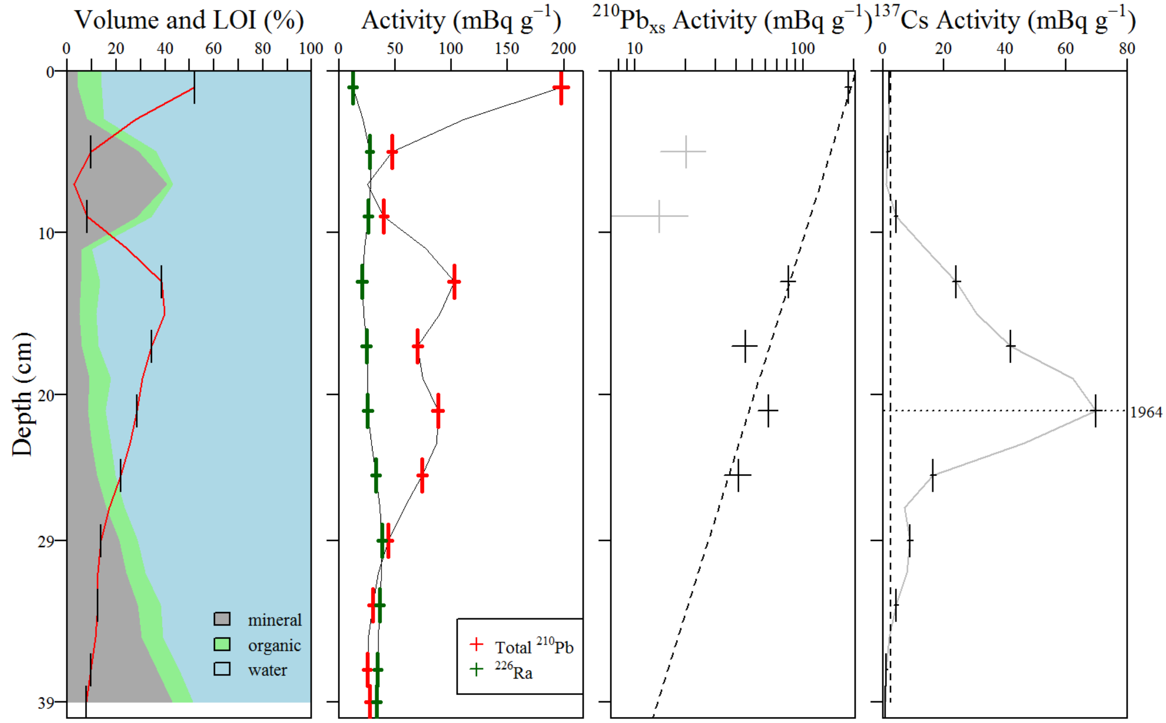
Volume and LOI (%)
Activity (mBq g−1)
210Pbxs Activity (mBq g−1)
137Cs Activity (mBq g−1)
Depth (cm)
mineral
organic
water
Total 210Pb
226Ra
1964

PM-2

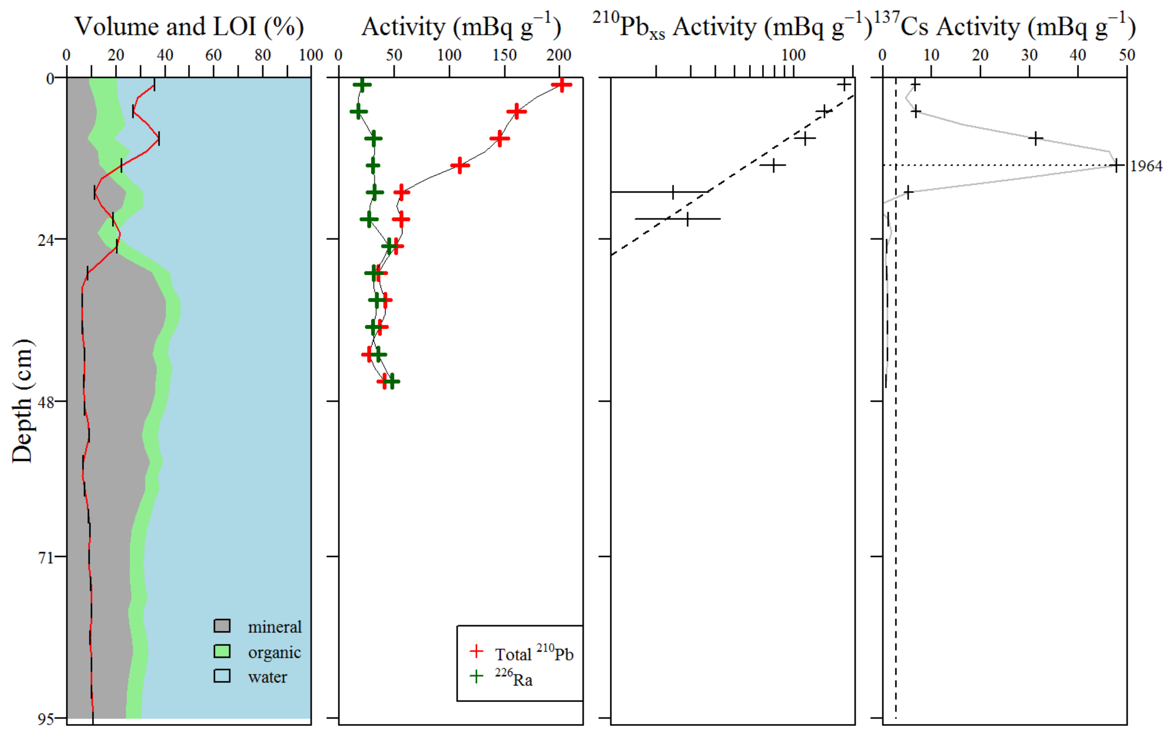
Volume and LOI (%)
Activity (mBq g−1)
210Pbxs Activity (mBq g−1)
137Cs Activity (mBq g−1)
Depth (cm)
mineral
organic
water
Total 210Pb
226Ra
1964

PM-3

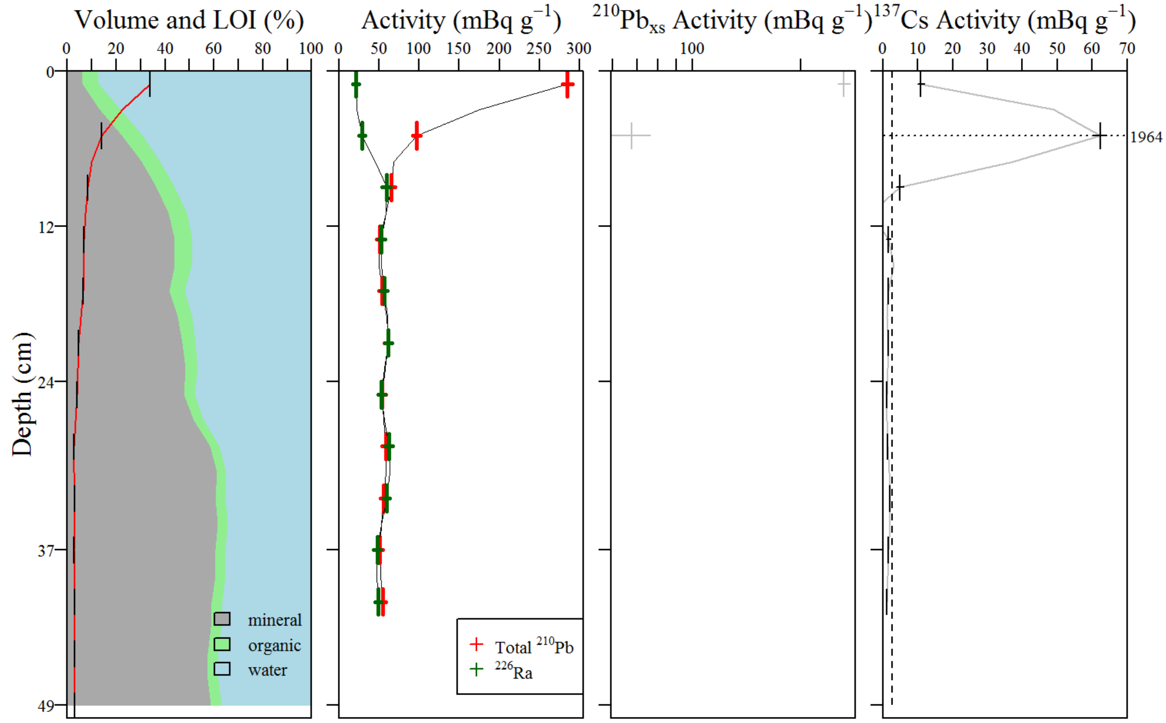

Volume and LOI (%)
Activity (mBq g^{-1})
$^{210}Pb_{xs}$ Activity (mBq g^{-1})
^{137}Cs Activity (mBq g^{-1})
Depth (cm)
mineral
organic
water
Total ^{210}Pb
^{226}Ra
1964

PM-4

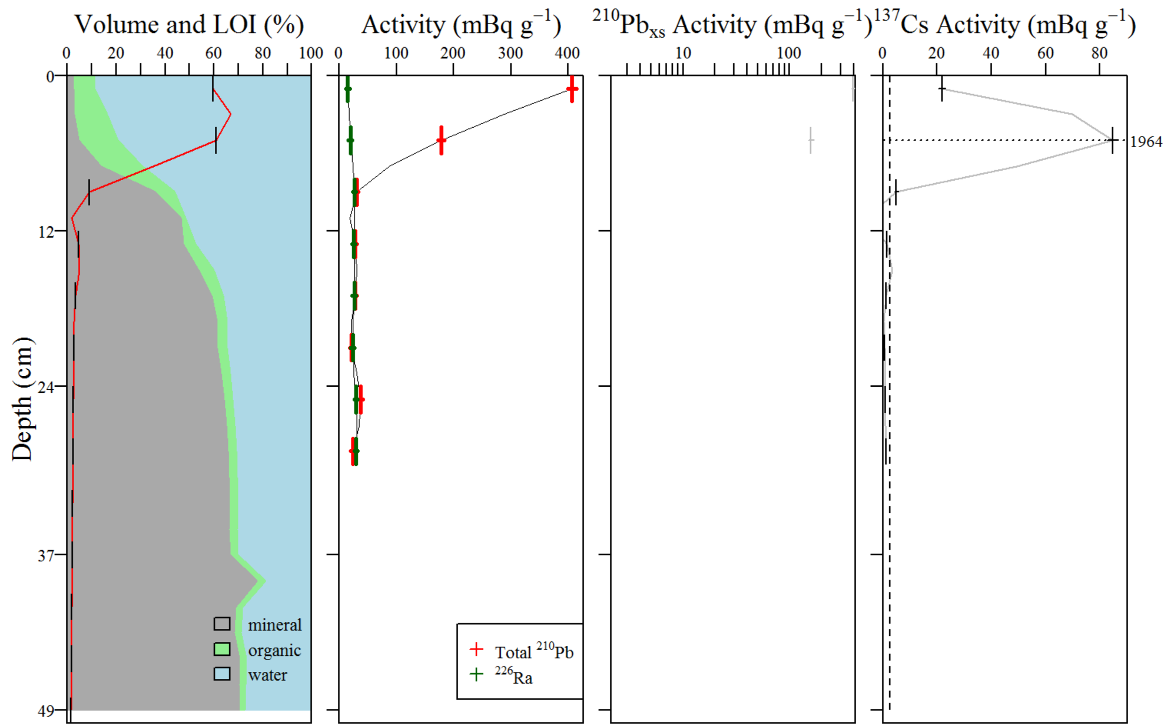

Volume and LOI (%)
Activity (mBq g^{-1})
$^{210}Pb_{xs}$ Activity (mBq g^{-1})
^{137}Cs Activity (mBq g^{-1})
Depth (cm)
mineral
organic
water
Total ^{210}Pb
^{226}Ra
1964

PM-5

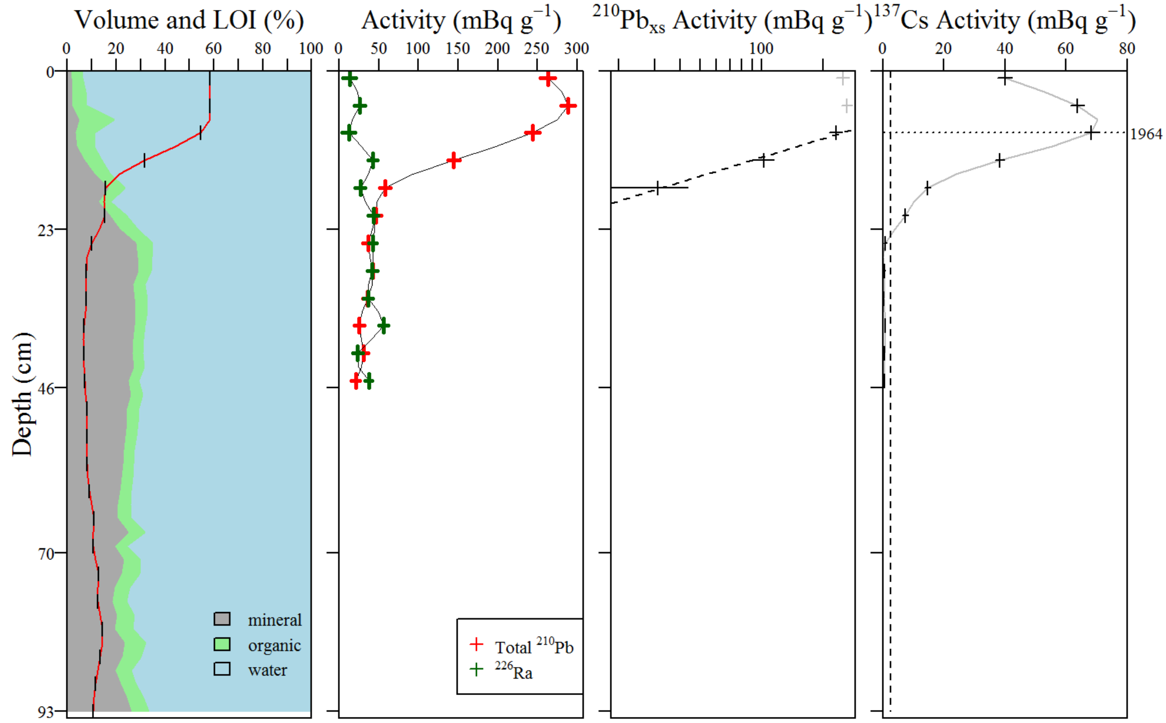

Volume and LOI (%)
Activity (mBq g⁻¹)
210Pbxs Activity (mBq g⁻¹)
137Cs Activity (mBq g⁻¹)
Depth (cm)
1964
mineral
organic
water
Total 210Pb
226Ra

PM-6

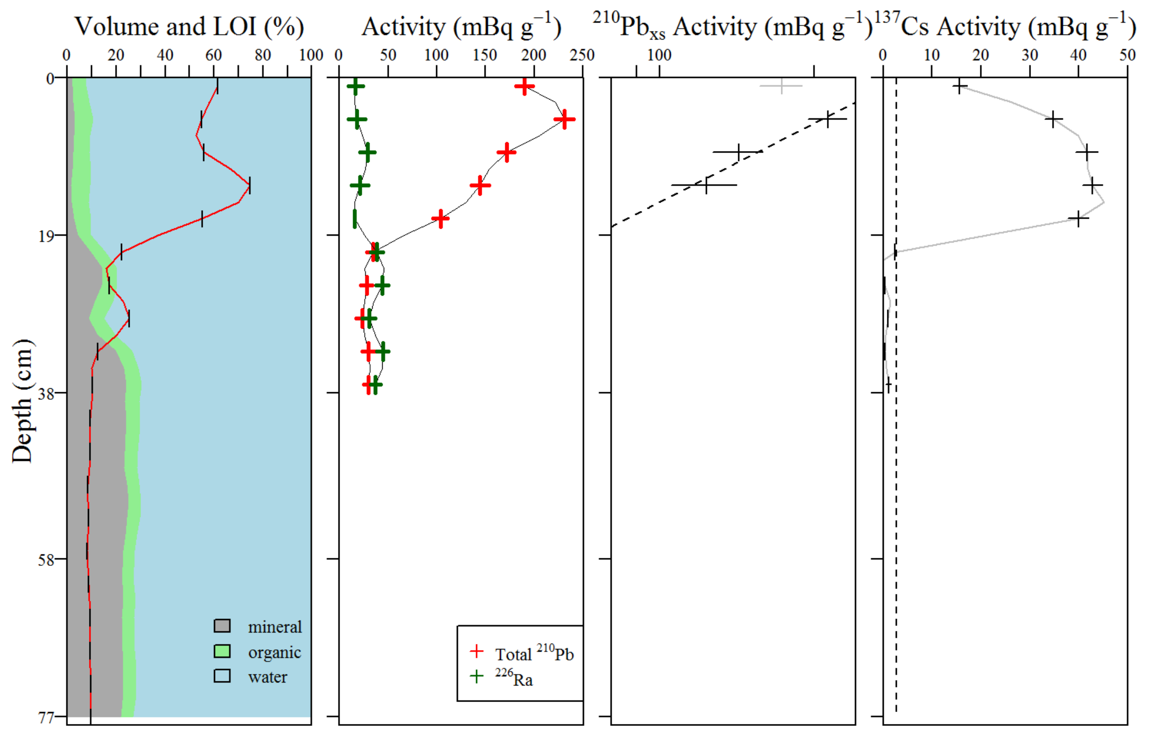

Volume and LOI (%)
Activity (mBq g⁻¹)
210Pbxs Activity (mBq g⁻¹)
137Cs Activity (mBq g⁻¹)
Depth (cm)
mineral
organic
water
Total 210Pb
226Ra

PM-7

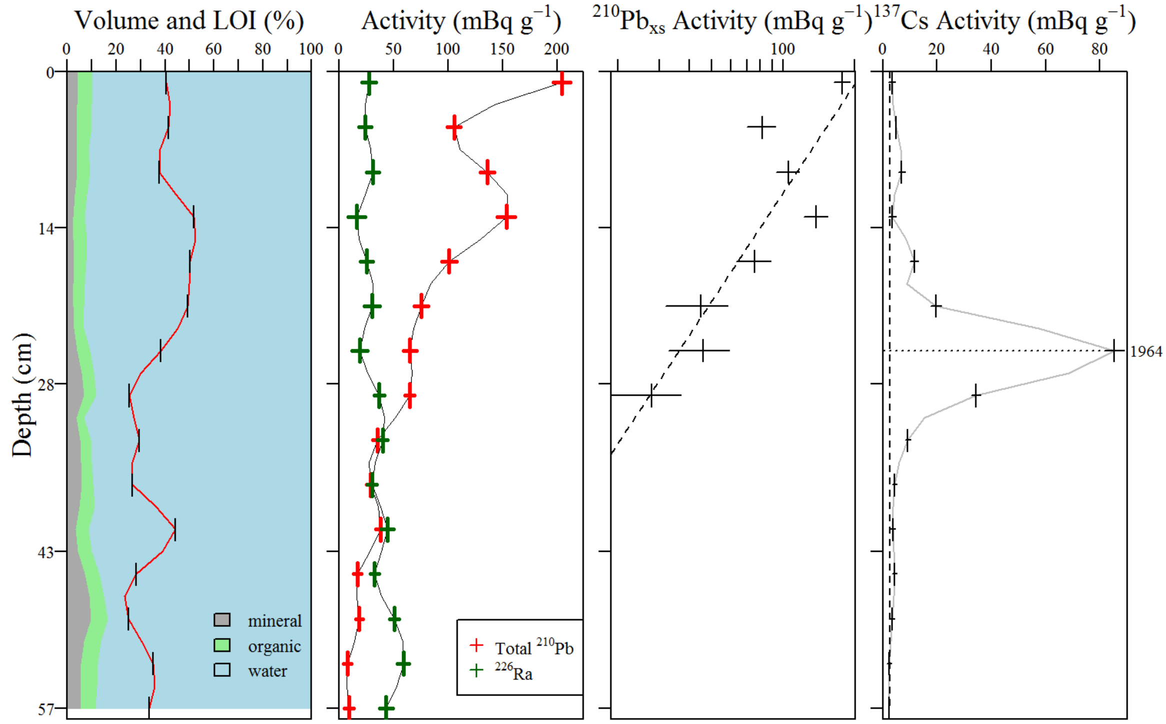

Volume and LOI (%)
Activity (mBq g^{-1})
$^{210}Pb_{xs}$ Activity (mBq g^{-1})
^{137}Cs Activity (mBq g^{-1})
Depth (cm)
mineral
organic
water
Total ^{210}Pb
^{226}Ra
1964

PM-8

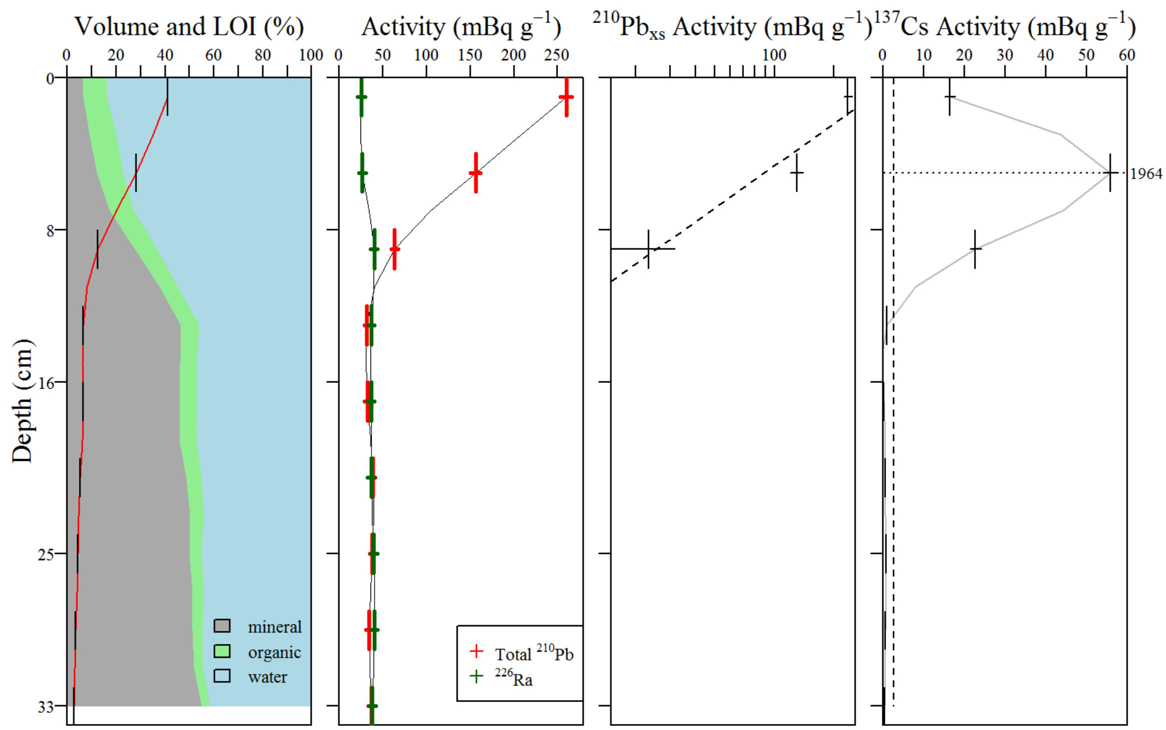

Volume and LOI (%)
Activity (mBq g^{-1})
$^{210}Pb_{xs}$ Activity (mBq g^{-1})
^{137}Cs Activity (mBq g^{-1})
Depth (cm)
mineral
organic
water
Total ^{210}Pb
^{226}Ra
1964

PM-9

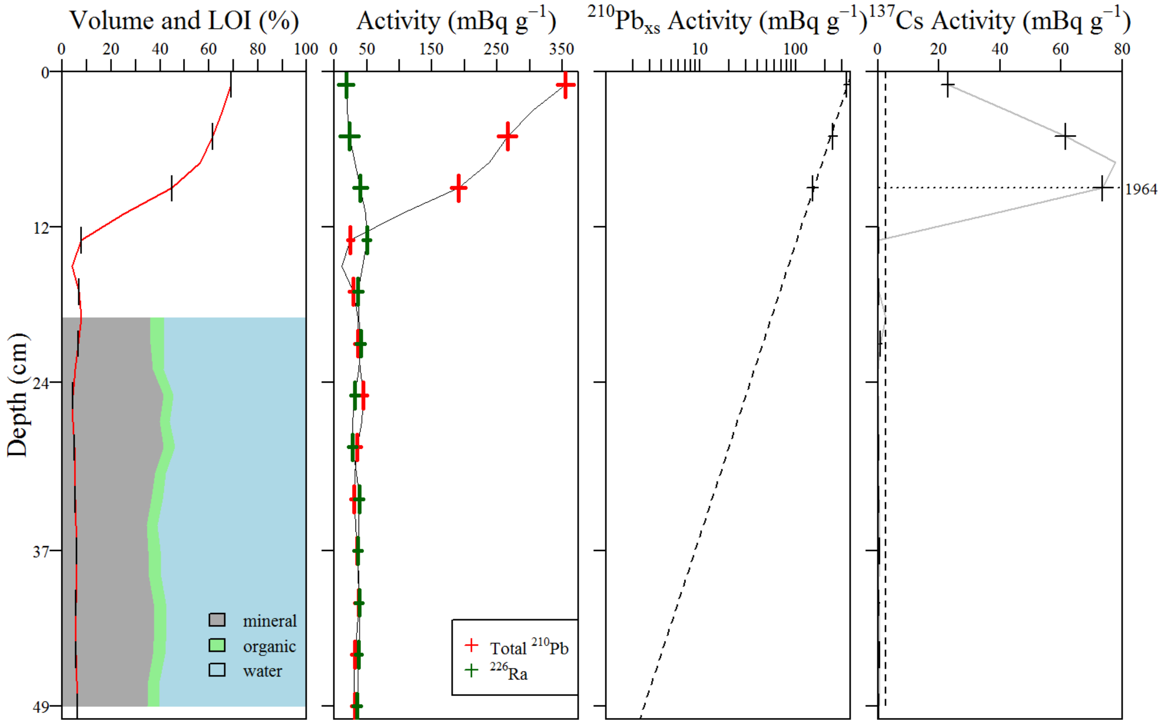
Volume and LOI (%)
Activity (mBq g^{-1})
$^{210}Pb_{xs}$ Activity (mBq g^{-1})
^{137}Cs Activity (mBq g^{-1})
Depth (cm)
mineral
organic
water
Total ^{210}Pb
^{226}Ra
1964

PM-10

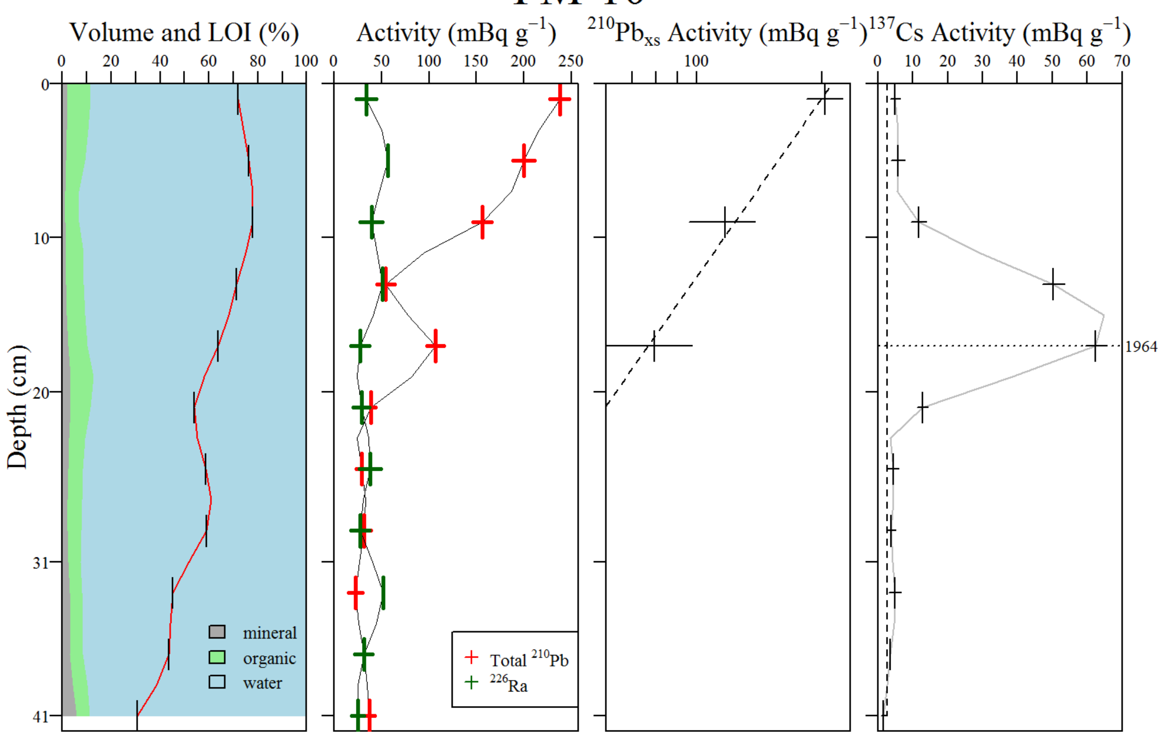
Volume and LOI (%)
Activity (mBq g^{-1})
$^{210}Pb_{xs}$ Activity (mBq g^{-1})
^{137}Cs Activity (mBq g^{-1})
Depth (cm)
mineral
organic
water
Total ^{210}Pb
^{226}Ra
1964

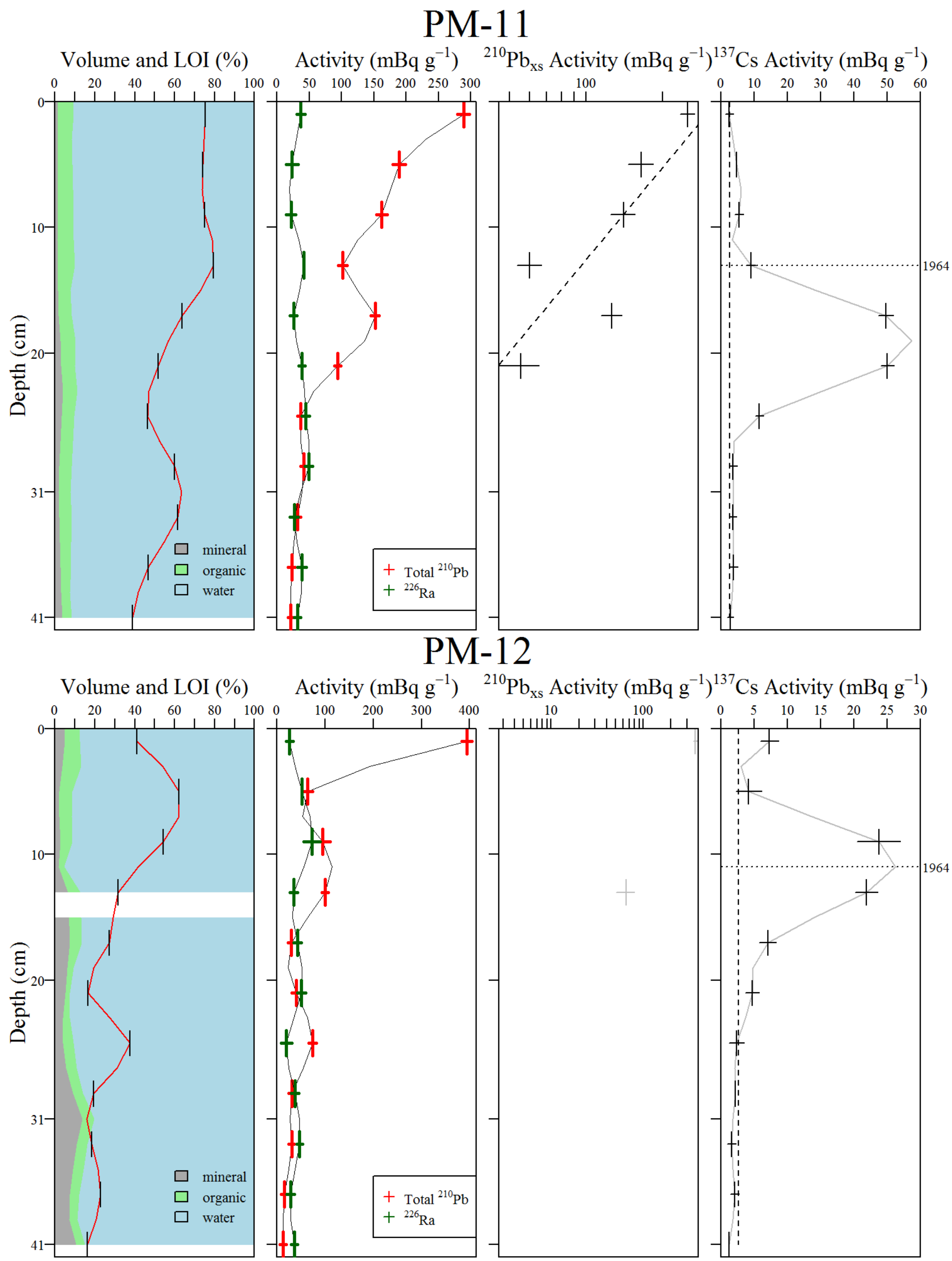
PM-11
Volume and LOI (%)
Activity (mBq g^{-1})
$^{210}Pb_{xs}$ Activity (mBq g^{-1})
^{137}Cs Activity (mBq g^{-1})
Depth (cm)
mineral
organic
water
Total ^{210}Pb
^{226}Ra
1964
PM-12
Volume and LOI (%)
Activity (mBq g^{-1})
$^{210}Pb_{xs}$ Activity (mBq g^{-1})
^{137}Cs Activity (mBq g^{-1})
Depth (cm)
mineral
organic
water
Total ^{210}Pb
^{226}Ra
1964

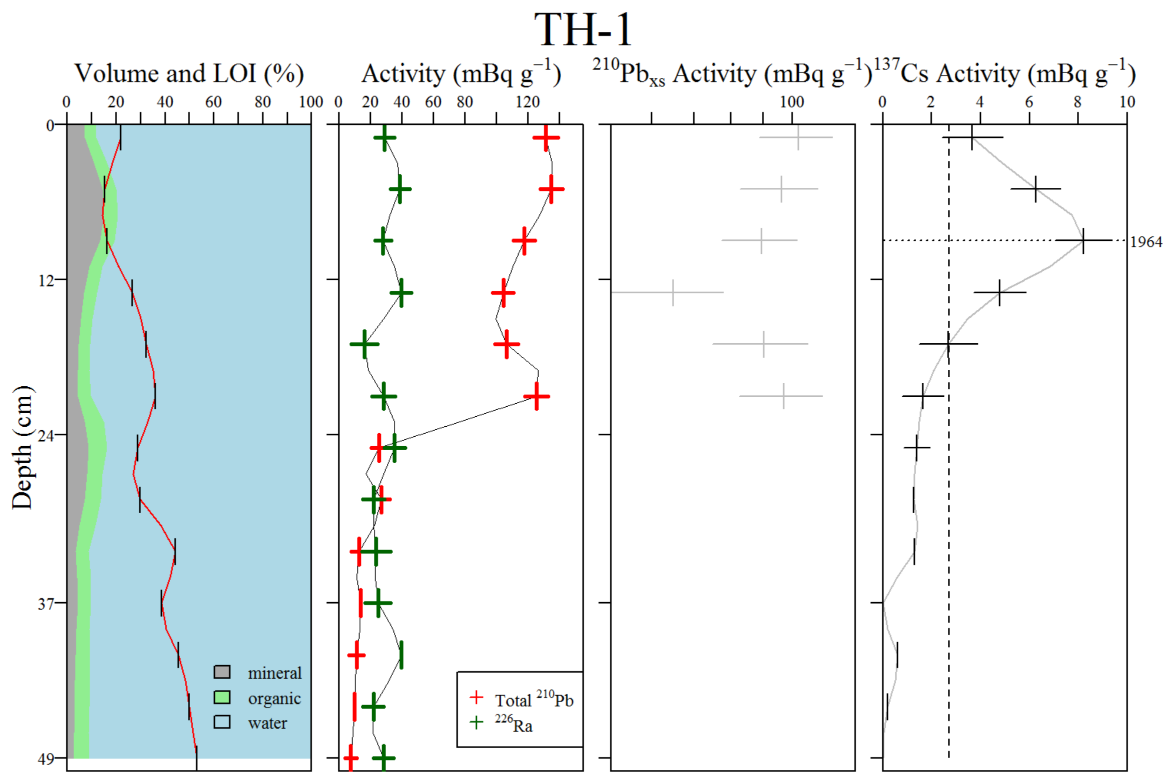
TH-1
Volume and LOI (%)
Activity (mBq g^{-1})
$^{210}Pb_{xs}$ Activity (mBq g^{-1})
^{137}Cs Activity (mBq g^{-1})
Depth (cm)
1964
mineral
organic
water
Total ^{210}Pb
^{226}Ra

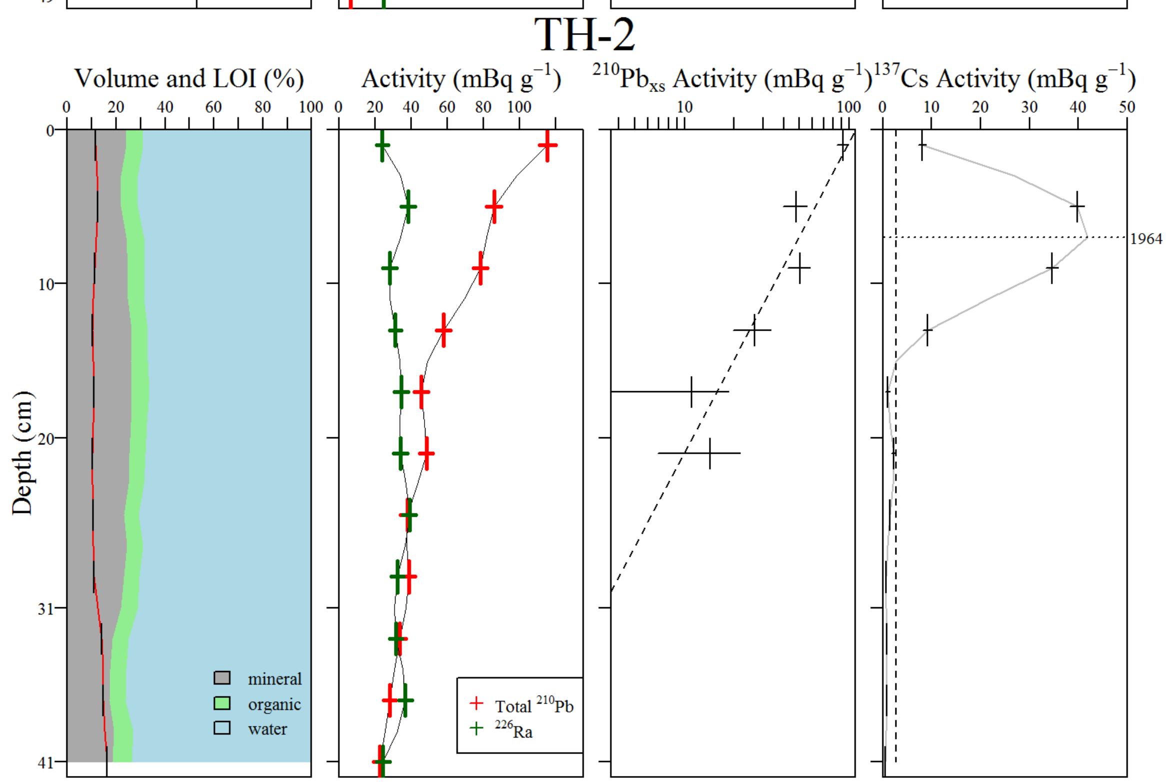
TH-2
Volume and LOI (%)
Activity (mBq g^{-1})
$^{210}Pb_{xs}$ Activity (mBq g^{-1})
^{137}Cs Activity (mBq g^{-1})
Depth (cm)
1964
mineral
organic
water
Total ^{210}Pb
^{226}Ra

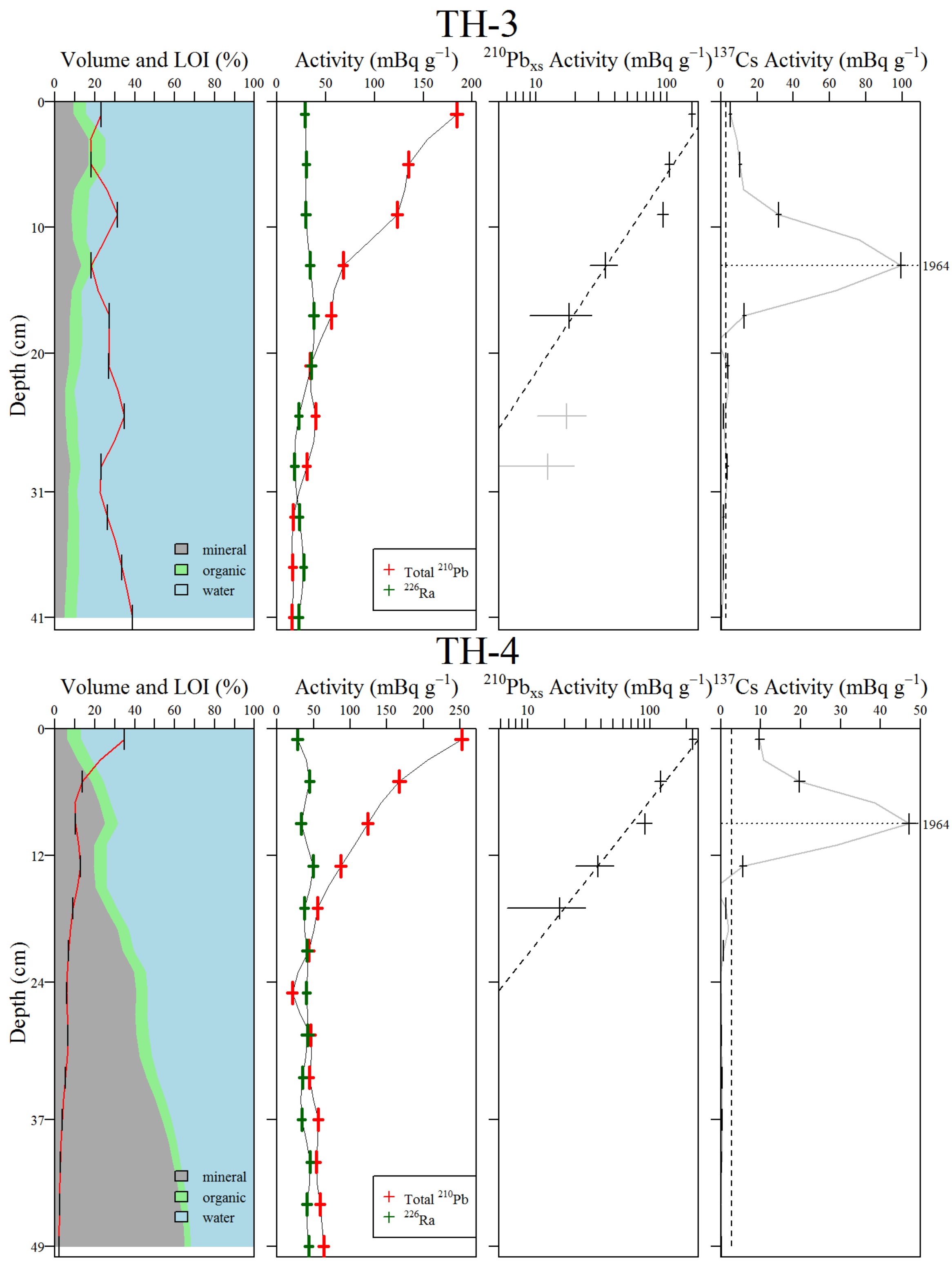

TH-3
Volume and LOI (%)
Activity (mBq g−1)
210Pbxs Activity (mBq g−1)
137Cs Activity (mBq g−1)
Depth (cm)
mineral
organic
water
Total 210Pb
226Ra
1964
TH-4
Volume and LOI (%)
Activity (mBq g−1)
210Pbxs Activity (mBq g−1)
137Cs Activity (mBq g−1)
Depth (cm)
mineral
organic
water
Total 210Pb
226Ra
1964

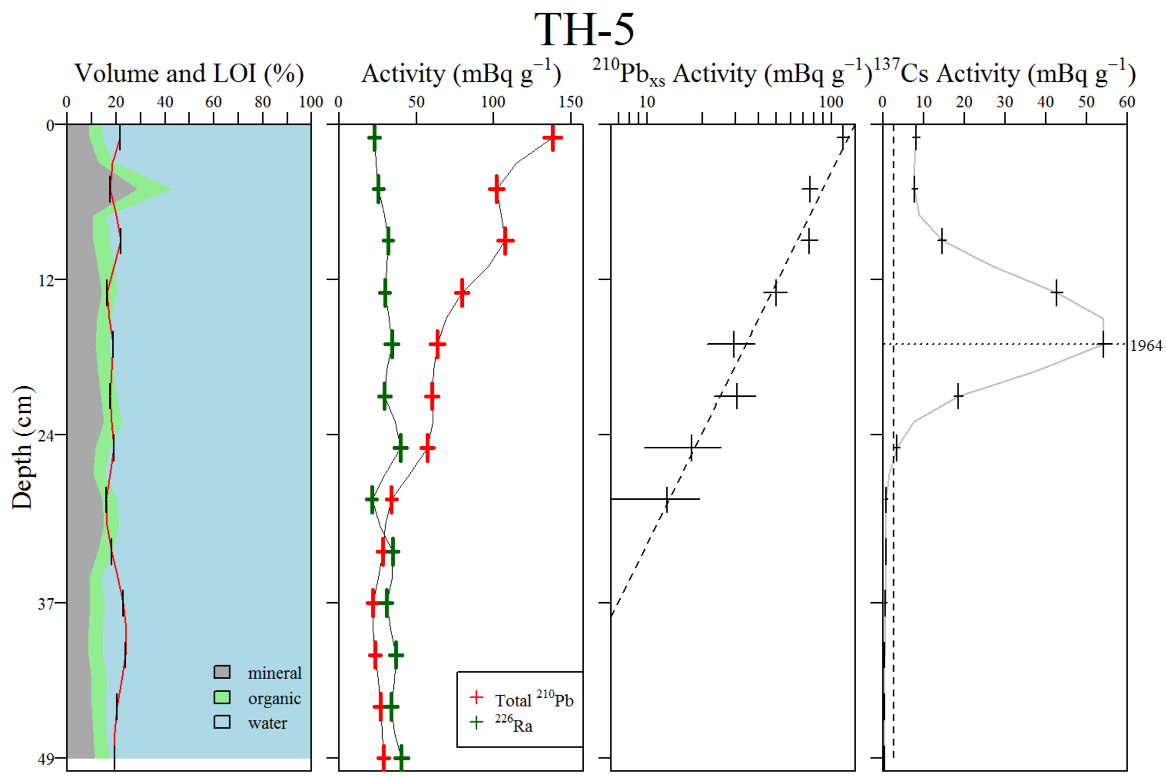

TH-5
Volume and LOI (%)
Activity (mBq g^{-1})
$^{210}Pb_{xs}$ Activity (mBq g^{-1})
^{137}Cs Activity (mBq g^{-1})
Depth (cm)
mineral
organic
water
Total ^{210}Pb
^{226}Ra
1964

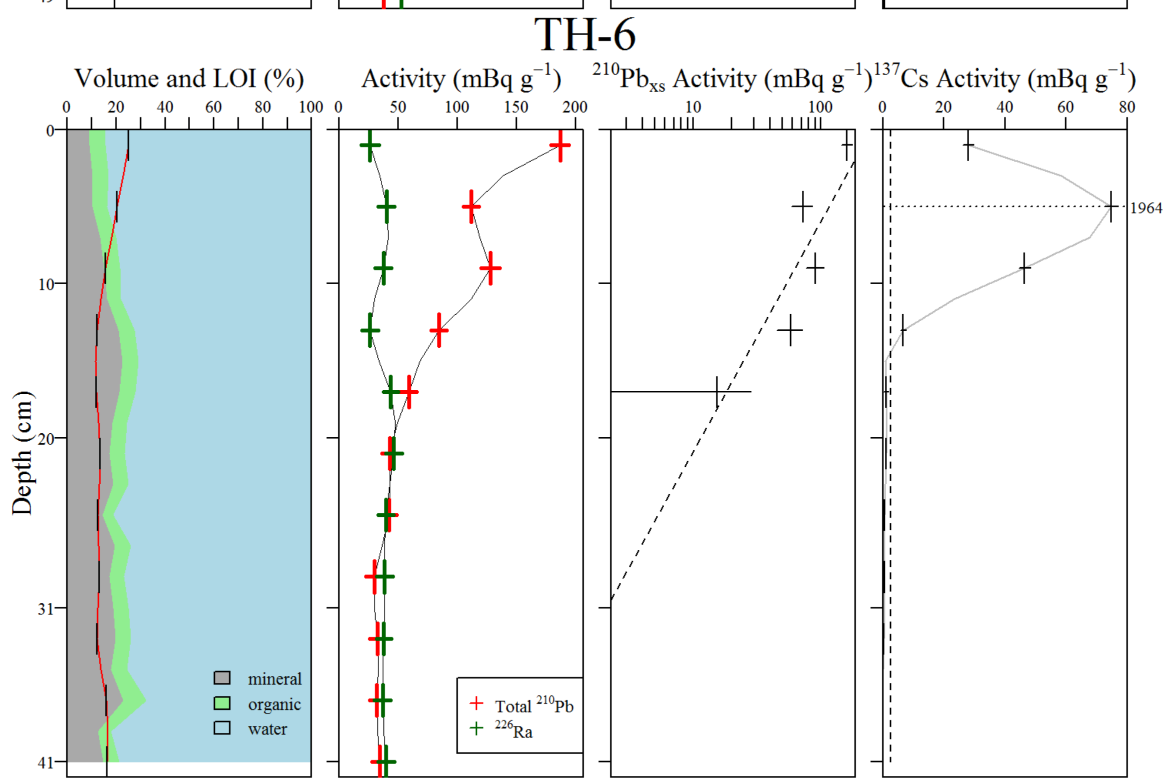

TH-6
Volume and LOI (%)
Activity (mBq g^{-1})
$^{210}Pb_{xs}$ Activity (mBq g^{-1})
^{137}Cs Activity (mBq g^{-1})
Depth (cm)
mineral
organic
water
Total ^{210}Pb
^{226}Ra
1964